Appendix X-6

Diavik Waste-Rock Research Program
2009 Progress Report

DIAVIK WASTE-ROCK RESEARCH PROGRAM

2009 Progress Report

for

Diavik Diamond Mines Inc.
International Network for Acid Prevention
Mine Environment Neutral Drainage

Research Partners

University of Waterloo
University of British Columbia
University of Alberta

Diavik Diamond Mine

NSERC CRSNG

MEND

INAP

Canada Foundation for Innovation
Fondation canadienne pour l'innovation

University of Alberta

University of Waterloo

UBC

Acknowledgements

Funding for this research was provided by: Diavik Diamond Mines Inc. (DDMI); a Canadian Foundation for Innovation (CFI) Innovation Fund Award, James F. Barker Principal Investigator; a Natural Sciences and Engineering Research Council of Canada (NSERC) Collaborative Research and Development Grant, David W. Blowes Principal Investigator; the International Network for Acid Prevention (INAP); and the Mine Environment Neutral Drainage (MEND) program. In-kind support provided by Environment Canada is greatly appreciated. We thank Diavik Diamond Mines Inc. and FDA Engineering for technical support and patience during the construction phase. We appreciate the support and assistance we have received from L. Smith, G. MacDonald, J. Reinson, L. Clark, and S. Wytrychowski, DDMI, throughout the project. Invaluable field support has been provided by numerous graduate students, co-op students, and technicians from the participating universities, as well as skilled equipment operators with DDMI.

Executive Summary

The Diavik Waste Rock Project is designed to evaluate the benefits of the proposed reclamation concepts for the Diavik Country Rock Stockpiles, and to evaluate techniques used to scale the results of laboratory studies to predict the environmental impacts of full-scale rock stockpiles. The Diavik Project includes laboratory testing of rock from the Diavik site, field lysimeters containing each rock type and three large-scale test piles. The test piles have been instrumented in detail and monitoring is underway. This report provides a brief update of progress over the 2009 field season. Results and interpretation presented in this report are preliminary and will be updated as new data are collected and more comprehensive quality control and data analysis are performed.

Gas transport studies of the Diavik test piles include gas pressure measurements in the Type III pile and oxygen and carbon dioxide measurements in the Type I, Type III and Covered piles. In the Type III pile gas pressure measurements indicate that pressures within the pile respond to observed changes in wind speed and wind direction exterior to the pile, suggesting that the wind is a major driver for gas transport in this pile. Gas concentration measurements in the Type I and Type III pile show no deviation from atmospheric concentrations suggesting that the rate of gas transport is fast relative to the rate of oxidation reactions. In the Covered pile modest depletions in O_2 concentrations have been observed below the till layer, indicating that the till layer provides a barrier to gas transport. O_2 depletion rates through the summer of 2008 are used to calculate a rate of sulfide oxidation. The calculated rate ranges from 1.7×10^{-11} to 4.1×10^{-11} kg O_2 m^{-3} s^{-1}. In comparison, humidity cell experiments on Type III rock from the Diavik site give average oxidation rates of approximately 2×10^{-12} kg O_2 m^{-3} s^{-1}.

Thermal data collected from 2007 to 2009 show freezing of the Type I and Type III piles each winter with a progressive decrease in observed winter temperatures. This trend suggests cooling of the piles. In the summer months the internal temperature throughout the piles continues to rise above 0 ^{o}C. The high permeability of the piles combined with the influence of the wind on gas transport led to these large temperature fluctuations. In the covered pile internal temperatures below the till cover remain near zero throughout the year, suggesting that the till layer moderates thermal transport. Above the till layer temperatures fluctuate in response to external temperatures, whereas within the till layer the temperatures drop below 0 ^{o}C in the

winter months but remain at 0 ^{o}C through the summer, suggesting that frozen water within the till layer is thawing.

Since construction of the test piles, two years have been well below average for rainfall totals (2007, 2009), whereas 2008 was slightly wetter than average. For the Type I and Type III piles outflow in 2009 was lower than in 2008; likely reflecting the much lower infiltration rate in 2009. Outflow for the Type III pile is much higher than the Type I pile, likely due to the artificial rainfall events conducted on the Type III pile in 2007. Covered pile outflow in 2009 also is much lower than 2008. Flow is reporting to a subset of the basal lysimeters in each of Type I and Type III piles. This behaviour is significant because it now provides the opportunity of examining trends in water chemistry for a flow path across the full height of the Type I and Type III test piles. A large scale field permeameter was constructed in 2009 (4 m x 4 m x 2 m). Estimates of matrix porosity as a proportion of total porosity are 5%, with a macroporosity of 22%. These estimates are consistent with the tests carried out in 2007 on a 1 m high permeameter. The saturated hydraulic conductivity for the 2 m high permeameter was approximately 6 x 10^{-3} m/s.

Effluent from the Type I and Type III basal drains contains high concentrations of ammonia, nitrite and nitrate, which are likely derived from residuals of blasting agents. The irregular concentrations and gradual dissipation of these by-products likely represents flushing along different flow paths. In both the Type I and Type III piles the pH rises and falls each year, possibly as a result of changes in the rates of sulfide oxidation reactions, and declines to below neutral for each pile. Sulfide oxidation in Type III rock is indicated by increased sulfate, release of acidity, depletion of alkalinity, and an increase in dissolved aluminum concentrations associated with dissolution of aluminosilicate minerals. Dissolved metal concentrations from the Type III basal drain effluent increase as the pH declines. Concentrations observed in 2009 are higher than observed in earlier years as the pH declines further each year. In the Type I basal drain effluent dissolved metal concentrations are significantly lower than in the Type III pile. Flow in the upper collection lysimeters is restricted to a few months in summer season. Effluent water quality from the upper collection lysimeters illustrates the difference in the Type I and Type III rock. Type I effluent has remained neutral since construction, whereas the Type III effluent annually falls below pH 4. Sulphate concentrations observed in Type III effluent are higher than the Type I, and alkalinity remains in Type I lysimeter but is completely depleted in

Type III. In the Covered pile, flow to the basal drains occurs throughout the winter, because the pile does not experience the same seasonal temperature cycle as the uncovered piles. As a consequence the pH remains low throughout the year, alkalinity remains low, sulfate concentrations consistently exceed 2000 mg L^{-1}, and dissolved metal concentrations are consistently high. In 2008, microbial populations in Type I and Type III test piles effluent were completely dominated by neutrophilic bacteria, T. thioparus and related species (Figure 2-25). In June 2009, increased numbers of acidophilic sulfur oxidizing bacteria were observed in all piles, and by September 2009 increased predominance of acidophilic iron oxidizers in the Covered and Type III piles was observed.

Instrumentation of the Type III full-scale waste rock dump will provide important information with respect closure planning at Diavik as well as provide the information necessary to complete the scale up characterization. Due to financial constraints drilling was postponed in 2009 and is tentatively planned for March 2010. Instrumentation is planned to include thermistors, gas sampling lines, tensiometers, soil moisture probes, and permeability instruments. Three attempts were made in 2009 to install instrumentation without drilling. The first two attempts were unsuccessful as the instrumentation was damaged during burial. The third attempt was made at the beginning of December 2009 by stringing a 150 m long instrument bundle horizontally at the base of the 50 m lift. This bundle includes gas lines and permeability samplers and was covered with approximately 0.5 m of crush to protect it during burial. Instrument survival will be assessed in the spring of 2010.

Preliminary scaling calculations based on time weighted load estimates, and volume and time based concentration estimates have been completed. Time weighted load estimates compare yearly geochemical loadings from the Type III humidity cell experiments to the Type III upper collection lysimeters and the Type III basal drains. Sulfur loadings calculated from the Type III humidity cells, based on mass of rock, surface area of rock, and mass of sulfur, are higher for the Type III upper collection lysimeters and the Type III test pile. Estimates based on the surface area of exposed sulfur provide a better estimate for the field-scale installations. Concentration values based on the time dependent loading rates derived from Type III humidity cells were used to estimate sulfur and metal concentrations for the Type III upper collection lysimeters. Initial calculations assume a constant residence time and a constant temperature. Estimates scaled on the basis of the mass of the rock and the mass of sulfur overestimate the dissolved concentration

observed in the field. Concentration estimates for sulfate and nickel scaled based on the surface area of exposed sulfur provide reasonable estimates of measured values, suggesting that scale-up calculations can provide reasonable estimates of sulfur and metal loadings in the field provided that the rock is adequately characterized at both scales.

Results from the Diavik Waste Rock Project have been presented at numerous Canadian and international conferences and published in various conference proceedings. One article has been published in a peer reviewed journal and several more are near completion and will be submitted in early 2010. The project has involved 11 graduate students from the three participating universities, including two that graduated in 2009, and has involved over 25 undergraduate students.

The Diavik Waste Rock Project research team is proposing to extend the research program for an addition 5 years beginning in 2010. A significant investment in research infrastructure at Diavik was made by the research partners including, Diavik, The Natural Science and Engineering Council of Canada, The Canadian Foundation for Innovation, INAP and MEND. This infrastructure represents a tremendous opportunity to continue to gain further insights into behaviour of the waste rock piles as the hydrology, thermal regime, and geochemistry evolve. Continuation of the project will; allow for a longer, richer data set to form the basis of scale up comparisons; provide additional full-scale data to be included in scale-up comparisons; further strengthen linkages between thermal, gas and water transport, and geochemical reactive transport aspects of the project; provide stronger support for closure planning for northern operations; and provide the opportunity to apply and evaluate sophisticated data interpretation and analysis techniques. Diavik has committed funding for the project extension and funding has been requested from INAP and MEND. It is anticipated that matching funding from NSERC will be requested in early 2010.

1 Introduction

1.1 Diavik Waste Rock Project

The Diavik Waste Rock Project is designed to evaluate the benefits of the proposed reclamation concepts for the Diavik Country Rock Stockpiles, and to evaluate techniques used to scale the results of laboratory studies to predict the environmental impacts of full-scale waste rock stockpiles. The Diavik Project includes laboratory testing of rock from the Diavik site using established, standardized testing procedures. Field lysimeters containing each rock type, constructed in duplicate, were installed at the Diavik site and are being monitored. Three large-scale test piles have been constructed. The test piles have been instrumented in detail and monitoring is underway.

The large-scale test piles consist of:

Type I pile: Type I rock with no cover ('best case' or baseline)

Type III pile: Type III rock with no cover

Covered pile: Type III rock with till (low permeability) and Type I rock (thermal) cover.

The Type I and Type III rock lysimeters and test piles simulate the extremes of the geochemical behaviour of the Diavik country rock, and provide valuable information to evaluate the approaches presently used to estimate solute loadings from waste rock stockpiles using small-scale testing procedures. The covered lysimeters and the covered test pile simulate the cover design proposed for the full-scale Country Rock Stockpiles.

This report provides an update of progress over the 2009 field season. Results and interpretations presented in this report are preliminary and will be updated as new data are collected and more comprehensive quality control and data analysis are performed. For more in-depth information on construction of field lysimeters and test-piles, and results from the experiments, the reader is referred to the Diavik Waste-Rock Research Project 2008 Progress report and a series of papers presented at the 2009 ICARD meeting. The publications are listed at the end of this report and have been made available on a CD distributed to the research partners.

2 Summary of Research Progress

2.1 Gas Transport

In 2007, an automated datalogging system was installed to measure gas pressures at 49 locations within, and 14 locations around, the Type III waste rock pile at 1 minute intervals (Figure 2-1; Amos et al; 2009). In addition, O_2/CO_2 concentrations are measured daily at 27 locations within the pile and wind speed and wind direction are recorded at 10 minute intervals using a wind monitor mounted approximately 7 m above the Type III pile. To facilitate frequent measurements (bi-weekly to monthly) of O_2/CO_2 concentrations at all sampling points in all three piles, a 22-port portable gas sampler, constructed at the University of Waterloo, is employed (Figure 2-2). Key features of this instrument are the AMI model 65 O_2 sensor, which is less sensitive to temperature fluctuations than previous instruments, and the automated two-point calibration of both the CO_2 and O_2. These features allow for small changes in gas concentrations to be detected.

Figure 2-1. Continuous gas pressure sampling system.

Figure 2-2. Portable 22 port O_2/CO_2 sampler and gas sample tubing bundle.

Measured differential gas pressures for gas sampling bundle 32N7 are shown in Figure 2-3. The data are shown as the differential pressure between the sampling point and the reference point on the top surface of the pile (32N2-0) and are plotted against the north wind vector. The pressure response at a given sampling point is a function of both wind speed and wind direction so that plotting the data against the wind vector provides a better understanding of the pressure response. Although the sampling points within sampling bundle 32N7 show a varied response to the wind, the general observation is that increases in wind speed result in greater pressures within the pile, particularly with the wind from the north (Figure 2-3). Sampling bundle 32N7 is located closer to the northern face of the pile.

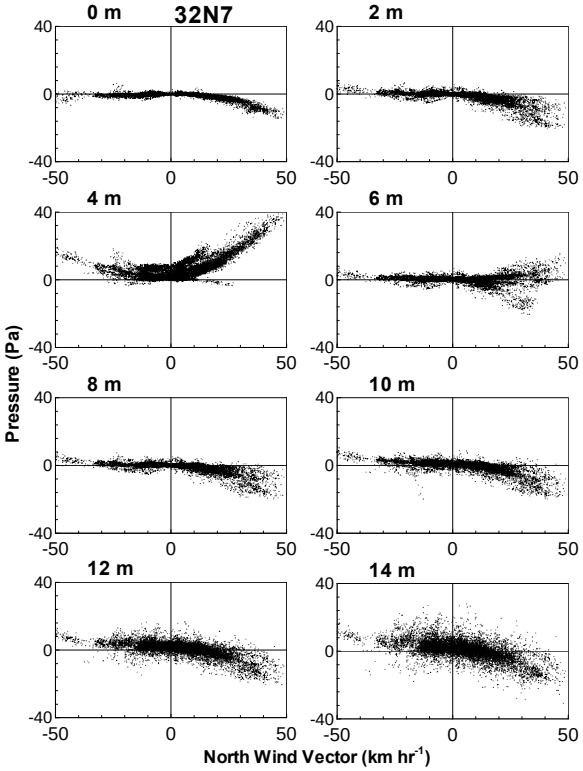

Figure 2-3. Measured differential pressures plotted against the north wind vector for the Diavik Type III test pile. Pressures are shown as the differential pressure between the sampling point and the reference point 32N2-0.

Figure 2-4 shows 2-D cross-sections of the differential pressure measurements along the north-south and east-west sampling transects on September 24 at 9:00 am with the winds speed at over 40 km/hr from the north. Although this is a relatively high wind speed, it is not uncommon at the Diavik site. With this strong wind from the north, high pressures develop along

the northern face of the pile, as is expected, although a low pressure zone at the toe of the northern face also develops. This anomaly is likely a result of a berm built close to the toe of the northern slope or other structural features around the test piles. Similarly, pressure gradients develop within the pile, although the irregularity of the pressure gradients suggests that the physical characteristics of the pile, and particularly the permeability distribution, may be major factors controlling the pressure distribution and air flow.

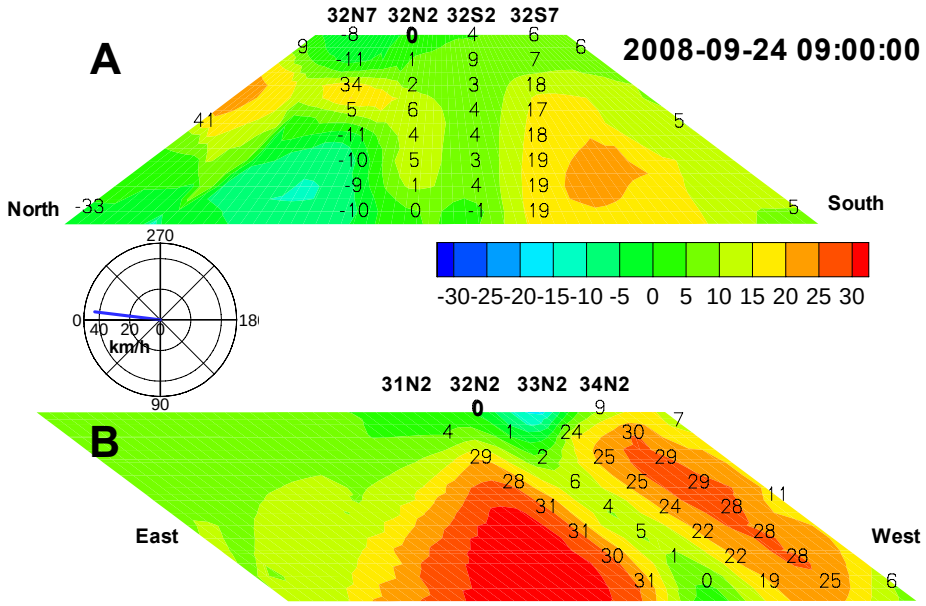

Figure 2-4. 2-D spatial profiles of differential pressure within and around the Type III test pile along with the prevailing wind conditions on September 24, 2008 at 9:00 am. Numbers on the contour plots represent measured data points spaced 2 m vertically. All differential pressures are referenced to point 32N2-0 (shown in bold). 2-D contours are obtained from 3-D kriging of all available data points. 2-D profiles shown are along North-South (A) East-West (B) sampling transects. Radial diagrams show wind direction in degrees plus wind speed along the radius in km/h.

In the Type I and Type III uncovered piles, O_2 and CO_2 concentrations have been measured monthly from May to November since the completion of the piles in September 2006. As of November, 2009, no deviation from atmospheric concentrations has been observed in either of the piles. This observation suggests that the rate of O_2 consumption through sulfide oxidation is slower than the O_2 transport rates.

In the Covered pile, gas concentrations were measured approximately monthly from June through October 2007, and twice per month from June to mid-November in 2008 and 2009. In most measured locations, gas concentrations remain near atmospheric; however, in a few

locations, the concentrations of O_2 are below atmospheric levels and the concentrations of CO_2 are elevated. An example of gas concentrations along sampling bundle C3W2 is shown in Figure 2-5. Gas concentrations remain near atmospheric from the surface to just below the till layer. At 7 to 8 m depth, O_2 concentrations decrease and CO_2 concentrations increase. Furthermore, at 7-8 m depth, the O_2 concentrations decrease with time and CO_2 concentrations increase with time. The observed changes in gas concentrations suggest that in certain locations within the pile, the rate of O_2 consumption through sulfide oxidation and the rate of CO_2 production through carbonate dissolution exceed the rate of gas transport.

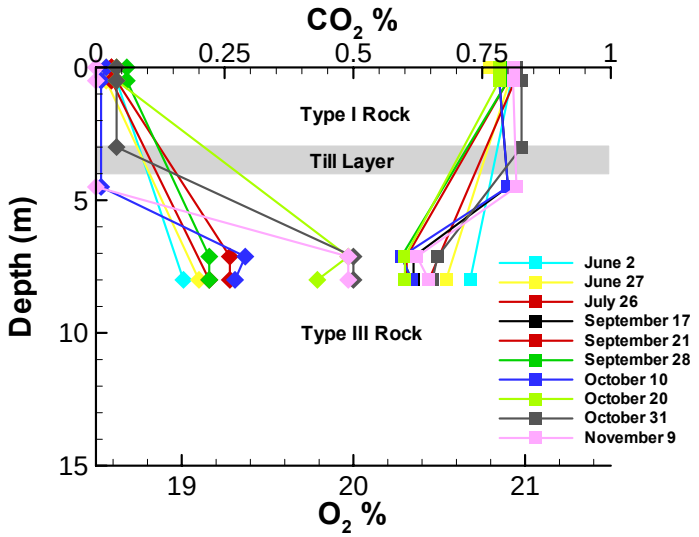

Figure 2-5. O_2 (squares) and CO_2 (diamonds) concentrations along sampling bundle C3W2 for June to Novemeber, 2008.

The temporal trends in O_2 concentrations are shown in greater detail for the three sampling locations within the Covered pile Type III core that showed depletions in O_2 concentrations and increases in CO_2 concentrations (Figure 2-6). For each of these locations, there is a period of decreasing O_2 concentrations starting in early June (≈day 0) and going to late august (≈day 110). Assuming a linear decrease in O_2 concentrations during this period, the rate of O_2 depletion ranges from 9.1×10^{-11} to 3.8×10^{-10} kg O_2 m^{-3} s^{-1} (Table 2-1). Assuming that diffusion is the dominant O_2 transport mechanism, the maximum O_2 transport rates can be estimated based on the lowest observed concentrations. Diffusion rates range from 2.2×10^{-12} to 7.7×10^{-12} kg O_2 m^{-2} s^{-1}. Therefore, for the period with the lowest observed O_2 concentrations, the total oxidation rate, equal to the sum of O_2 depletion rates and the influx of O_2 through

diffusion, range from 9.9 x 10^{-11} to 3.9 x 10^{-10} kg O_2 m^{-3} s^{-1} for the three sampling points analyzed. Humidity cell experiments on Type III rock from the Diavik site give average oxidation rates of approximately 3 x 10^{-11} kg O_2 m^{-3} s^{-1}. Further analysis is required to investigate the relationship between the lab measured rates and those determined from the gas concentration measurements.

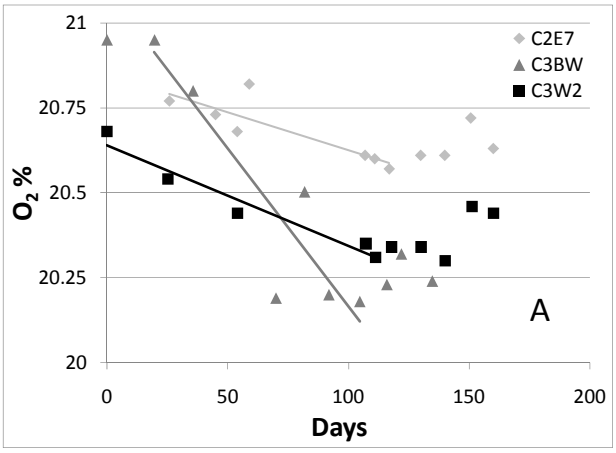

Figure 2-6. O_2 concentrations with time for selected sampling locations C2E7-4.5, C3BW-24, and C3W2-8. Lines are linear regressions of data points during the period of decreasing O_2 concentrations. Day '0' is June 2, 2008.

Table 2-1. Oxidation rate calculation results from Covered pile O_2 data.

	C2E7	C3BW	C3W2
O_2 depletion rate (kg O_2 m^{-3} s^{-1})	9.1 x 10^{-11}	3.8 x 10^{-10}	1.2 x 10^{-10}
Maximum O_2 diffusion rate (kg O_2 m^{-2} s^{-1})	7.7 x 10^{-12}	2.2 x 10^{-12}	4.6 x 10^{-12}
Total oxidation rate (kg O_2 m^{-3} s^{-1})	9.9 x 10^{-11}	3.9 x 10^{-10}	1.3 x 10^{-10}

In 2009 and automated gas pressure and gas concentration sampling system was installed on the Covered pile (Figure 2-7). This system is similar to that previously installed on the Type III pile and includes gas pressure measurements at 105 sample locations within the pile and 14 locations on the surface of the pile at 1 minute intervals. Gas concentration measurements are taken at all 105 internal locations daily. The extensive data set collected from this system is currently being evaluated.

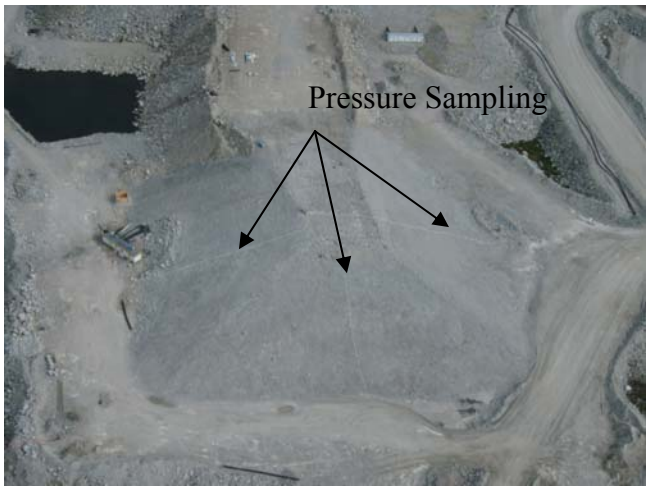

Figure 2-7. Arial view of Covered test pile showing surface pressure sampling conduit; part of the automated pressure and gas sampling system installed in 2009.

2.2 Thermal Regime

Internal temperatures in the uncovered test piles show a cooling trend. This is demonstrated for Face 4 of the Type III pile in Figure 2-8. These plots show progressively lower temperatures in January of each year. Figure 2-9 shows temperature versus time plots for individual thermistor strings on Face 1 of the Type I and Type III piles. These plots show that temperatures from 1 to 12 m depth drop well below 0 ^{o}C in the winter of each year and also demonstrate the cooling trend, with lower temperatures observed each year. In the summer months temperatures along the length of the thermistor string exceed 0 ^{o}C, demonstrating that the piles continue to thaw each year. The continued annual freezing and thawing of the piles is due to the high rate of thermal transport in the pile, as a result of the high permeability and gas transport rates observed.

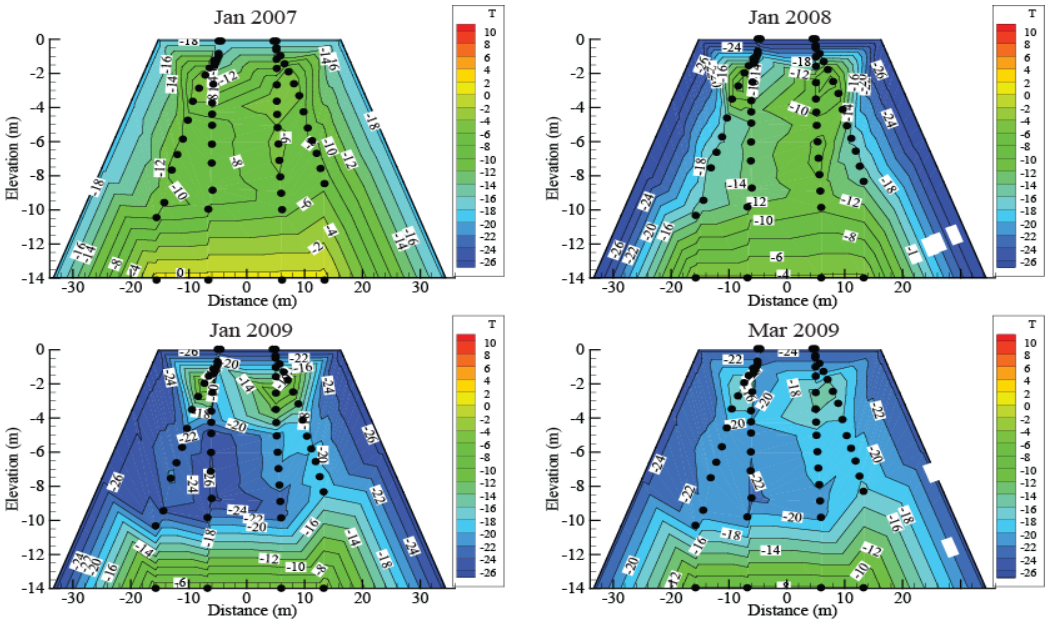

Figure 2-8. Contour temperature in Jan at face 4 type III pile since 2007.

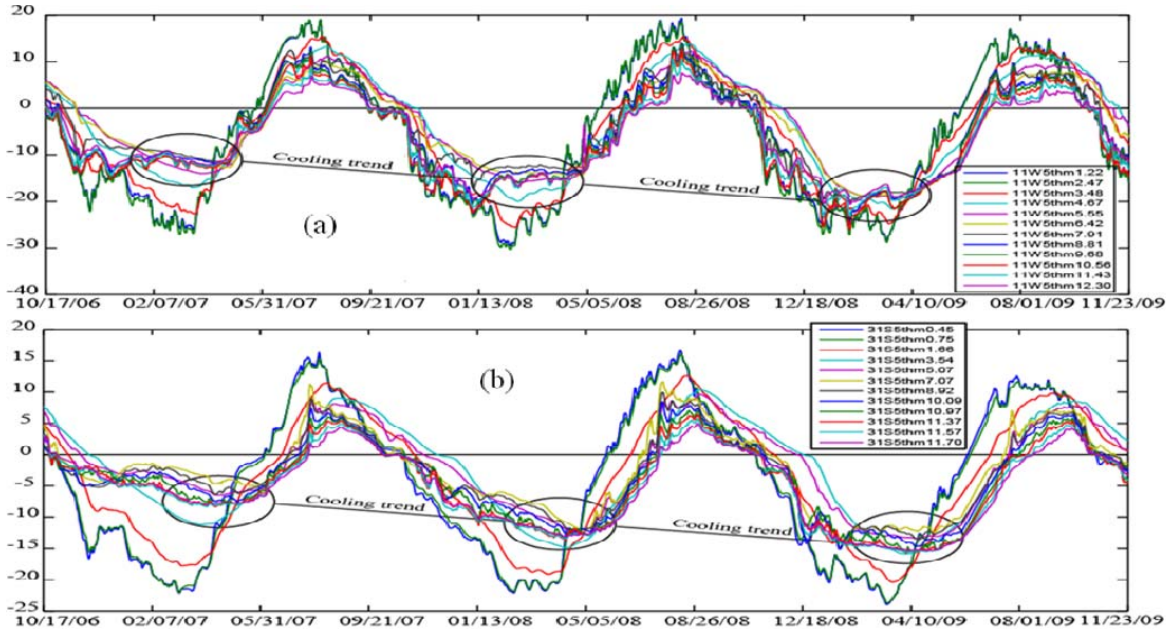

Figure 2-9. Thermistor string at face 1 Type I (a) and Type III (b) pile shows cooling trend.

In the covered pile a cooling trend has not been observed (Figure 2-10). Below the till layer temperatures remain relatively constant throughout the year as the till layer limits gas and thermal transport. Above the till layer temperatures cycle annually under the influence of the external temperature (Figure 2-11). Within the till layer the temperatures drop below 0 ^{o}C in the winter months but remain at 0 ^{o}C through the summer suggesting that frozen water within the till layer is thawing.

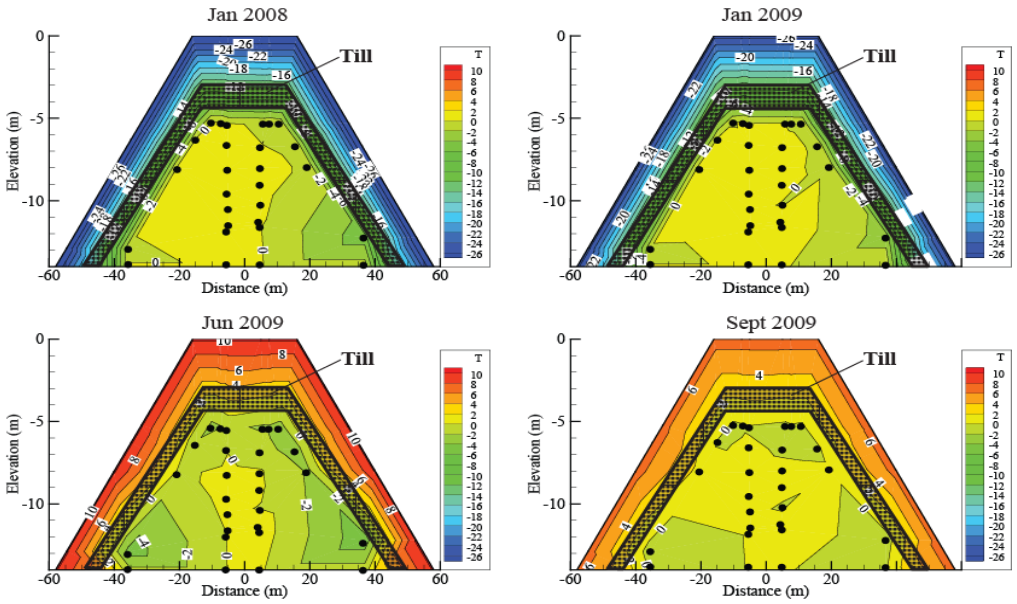

Figure 2-10. Contour temperature at face 4 covered pile since 2007.

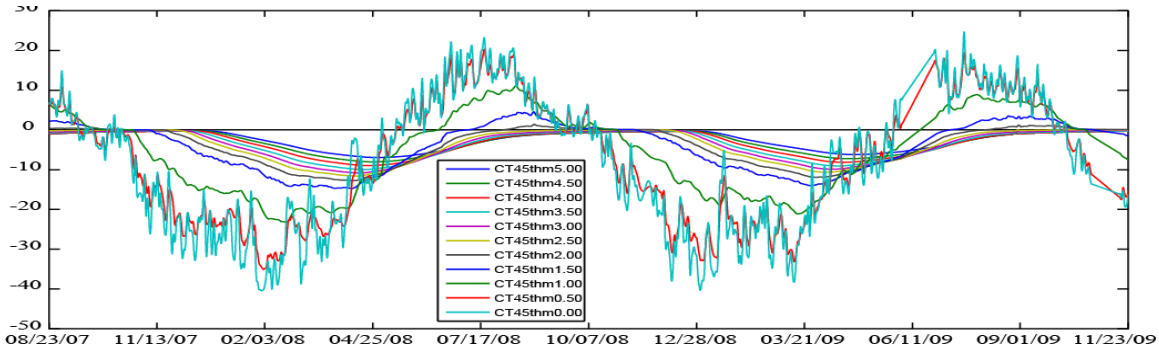

Figure 2-11. Thermistor string drilled from the top of covered pile shows an active layer of 3m at this string since 2008.

2.3 Hydrology

Precipitation in 2009 (excluding snowfall) was approximately one half of the average annual rainfall at Diavik (81 mm versus 154 mm; Figure 2-12). Since construction of the test piles, two years have been well below average for rainfall totals (2007, 2009), while 2008 was slightly wetter than average. Although there were frequent small rainfall events in 2009, no large events occurred in 2009 (unlike the pattern in 2008).

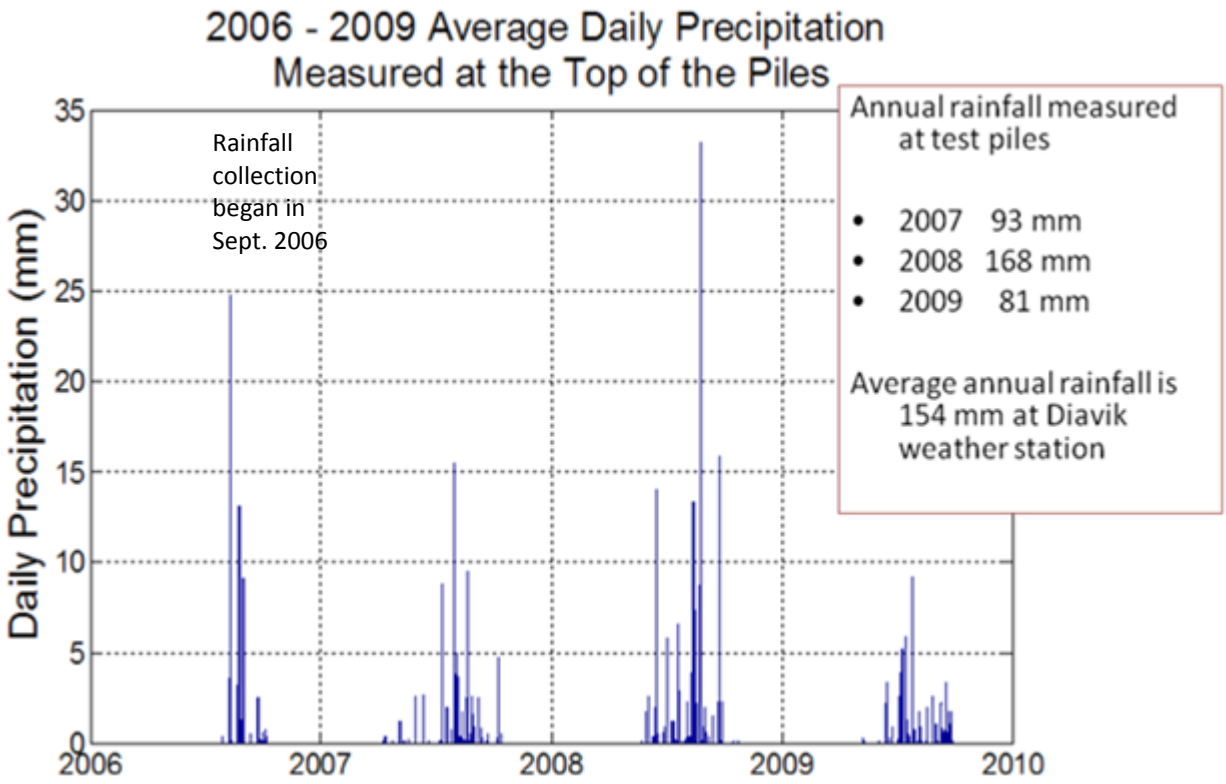

Figure 2-12. Average daily precipitation at top of test piles.

There was outflow from the basal drains in each of the three test piles (Figure 2-13, Figure 2-14). For the Type I pile, which has experienced only natural rainfall events, the outflow in 2009 (10,000 L) was substantially lower than that in 2008 (70,000 L); likely reflecting a much lower to negligible infiltration rate at the top surface of the test pile in 2009. For the Type III pile, the outflow was also smaller in comparison to the previous year (110,000 L versus 130,000 L), but still much higher than the Type I pile, likely reflecting a residual drain down effect from the artificial rainfall events applied on this pile in September 2007. At the Covered pile, outflow

in the late summer and fall of 2009 was also much lower than that which occurred in 2008 (Figure 2-14).

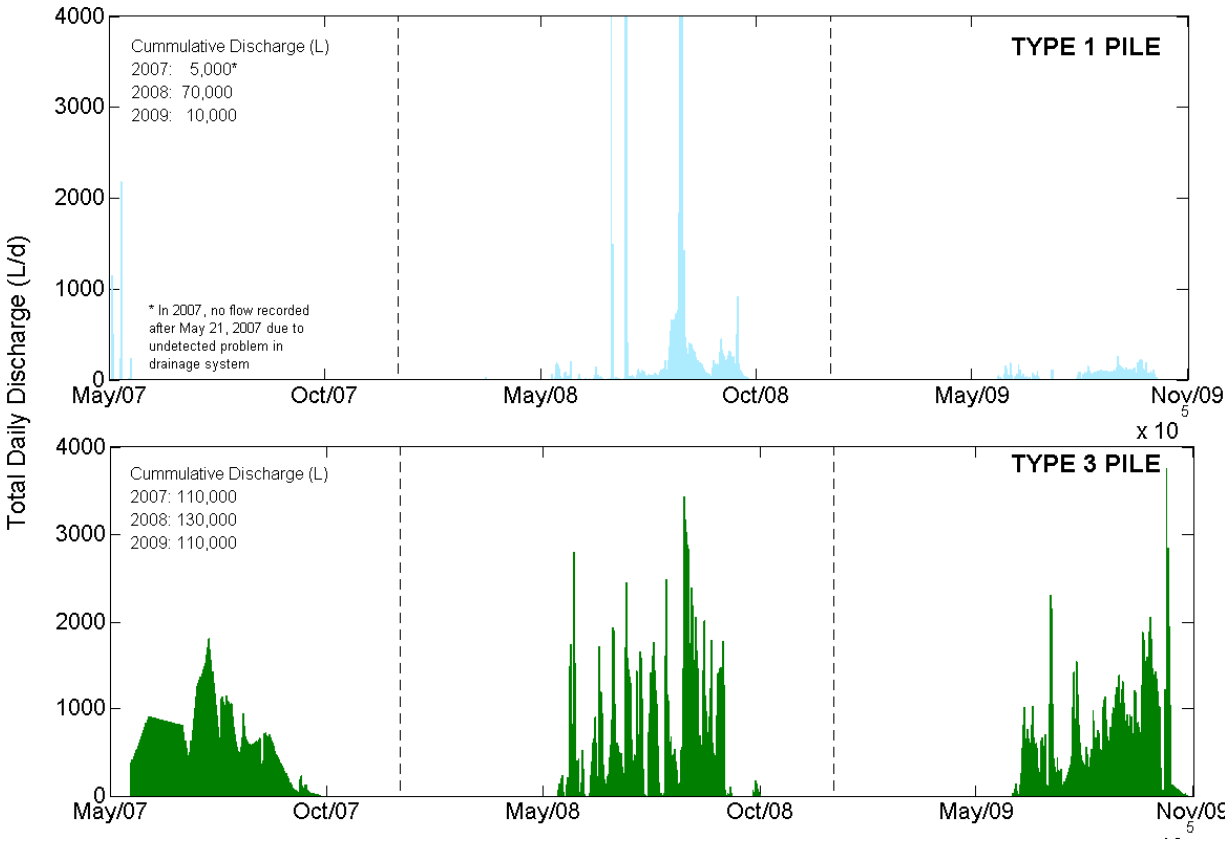

Figure 2-13. Total daily outflow volume at Type I and Type III basal drains.

Flow is reporting to a subset of the basal lysimeters in each of Type I and Type III piles (Figure 2-15; Figure 2-16). At the Type III pile, flow from the central basal lysimeters in 2009 (250 L) was much less than the reporting to the central lysimeters in 2008 (2200 L), however, flow did initiate in 2009 in a subset of the basal lysimeters under the batter of the Type III pile. Small amounts of flow also reported to the basal lysimeters located beneath the Type I pile (150 L in the central zone, 60 L in a batter lysimeters). This behaviour is significant because it now provides the opportunity of examining trends in water chemistry for a flow path across the full height of the Type I and Type III test piles.

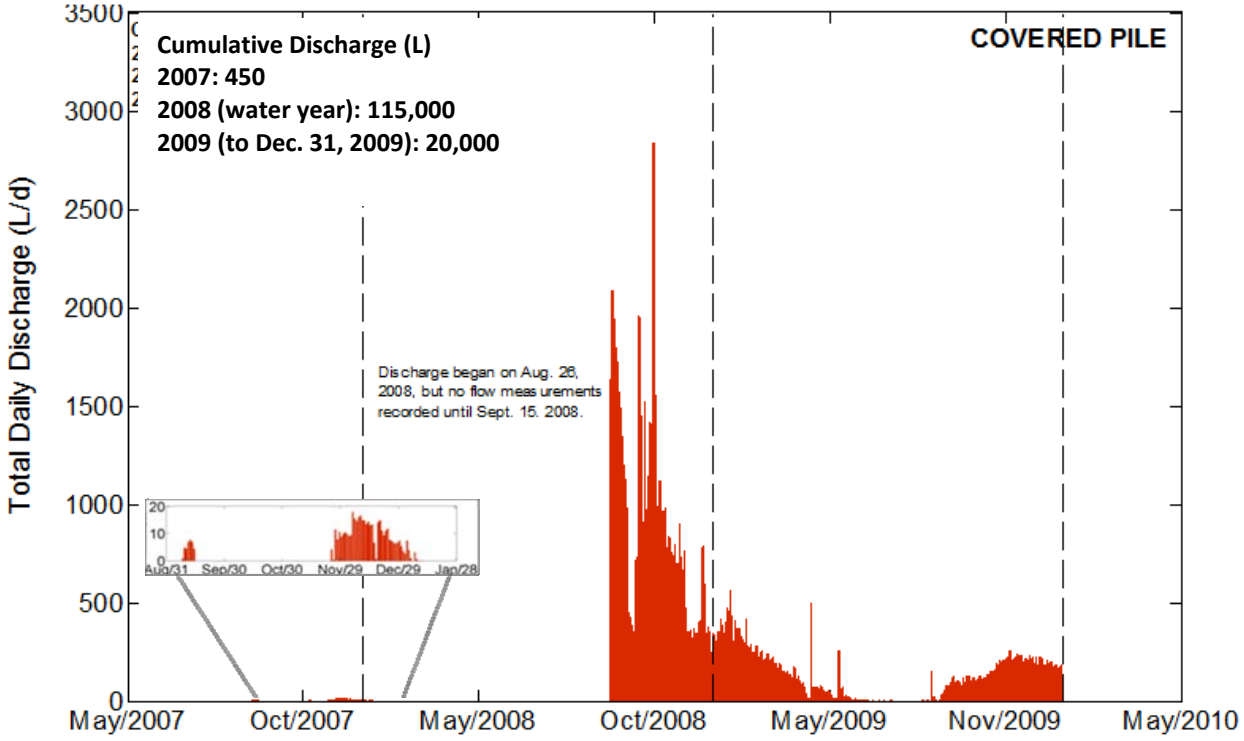

Figure 2-14. Total daily outflow volume at Covered pile basal drain.

TDR data has been collected and processed to document the seasonal variation in moisture content within each of the test piles. Results are qualitatively similar to the previous two years. Moisture content data for 2009 for the till layer within the covered pile has recently been processed and is now being evaluated to examine the movement of wetting fronts across the till layer.

A large scale field permeameter (Figure 2-17) was constructed in 2009 (4 m x 4 m x 2 m) to obtain a comparison to the hydraulic properties of waste rock obtained in 2007 in a permeameter with the same lateral dimensions, but a height of 1 m. Estimates of matrix porosity (Figure 2-18) as a proportion of total porosity are 5%, with a macroporosity of 22% (total porosity of 27%). These estimates are consistent with the tests carried out in 2007. The saturated hydraulic conductivity for the 2 m high permeameter was approximately 6 x 10^{-3} m/s. The field permeameter, filled with Type I rock, will now be used as another collection lysimeter to focus on water chemistry questions.

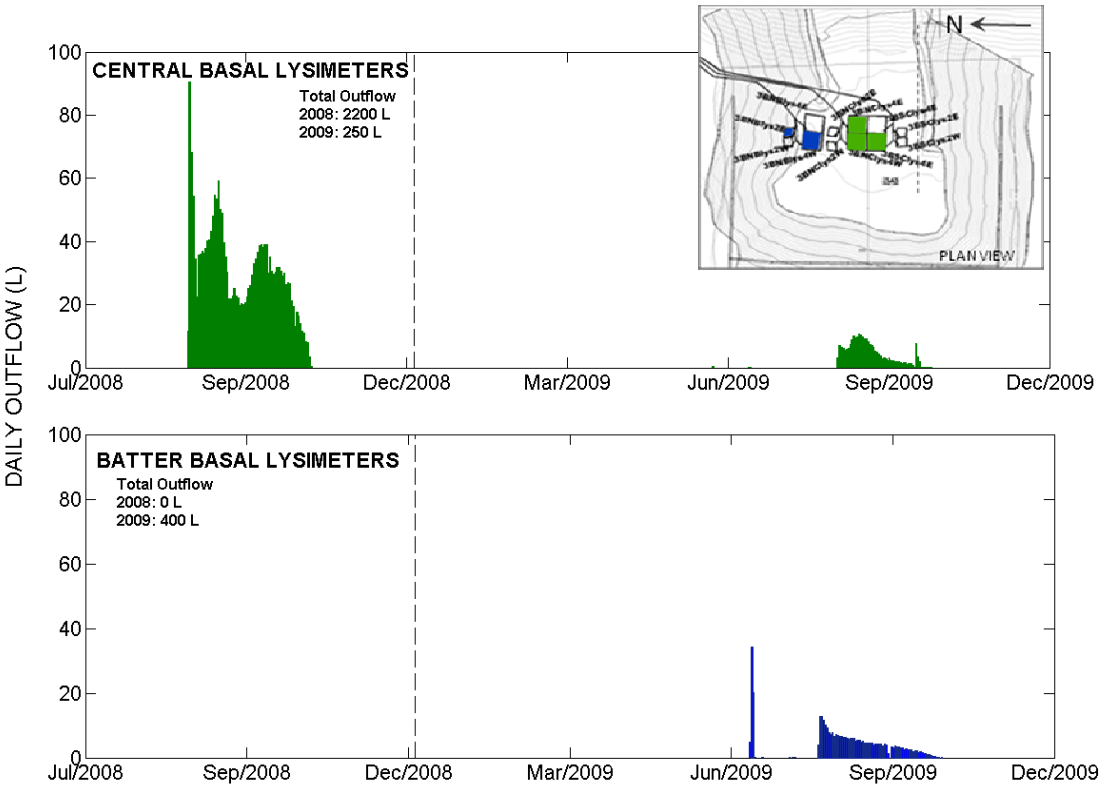

Figure 2-15. Total daily outflow volume at Type III basal lysimeters.

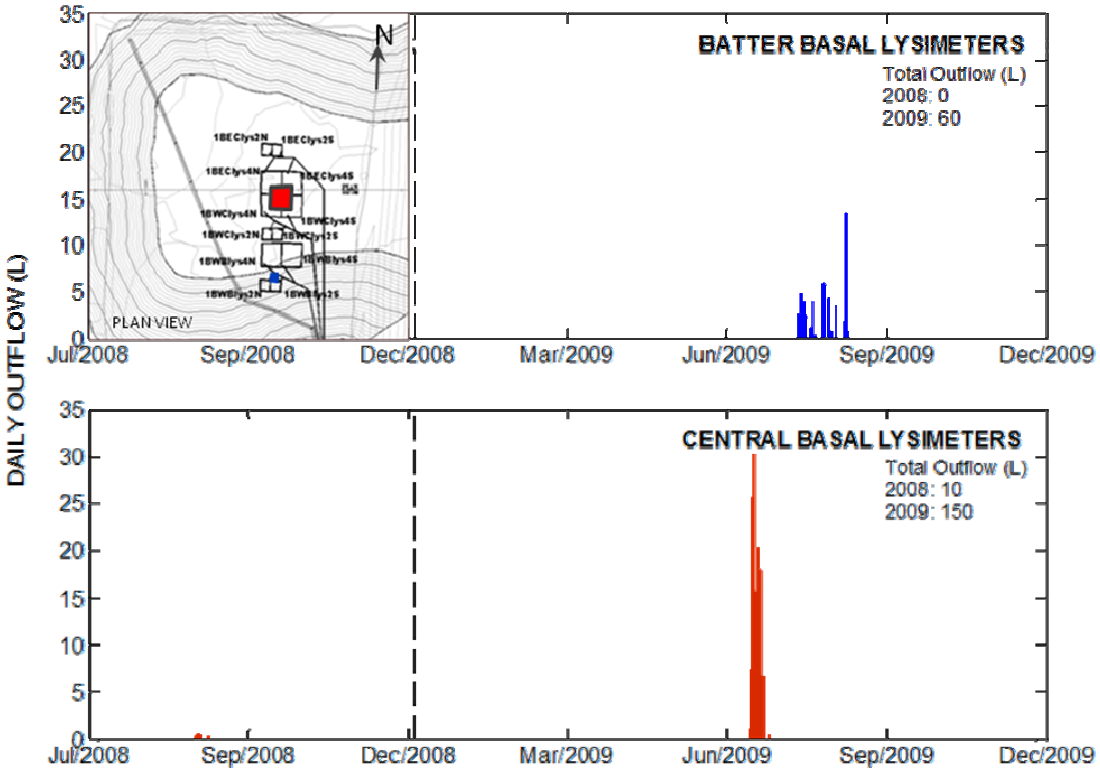

Figure 2-16. Total daily outflow volume at Type I basal lysimeters.

Figure 2-17. Construction of 32 m^3 field permeameter experiment.

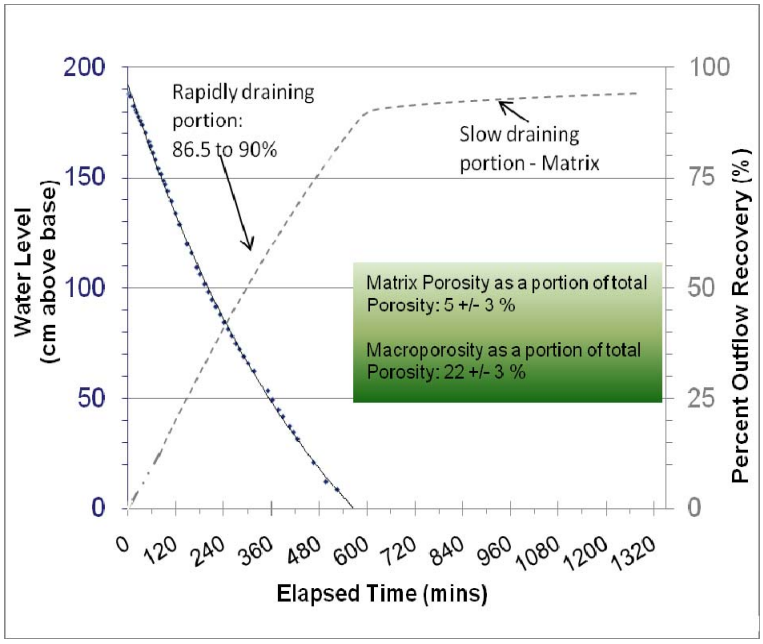

Figure 2-18. Results of 32 m^3 field permeameter experiment.

Monitoring continued to record the movement of tracers released onto the surface of the Type III test pile in September 2007 (Figure 2-19). A definitive tracer arrival in the basal drain was detected in September 2009 (chloride and bromide). Data are being processed to estimate

solute velocities, using the TDR and temperature data to determine the time window under which free water can move downward through the pile. Note the tracer was first detected in several of the basal lysimeters in 2008, and again in 2009 (Figure 2-20). Tracer arrival at the bottom of the Type III pile is currently being correlated with tracer concentrations recorded in the soil water solution samplers internal to the test pile.

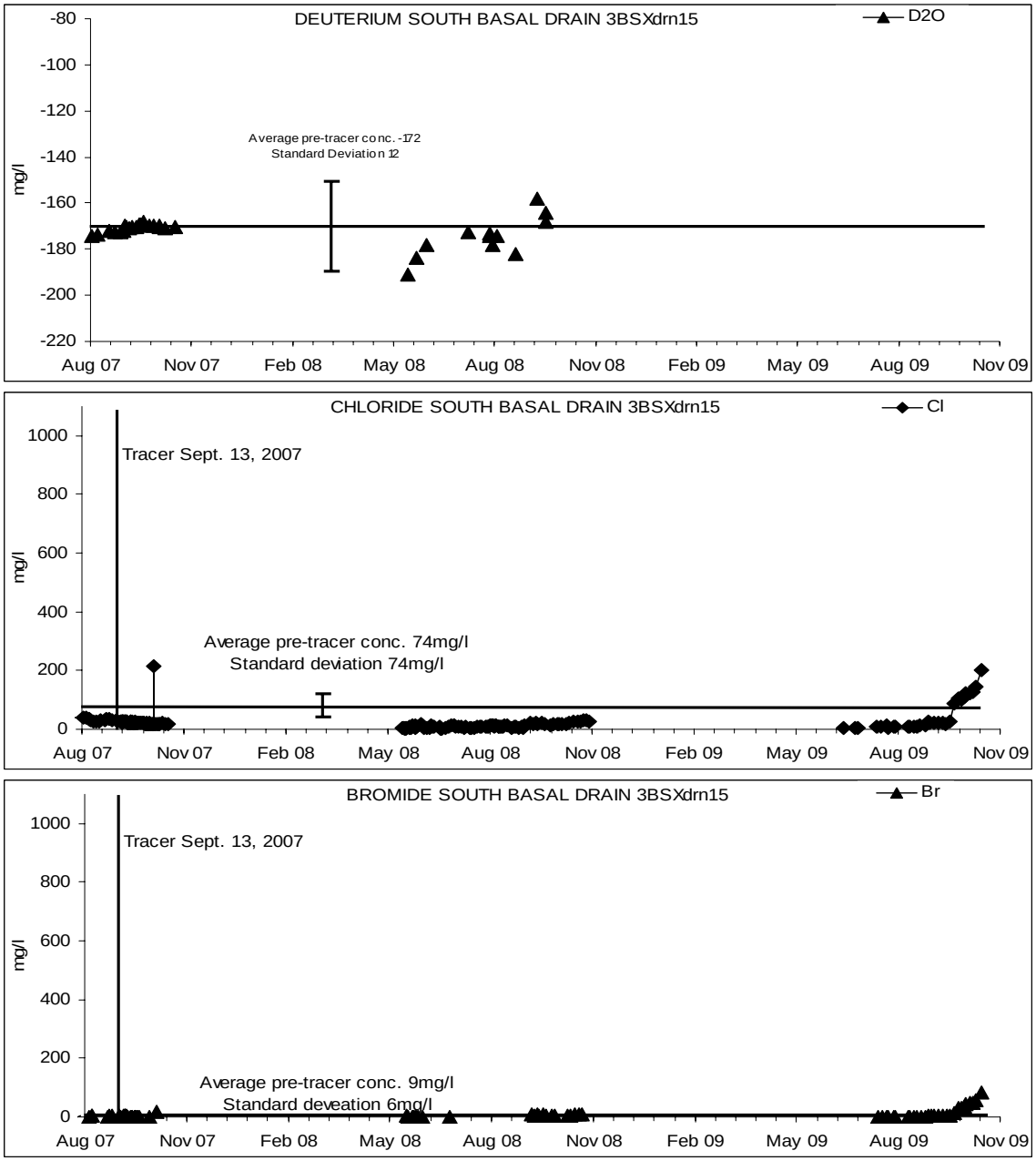

Figure 2-19. Tracer breakthrough at Type III basal drain.

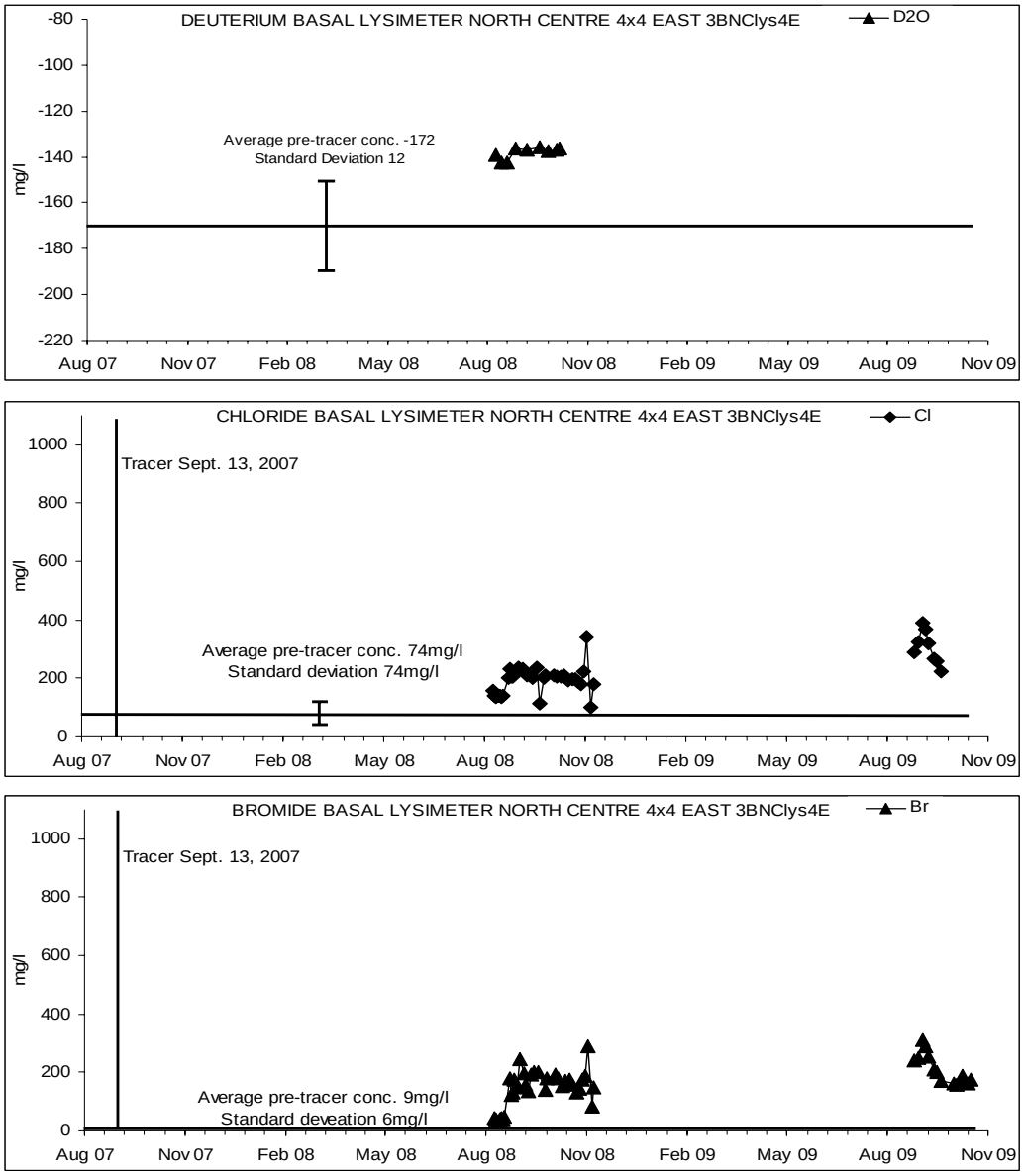

Figure 2-20. Tracer Breakthrough at Type III north centre 4 m by 4 m lysimeter.

2.4 Geochemistry and Microbiology

Effluent from the Type I and Type III basal drains contains high concentrations of ammonia, nitrite and nitrate, which are derived from residuals of blasting agents (Figure 2-21). Other by-products of blasting are chloride, derived from perchlorate, which is used as an accelerant in blasting materials, and sulfate, derived from oxidation of sulfide minerals during

blasting. The release of blasting by-products can be used as an indicator of the first flush of water through the pile, while irregular concentrations and gradual dissipation of these by-products likely represents flushing along different flow paths.

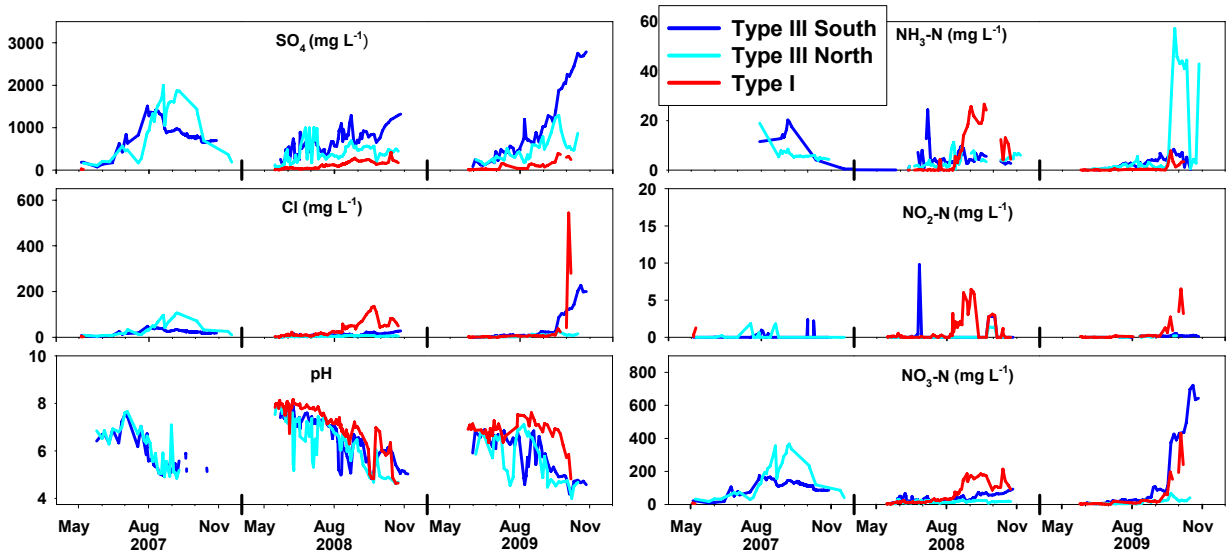

Figure 2-21. Type I and Type III basal drains general geochemistry and blasting residuals.

In both the Type I and Type III piles pH rises and falls each year, likely as a result of changes in the sulfide oxidation reaction rates (Figure 2-21). The pH falls more rapidly and to lower values in the Type III pile than in the Type I pile, however, by the end of the season the pH in both piles has declined below neutral. Sulfide oxidation in Type III rock is indicated by increased sulfate concentrations, exceeding 1000 mg L^{-1} each year. Sulfate in the north and south drains are similar, although slightly higher in south drain. As a result of sulfide oxidation, effluent from the Type III north and south drains become acidic early each year. The release of acidic water is accompanied by the depletion of alkalinity and an increase in dissolved aluminum concentrations, exceeding 5 mg L^{-1} in 2009 (Figure 2-22). This increase is associated with the dissolution of aluminosilicate minerals, which is enhanced at low pH. Aluminosilicate dissolution also releases cations such as K, Mg, Ca.

Dissolved metal concentrations in the Type III basal drain effluent increase as the pH declines, with high concentrations of nickel, exceeding 3 mg L^{-1}, cobalt reaching 0.5 mg L^{-1}, zinc up to 1 mg L^{-1}, and cadmium exceeding 5 µg L^{-1}, observed each year. Concentrations observed in 2009 are higher than observed in previous years. The dissolved metal concentrations in the

Type I basal drain effluent were significantly lower than in the Type III with concentrations of nickel less than 1.4 mg L^{-1}, cobalt less than 0.3 mg L^{-1}, cadmium less than 0.01 µg L^{-1}, and zinc below 1.5 mg L^{-1} (Figure 2-22).

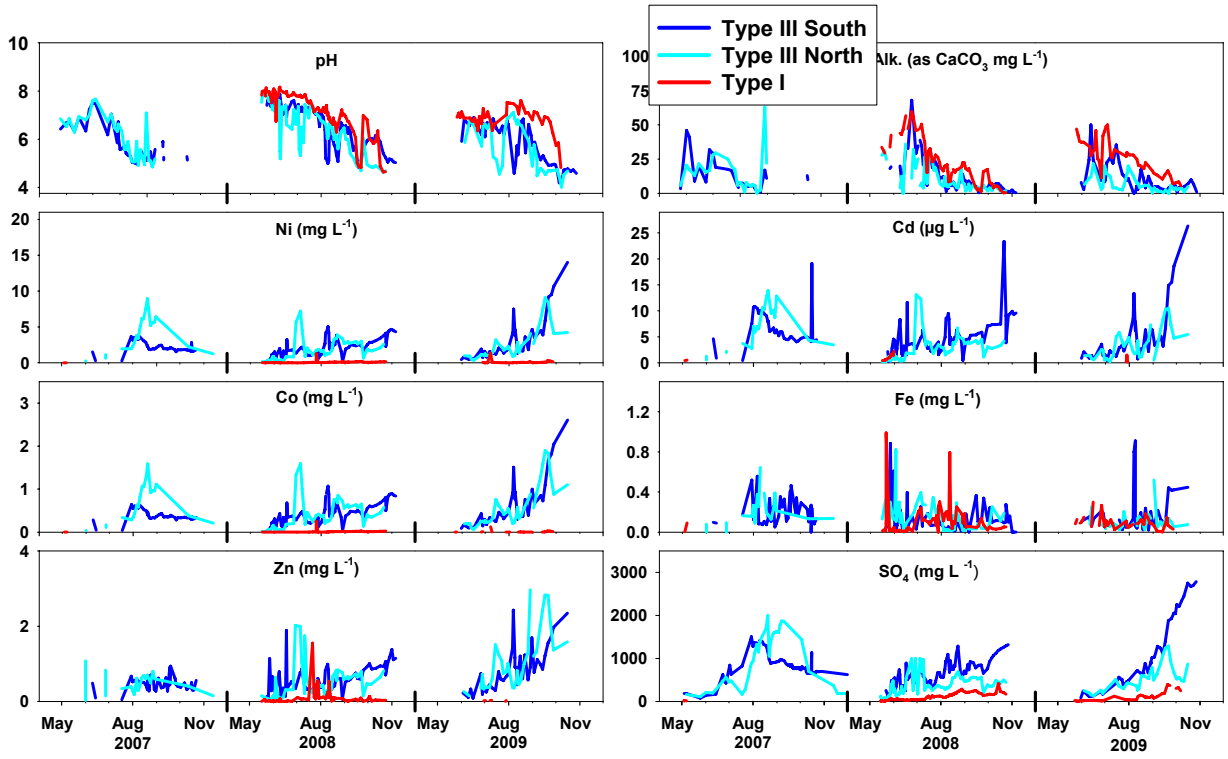

Figure 2-22. Type I and Type III basal drains geochemistry including major ion and metals.

The Covered pile does not experience the same amplitude in the temperature cycles, in contrast to the seasonal cycles observed in the uncovered piles Type I and Type III piles. As a result the Covered pile basal drain flows throughout the year (Figure 2-23). Alkalinity was depleted in late 2007 and has remained low since then. The pH remains below 5, sulfate concentrations consistently exceed 2000 mg L^{-1}, and increased concentrations of dissolved metals persist, including nickel above 5 mg L^{-1}, zinc exceeding 2 mg L^{-1}, cobalt in excess of 1 mg L^{-1}, and cadmium above 20 µg L^{-1} (Figure 2-23).

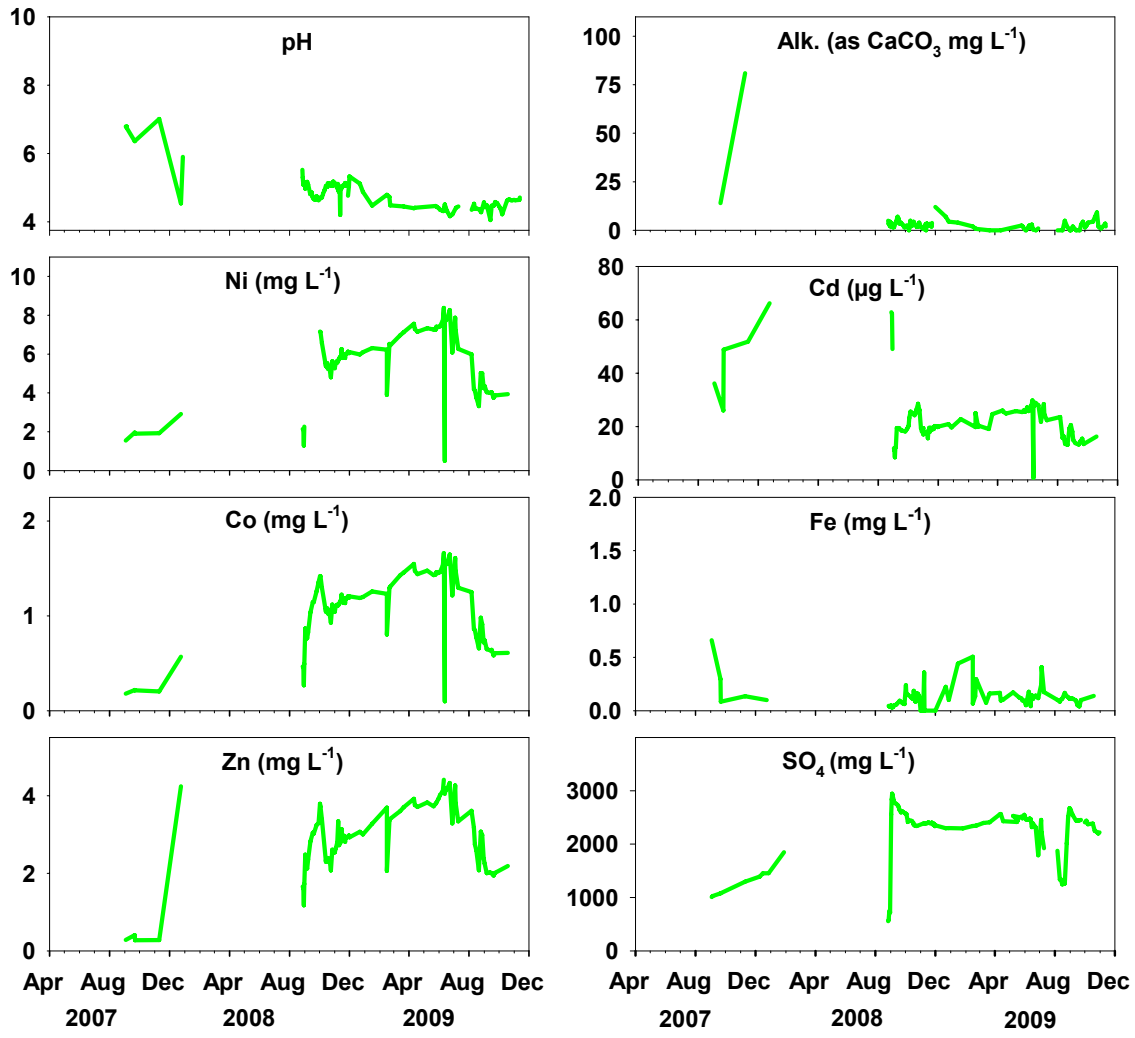

Figure 2-23. Covered pile basal drain geochemistry.

Flow in the upper collection lysimeters is more episodic than the basal drains in the test piles, with most flow occurring in a few months in summer season (Figure 2-24). Effluent water quality from the upper collection lysimeters illustrates the difference in the Type I and Type III waste rock. Type I effluent has remained neutral since construction, whereas the Type III effluent annually falls below pH 4. In addition, increased sulfate concentrations associated with sulfide oxidation are observed in Type III effluent compared to the Type I effluent, and alkalinity remains in the Type I lysimeter but is completely depleted in the Type III lysimeter.

Microbial enumerations conducted on samples collected in 2008 indicated that microbial populations in Type I and Type III test piles were dominated by neutrophilic bacteria, T. thioparus and related species (Figure 2-25). No significant populations of acidophilic sulfur

oxidizers or acidophilic iron oxidizers were detected. Succession of bacterial species was evident in 2009, with increased numbers of acidophilic sulfur oxidizing bacteria observed in all piles in June, and increased predominance of acidophilic iron oxidizers in the Covered and Type III piles by September of 2009 (Figure 2-26).

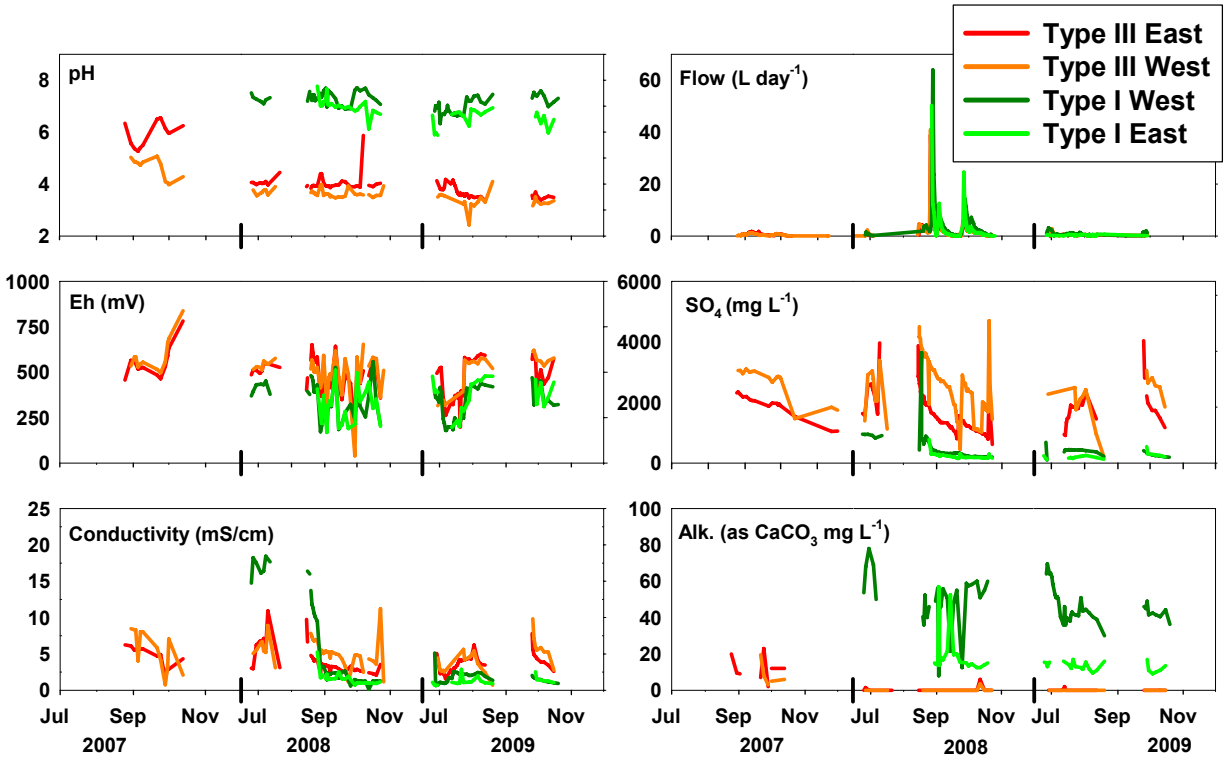

Figure 2-24. Upper collection lysimeter geochemical parameters and flow data.

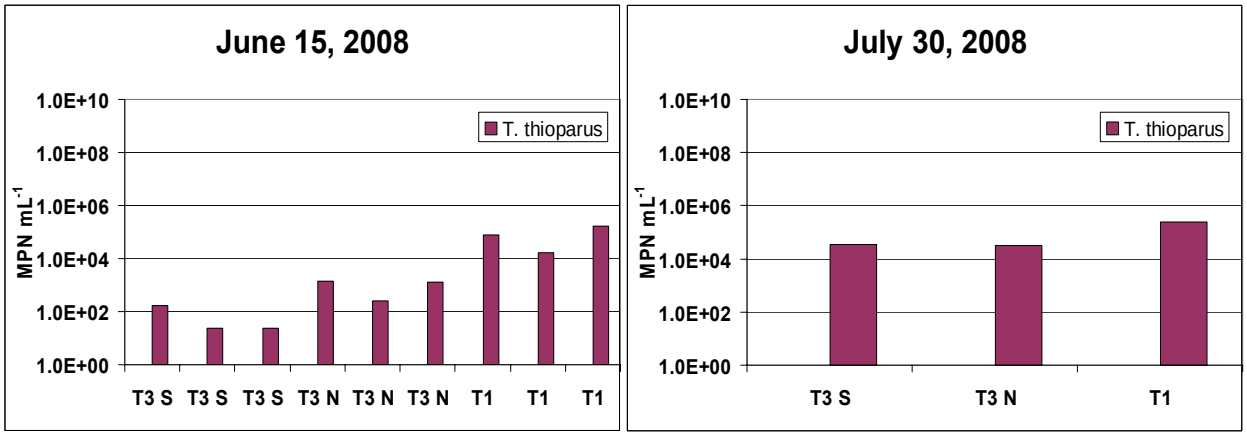

Figure 2-25. Type I and Type III pile microbial enumerations for 2008 – effluent water samples.

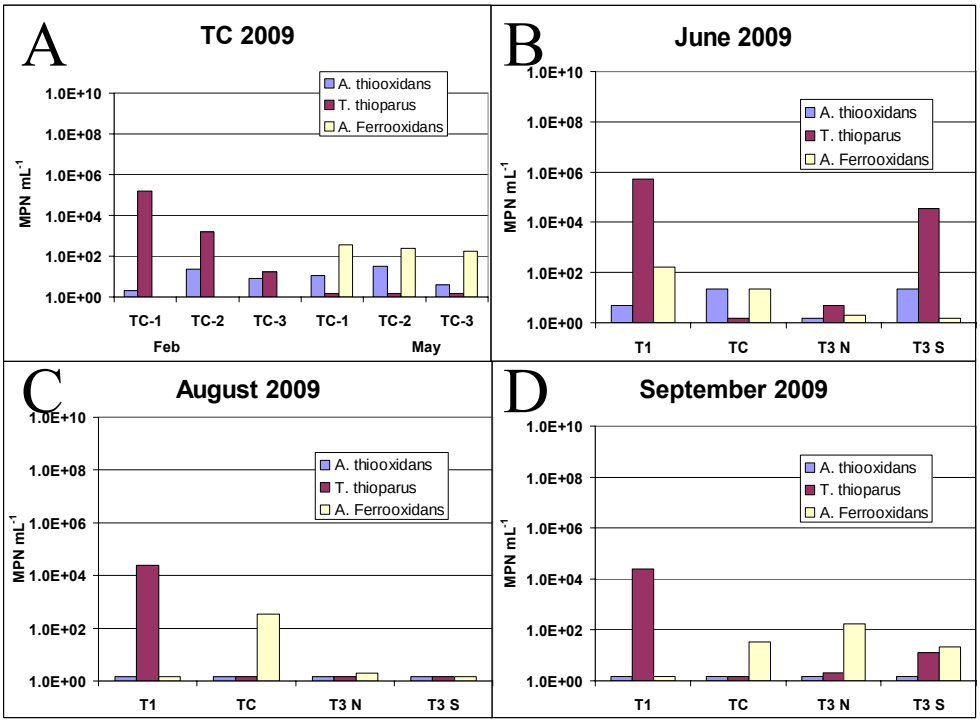

Figure 2-26. A: Covered pile microbial enumerations in 2009. B-D: Type I, Type III and Covered pile microbial enumerations in June (B), August (C) and September (D) 2009 – effluent water samples.

2.5 Full Scale Installations

Instrumentation of the Type III full-scale waste rock dump will provide important information with respect closure planning at Diavik as well as provide the information necessary to complete the scale up characterization from small (< 1 kg) samples to the full-scale pile. Due to financial constraints drilling was postponed in 2009 and is currently tentatively planned for March 2010. Instrumentation is planned to include thermistors, gas sampling lines, tensiometers, soil moisture probes, and permeability instruments.

In 2009, three attempts were made to install instrumentation in the full-scale Type III waste rock pile without drilling. The first attempt was along a 50 m high tip face of the Type III dump. Due to difficulties in stringing the instrument lines down the 50 m high slope, damage sustained during burial of the instruments, and subsequent damage by working mining equipment, no instruments survived this installation. A second attempt was made by stringing a 120 m long instrument bundle horizontally extending from the base of a 50 m lift in the Type III dump (Figure 2-27). These instruments were left uncovered and buried when end dumping

resumed from the top of the dump. This method proved to be too harsh for the instruments and none survived.

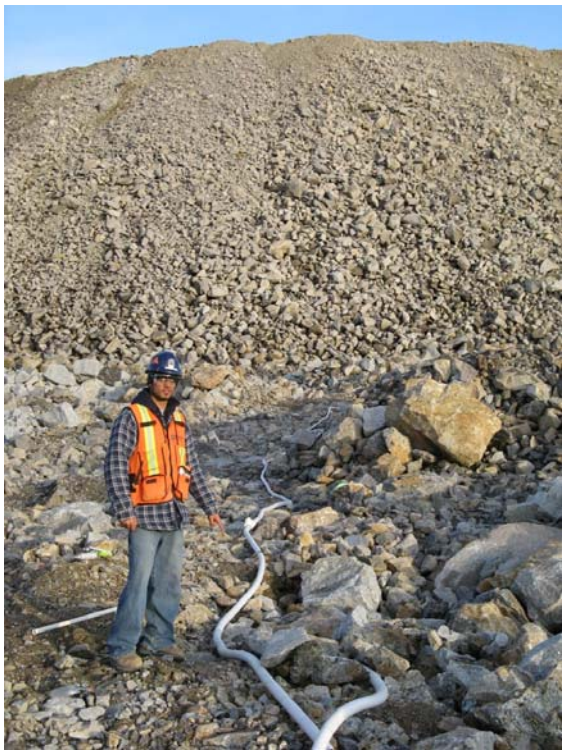

Figure 2-27. Horizontal instrument installation in full-scale Type III dump.

A third attempt was made at the beginning of December 2009 by stringing a 150 m long instrument bundle horizontally at the base of the 50 m lift. The length of the bundle includes an 80 m long lead to clear the planned roadway so that approximately 70 m of the bundle will be buried within the dump. This bundle includes only gas lines and permeability samplers and was covered with approximately 0.5 m of crush to protect it during burial. Burial of this line is in progress and instrument survival will be assessed in the spring.

3 Scale-up Calculations

Several methods can be used to scale geochemical loading rates from small-scale laboratory experiments to large-scale field experiments and ultimately to full-scale waste rock piles. Here we present preliminary scaling results based on time weighted load estimates, and volume and time based concentration estimates. Future concentration estimates will include more

refined estimates of water flow and temperature. In addition, reactive transport models will be used to simulate spatially and temporally distributed loadings with temperature corrections and gas transport constraints.

3.1 Time Weighted Load Estimates

Several humidity cell experiments have been underway, in both room temperature and cold room environments and for each of the Type I, Type II, and Type III rock classifications, for more than 3 years (Figure 3-1). Geochemical loading estimates derived from these experiments, including sulfate release rates and metal release rates, form the basis of the scale-up calculations (Figure 3-2). Material properties, including sulfur content and grain size, have been determined to provide a basis of comparison to field experiments.

Figure 3-1. Room temperature humidity Cell Experiments

For both the upper collection lysimeter experiments and the test piles the Type III installations provide the best data sets for scale-up comparisons. This is because of the additional volume of water applied to these experiments through artificial rainfall. For each of the Type III humidity cells, the Type III upper collection lysimeters, the Type III basal drains, and the Type III basal lysimeters, yearly sulfur loads are calculated using the measured sulfur concentrations and the measured water volumes from each of the experiments. The sulfur loads are then normalized to the mass of the rock, the surface area of the rock, the mass of sulfur in the rock, and estimated surface area of the sulfur (Table 3 1). For the field installations, rock masses are

estimated based on as-built drawings. For the Type III basal drains two loading estimates are provided; one uses the rock mass of the entire pile and the second uses the rock mass of only the batters of the pile. This difference reflects the assumption that flow to the basal drains is from the entire pile *versus* the assumption that flow is only derived from the batters of the piles.

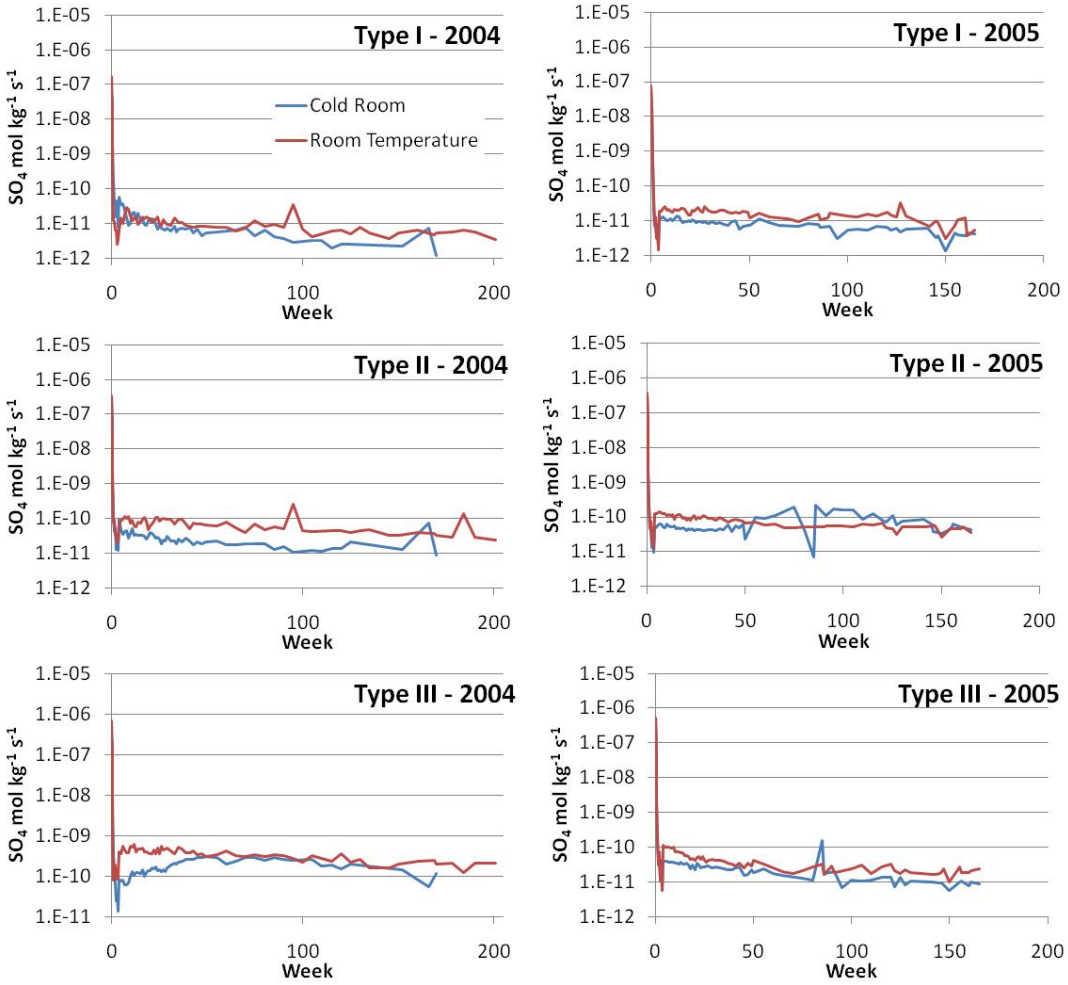

Figure 3-2. Average sulfate release rates from Type I, II and III rock collected in 2004 and 2005 for both cold room and room temperature experiments.

The surface area of the rock is estimated based on surface area measurements performed on humidity cell charges and comparison of grain-size analysis of both humidity cells and field scale experiments. Comparison of the grain-size results from the humidity cells and the material from the Type III test pile indicate that the grain-size distribution of the material in the humidity cells is representative of the fine fraction in the Type III pile. In addition, this comparison

indicates that the size fraction used in the humidity cells (< ¼ inch) represents approximately 16 % of the material in the Type III pile. Since the fine fraction of a rock sample contains the vast majority of the surface area, it is assumed that the surface area of the field installations is 16 % of that measured in the humidity cells on a per mass basis.

Sulfur content of the Type III material was measured on multiple samples during construction of the Type III pile. Material from the Type III upper collection lysimeter has not yet been analyzed so it is assumed here to be the same as the Type III test pile. Surface area of the sulfur is calculated assuming that the ratio of surface area of the sulfur to the surface area of the rock is proportional to the sulfur content of the rock.

Table 3-1. Preliminary Yearly Load Estimates

Type III Rock		g S (kg rock)$^{-1}$	g S (m^2 rock)$^{-1}$	g S (Kg S)$^{-1}$	g S (m^2 S)$^{-1}$
Humidity Cells	2004 Room Temperature	0.44	2.7E-04	273	0.17
	2005 Room Temperature	0.18	3.0E-05	294	0.05
	2004 Cold Room	0.23	1.4E-04	144	0.09
	2005 Cold Room	0.14	2.4E-05	241	0.04
Upper Collection Lysimeters	West	0.0062	3.5E-05	9.89	0.06
	East	0.0042	2.3E-05	6.66	0.04
Test Pile	Basal Drain	0.00038	2.1E-06	0.61	0.003
	Basal Drain - Batters	0.00064	3.6E-06	1.02	0.006
	Basal Lysimeter - 3BNClys4E	0.0018	9.9E-06	2.83	0.02
	3BNClys4W	0.0017	9.3E-06	2.64	0.01
	3BSClys4E	0.00044	2.5E-06	0.70	0.004

In general, the sulfur loadings calculated from the Type III humidity cells based on mass of rock, surface area of rock, and mass of sulfur, are much higher than for the Type III upper collection lysimeters and the Type III test pile. For estimates based on the surface area of the

sulfur the sulfur loading rates derived from the humidity cells provide a better estimate of loading rates from the field-scale installations (Table 3 1).

3.2 Concentration Estimates

Time dependent loading rates from Type III humidity cells (Figure 3-2) are used to estimate sulfur and metal concentrations for the Type III upper collection lysimeters and estimated concentrations are compared to measured concentrations (Figure 3-3). Calculations are based on a specific date, corresponding to a certain elapsed time since the upper collection lysimeters were installed. Taking this and an estimated residence time of 400 days (based on observed water flow and tracer breakthrough), release rates based on the mass of rock are determined from the humidity cells corresponding to the same elapsed time. A total sulfur loading is calculated based on the residence time and a concentration estimate is calculated by estimating the volume of water within the rock mass. Concentrations are then corrected for mass of sulfur and surface area of sulfur in a similar manner as in section 3.1.

Estimates based on the mass of the rock and the mass of sulfur overestimate the dissolved concentrations observed in the field. However, concentration estimates for sulfate and nickel based on the surface area of the exposed sulfur are in reasonable agreement compared to values measured in the field. For iron the estimated concentrations are well above the measured concentrations, likely indicating a solubility control on iron in the system. The good agreement between estimated and observed concentrations shows that scale-up calculation can provide reasonable estimates of sulfur and metal loadings in the field provided that the rock is adequately characterized at both scales, particularly with respect to grain size and sulfur content.

These estimates assume a constant residence time and utilize room temperature rate estimates. Better predictions should be achievable by applying correction for the dependence of reaction rate on temperature and the variations in residence times actually observed in the field. The concentration estimates presented here provide scale-up estimates from lab-scale experiments to the 2 m-scale upper collection lysimeters. Ongoing work includes scaling to the 15 m-scale test piles.

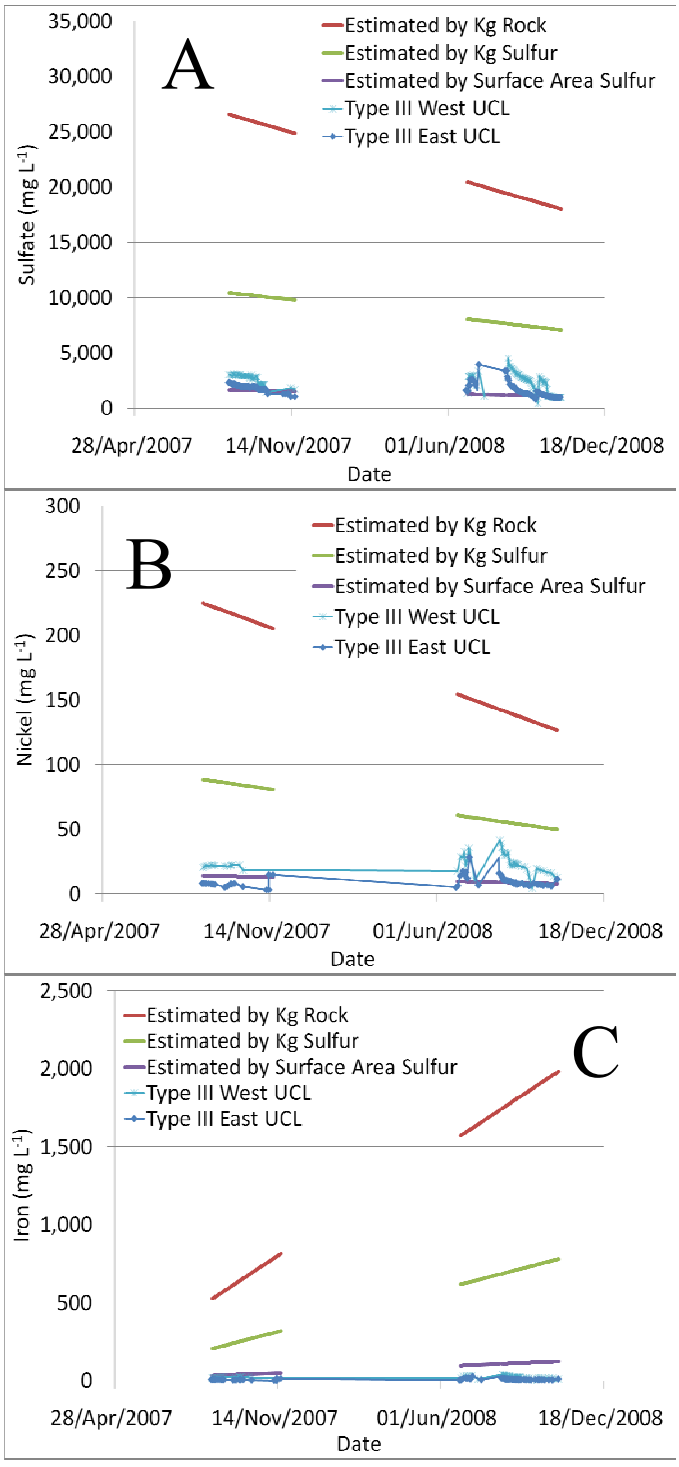

Figure 3-3. Concentration estimates for A: sulfate, B: nickel and C: iron for Type III upper collection lysimeters based on release rates derived from room temperature humidity cell experiments.

4 Results and Reporting

Results from the Diavik Waste Rock Project have been presented at numerous Canadian and international conferences and published in various conference proceedings (Table 4-1). These presentations and publications cover construction, hydrological, thermal, gas transport, and geochemical aspects of the project. In 2009, initial results from the gas transport studies were published in the Vadose Zone Journal, a highly regarded journal published by the Soil Science Society of America. This article was featured on the cover of the journal and was also featured in the society's monthly newsletter, providing a broader exposure for the research project. The project has involved 11 graduate students from the three participating universities, including two that graduated in 2009, and has involved over 25 undergraduate students (Table 4-2).

Table 4-1. Diavik Waste Rock Project Publication and Presentations

Publications
Blowes et al., Proceedings of the Sea to Sky Geotechnique, 2006.
Blowes et al., ICARD, 2006.
Blowes et al., IMWA Symposium 2007.
Arenson et al., Proceeding of the 60th Canadian Geotechnical Conference, 2007.
Blowes et al., Proceedings of the CIM Symposium 2008.
Pham et al., Ninth International Conference on Permafrost, 2008
Pham et al., Proceeding of the 61th Canadian Geotechnical, 2008
Amos et al., Vadose Zone Journal, November 2009
Amos et al., Proceedings of Securing the Future and 8th ICARD, 2009
Bailey et al., Proceedings of Securing the Future and 8th ICARD, 2009
Neuner et al., Proceedings of Securing the Future and 8th ICARD, 2009
Pham et al., Proceedings of Securing the Future and 8th ICARD, 2009
Smith et al., Proceedings of Securing the Future and 8th ICARD, 2009
Theses
Neuner, M., MSc. Thesis, University of British Columbia, 2009
Smith, L.J.D., MSc. Thesis, University of Waterloo, 2009

Reports
Diavik Waste Rock Project Annual Update – 2005, 2006, 2007, 2009
INAP test piles site tour and update - August 2008
Diavik Waste Rock Project Comprehensive Progress Report - 2008
Conference Presentations
Canadian Geotechnical Conference 2006, 2007, 2008
ICARD 2006, 2009 – *6 Presentations*
Yellowknife Geoscience Forum 2006, 2008, 2009 - *5 Presentations*
Sudbury 2007
AGU 2007
IMWA 2008
Goldschmidt 2008 - *2 Presentations*

Table 4-2. Graduate Student Participation in Diavik Waste Rock Project

Student	Project Description	Graduation Year
Mandy Moore	Humidity cells – years 1 to 4	2010
Matt Neuner	Hydrology years 1 and 2	2009*
Lianna Smith	Pile Construction, characterization and early geochemical results	2009*
Renata Klassen	Thermal Modelling	2010
Mike Gupton	Tracer tests and hydrology	2010
Nam Pham	Thermal characterization and modelling	2010
Steve Momeyer	Hydrology years 3 and 4	2010
Brenda Bailey	Geochemistry and Microbiology	2011
Sheldon Chi	Gas Transport analysis and modelling	2011
Ashley Stanton	Humidity cells years 4 to 6, database management	2012
Stacey Hannam	Mineralogy	2012

* Graduated

5 Summary of Progress and Future Outlook

The objectives of the Diavik Waste Rock Research Program are to evaluate the benefits of the proposed reclamation concepts for the Diavik Country Rock Stockpiles, and to evaluate techniques used to scale the results of laboratory studies to predict the environmental impacts of full-scale rock stockpiles. Laboratory experiments have been underway for more than 3 years to evaluate leaching rates from Diavik waste rock. Data collection from the field experiments has been underway for 3 full field seasons from 2007 to 2009. The extensive data sets reveal clear hydrological, thermal and geochemical trends and demonstrate that the hydrology, geochemistry and thermal states of the test piles continue to evolve. The data sets have allowed for preliminary scaling calculations to be completed. These calculations suggest that small-scale experiments can give reasonable estimates of field scale leaching rates provided that the material properties are well characterized at each scale. In 2009, instrumentation of the full scale Type III waste rock type at Diavik was attempted; although the success of the installation is unknown to date.

The Diavik Waste Rock Project Research Team is proposing to extent the research program for an addition 5 years beginning in 2010. A significant investment in research infrastructure at Diavik was made by the research partners including, Diavik, The Natural Science and Engineering Council of Canada (NSERC), The Canadian Foundation for Innovation (CFI), INAP and MEND. This infrastructure represents a tremendous opportunity to continue to gain further insights into behaviour of the waste rock piles as the hydrology, thermal regime, and geochemistry evolve toward steady state conditions. Continuation of the project will; allow for a longer, richer data set to form the basis of scale up comparisons; provide additional full-scale data to be included in scale-up comparison; further strengthen linkages between thermal, gas and water transport, and geochemical reactive transport aspects of the project; provide stronger support for closure planning for northern operations; and provide the opportunity to apply and evaluate sophisticated data interpretation and analysis techniques. Diavik has committed funding for the project extension and funding has been requested from INAP and MEND. Matching funding from NSERC will be request in March, 2010.

6 References

Amos, R.T., Blowes, D.W., Smith, L., Sego, D.C., 2009. Measurement of wind induced pressure gradients in a waste rock pile. *Vadose Zone Journal, November 2009.*

Amos, R.T., Smith, L., Neuner, M., Gupton, M., Blowes, D.W., Smith, L., Sego, D.C., 2009. Diavik Waste Rock Project: Oxygen Transport in Covered and Uncovered Piles. *Proceedings of Securing the Future and 8th ICARD*, June 22-26, 2009, Skellefteå, Sweden.

Arenson, L.U., Pham, N-H., Klassen, R., Sego, D.C., 2007. Heat Convection in Coarse Waste Rock Piles. Proceeding of the 60th Canadian Geotechnical Conference and 8th Joint CGS/IAH-CNC Groundwater Specialty Conference, October 22-24, 2007 Ottawa, ON (CD) pp: 1500-1507.2008

Bailey, B.L., Smith, L., Neuner, M., Gupton, M., Blowes, D.W., Smith, L., Sego, D.C., 2009. Diavik Waste Rock Project: Early Stage Geochemistry and Microbiology. *Proceedings of Securing the Future and 8th ICARD*, June 22-26, 2009, Skellefteå, Sweden.

Blowes, D.W., Moncur, M.C., Smith, L., Sego, S., Klassen, R., Neuner, M., Smith, L., Garvie, A., Gould, D., Reinson, J., 2006. Mining in the continuous permafrost: construction and instrumentation of two large-scale waste rock piles. In*: Proceedings of the Sea to Sky Geotechnique 2006*, 59th Canadian Geotechnical Conference, October 1-4, 2006, Vancouver, BC, pp. 1041-1047.

Blowes, D., Moncur, M., Smith, L., Sego. D., Bennett, J., Garvie, A., Gould, D., Reinson, J., 2006. Construction of two large-scale waste rock piles in a continuous permafrost region. In: *ICARD, 2006, Proceedings of the Seventh International Conference on Acid Rock Drainage*, March 26-29, 2006, St. Louis, MO, USA.

Blowes, D., Smith, L., Sego, D., Smith, L., Neuner, M., Gupton, M., Moncur, M., Moore, M., Klassen, R., Deans, T., Ptacek, C., Garvie, A., Reinson, J., 2007. Prediction of effluent water

quality from waste rock piles in a continuous permafrost region. In: *IMWA Symposium 2007: Water in Mining Environments*, R. Cidu & F. Frau (Eds), May 27-31, 2007, Cagliari, Italy, pp 3-9.

Blowes, D.W., Smith, L., Sego, D., Smith, L., Neuner, M., Gupton, M., Bailey, B.L., Moore, M., Pham, N., Amos, R.., Gould, W.D., Moncur, M., Ptacek, C., 2008. The Diavik Waste Rock Research Project. Proceedings of the CIM Symposium 2008 on Mines and the Environment, Rouyn-Noranda, Québec, Canada, November 3, 2008.

Diavik Waste Rock Project, 2008. Progress Report. Report prepared for Diavik, INAP and MEND.

Pham, H-N, Arenson, L.U. and Sego D.C., 2008. Numerical Analysis of Forced and Natural Convection in Waste-Rock Piles in Permafrost Environments. Ninth International Conference on Permafrost, University of Alaska, Fairbanks, June 29-July 3, 2008, 2: 1411-1416

Pham, H-N., Sego, D.C., Arenson, L.U., Blowes, D.W., and Smith, L. 2008. Convective heat transfer in waste rock piles under permafrost environment. Proceeding of the 61th Canadian Geotechnical Conference and 9th Joint CGS/IAH-CNC Groundwater Specialty Conference, September 21-24, 2008 Edmonton, AB (CD) pp. 940-947.

Neuner, M., Gupton, M., Smith, L., Smith, L., Blowes, D.W., Sego, D.C., 2009. Diavik Waste Rock Project: Unsaturated Water Flow. *Proceedings of Securing the Future and 8th ICARD*, June 22-26, 2009, Skellefteå, Sweden.

Neuner, M., 2009. Water flow through unsaturated mine waste rock in a region of permafrost. MSc. Thesis, University of British Columbia, Vancouver, British Columbia, Canada, February 2009.

Pham, N., Sego, D.C., Arenson, L.U., Smith, L., Gupton, M., Neuner, M., Amos, R.T., Blowes, D.W., Smith, L., 2009. Diavik Waste Rock Project: Heat Transfer in a Permafrost

Region. *Proceedings of Securing the Future and 8th ICARD*, June 22-26, 2009, Skellefteå, Sweden.

Smith, L., Moore, M., Bailey, B.L., Neuner, M., Gupton, M., Blowes, D.W., Smith, L., Sego, D.C., 2009. Diavik Waste Rock Project: From the Laboratory to the Canadian Arctic. *Proceedings of Securing the Future and 8th ICARD*, June 22-26, 2009, Skellefteå, Sweden.

Smith, L.J.D., 2009. Building and characterizing low sulfide instrumented waste rock piles: Pile design and construction, particle size and sulfur characterization, and initial geochemical response. MSc. Thesis, University of Waterloo, Waterloo, Ontario, Canada, 2009

Appendix X-7

Reclamation Materials Inventory and Mapping
1996 Environmental Baseline Program

TECHNICAL MEMORANDUM
DIAVIK DIMOND MINES INC. PROJECT

TO: Erik Madsen, Murray Swyripa, File

DATE: 1/17/97
PROJECT: 962-2309-5551

AUTHOR(S): Tim R. Bossenberry

FINAL REPORT

TITLE: Technical Memorandum #4-revision #1
Reclamation Materials Inventory and Mapping
1996 Environmental Baseline Program

OBJECTIVES

The objectives of the 1996 terrain and soils programme for the Diavik Diamond Mines Inc. Project were to:

- describe the terrain of the east island.
- inventory and classify the surficial deposits and soils of the east island.
- identify the surficial materials on the east island that would be suitable for reclaiming the areas disturbed by mining activities.
- interpretation of surficial materials on the mainland and west island, based on the investigations and mapping completed for the east island.

INTRODUCTION

The field component of the terrain and soils programme was carried out from July 29 through August 3, 1996. Personnel involved in the field programme included Tim R. Bossenberry (Golder) and Phoebe Ann Wetrade, an a assistant provided by the camp. Field work was confined to the east island (a portion of the Local Study Area), since at that time, that was where the majority of the disturbance was to occur. Interpretation of the surficial materials on the

mainland and west island (remainder of the Local Study Area) will be forthcoming (end of November, 1996), and will be based on the investigations and mapping completed for the east island.

- A total of 47 sites were investigated on the east island to determine local terrain and soils characteristics (Figure 14).
- Numerous photographs were taken at various locations on the east island, including the soil inspection sites, to fully characterise the terrain conditions and the extent of surficial materials (Plates 1 through 80).
- Surficial materials mapping was done on a series of 1:10,000 colour aerial photographs of the east island (Figures 2 through 13). The aerial photographs were interpreted and provided a base for defining the surficial materials polygons.
- Orientation of the twelve (12) aerial photographs is included on Figure 1.
- Each of the eighty (80) photographs taken from the ground on the east island and the direction in which these photos were taken are indicated on Figures 2 through 13.

METHODS

Technical Procedure 8-11-0 (Soil Investigation and Sampling) was followed for the investigation of terrain and soils on the east island of the Diavik Dimond Mines Inc. Project. Specific Work Instructions SWI-15.0 were also followed for this investigation. There were no deviations to the Technical Procedure or the Specific Work Instructions. Technical Procedure TP 8-11-0 and Specific Work Instructions SWI-15.0 are included at the end of this Technical Memorandum.

RESULTS

Terrain

The landscape conditions on the east island are described in Table 1 (Landscape and Soil Profile Characteristics) for the 47 Soil Investigation Sites, and visually by the 80 photographic plates included at the end of this Technical Memorandum.

The project area is a glaciated landscape characterised by:

- steep sided bedrock ridges (examples on Plates 18, 21, 26 and 32);
- undulating to strongly rolling (2% to 30% slopes) morainal deposits (examples on Plates 4, 6, 25 and 80);
- ridged (eskers) and hummocky (kames) glaciofluvial deposits (examples on Plates 51, 52 and 73); and
- level to depressional glaciolacustrine (examples on Plates 7, 18, 24, 32, 34, 50, 58, 60 and 61) and organic deposits (examples on Plates 1, 22, 23, 42, 44, 48, 50, 54, 65, 69 and 76).

There are numerous solifluction lobes on the east island (examples on Plates 13, 14 and 16). These lobes are most defined on slopes ranging from 10% to 25%, however, may occur on slopes as shallow as 2%.

There are a few small creeks that dissect the east island (examples on Plates 11 and 36). The creeks are not incised, therefore, do not affect the condition of the landscape.

Most of the terrain features on the east island are controlled by shallow bedrock (examples on Plates 4, 40 and 48). There are veneers (<one metre thick) and blankets (one to three metres thick) of morainal and glaciolacustrine deposits overlying the bedrock. There are also veneers and blankets of glaciolacustrine deposits overlying morainal deposits on the east island.

Surficial Geology

Parent materials on the east island consist of morainal, glaciolacustrine, glaciofluvial and organic deposits. The spatial distribution of surficial deposits on the east island is illustrated on Figures 2 through 13.

- Morainal (material deposited by glaciers) deposits overlie most of the bedrock in the area. These deposits are: moderately coarse (sandy loam) to coarse (loamy sand, sand) textured; moderately well to imperfectly drained on undulating to strongly rolling topography (2% to 30% slopes); and moderately to exceedingly stony.
- Glaciolacustrine (material deposited by glacial lakes) deposits occupy most of the lowland areas that are within 10 metres of the current level of Lac de Gras. These deposits are: medium (silt loam, loam) to moderately coarse (sandy loam) textured; imperfectly to poorly drained on level to gentle slopes (0% to 5% slopes); and nonstony to slightly stony. Glaciolacustrine deposits overlie bedrock and morainal deposits on the east island.
- Glaciofluvial (material deposited by glacial rivers) deposits are generally in the form of eskers and kames. These deposits are: coarse (sand, loamy sand) textured; well to rapidly drained on moderate to strong slopes (6% to 30% slopes); and generally nonstony. Glaciofluvial deposits in this area may have lenses of fine gravel throughout their profiles.
- Organic deposits are: poorly to very poorly drained on level to depressional topography; and nonstony. Most of the shallow (<1 metre) organic deposits have large remanant stones (bedrock or glacial till) exposed at the surface.

Regional Soils

The east island lies within the continuous permafrost zone of the North West Territories. Soils in this zone are of the Cryosolic order. Cryosolic soils are formed in either mineral or organic materials under the influence of cryoturbation, or frost boiling, and are characterised by disrupted, mixed or broken horizons. Cryosolic soils form where permafrost occurs within 2 metres of the ground surface.

The Cryosolic order is divided into:

- Turbic Cryosols, where there is marked cryoturbation in mineral material, as evidenced by patterned ground (circles, polygons) or surface frost boils (earth hummocks);
- Static Cryosols, where there is no visible evidence of patterned ground or surface frost boils in mineral material; and
- Organic Cryosols, which occur in organic material.

There is a high risk of mass movement (solifluction) in Cryosolic soils on slopes greater than 2%. Solifluction occurs when thaw water:

- infiltrates to the permafrost layer, which;
- saturates the thaw layer, which;
- increases the materials weight, which;
- lubricates the thawed/frozen interface, which;
- decreases the shear strength of the material, which;
- results in a slow, downslope movement of the material.

Solifluction, like cryoturbation, causes soil horizons to become mixed together.

Areas of the east island that have been significantly cryoturbated and soliflucted are indicated on Figures 2 through 11 by the symbols C and S, respectively. Most of the soils on the east island have been cryoturbated to a certain extent, and if on a slope greater than 2%, soliflucted.

A soil investigation was completed for the east island, the results of which are included on Table 1 at the end of this Technical Memorandum. This information was used as part of the baseline map created for the Local Study Area.

Materials Suitable for Reclamation

The suitability of the morainal, glaciolacustrine and glaciofluvial materials on the east island for reclamation purposes are indicated on Table 1. Suitability for reclamation is rated based primarily on soil texture, soil consistence, and stone content.

All of the organic materials on the east island are particularly suitable for reclamation, since they:

- have a very high moisture retention capacity; and

- contain an abundant reserve of native seeds and stolons.

The glaciolacustrine materials on the east island are suitable for reclamation, since they generally:

- have a fine sandy loam to silty loam texture;
- have a friable to very friable consistence; and
- have less than a 10% stone content.

The glaciofluvial materials (eskers and kames) on the east island are marginally suitable for reclamation, since they:

- have a sand to loamy sand texture;
- have a loose consistence; and
- may contain a significant content of gravel.

The morainal materials on the east island are marginally suitable for reclamation, since they:

- have a sand to gravelly sandy loam texture;
- have a friable to loose consistence; and
- have a stone content generally exceeding 20% and a very (stones 1 to 2 metres apart) to exceedingly (stones 0.1 to 0.5 metres apart) stony surface.

The frost boiled materials (Turbic Cryosols), particularly those developed in thin organic over glaciolacustrine or glaciofluvial deposits, on the east island are suitable for reclamation, since they:

- have had organic and mineral materials naturally mixed together;
- have had only the finer mineral fractions boiled to the surface, with large stones being left at depth; and
- have a noncompacted consistency, due to the constant frost boiling.

The soliflucted materials on the east island are suitable for reclamation, since they:

- have had organic and mineral material naturally mixed together, similar to the Turbic Cryosols; and
- have a noncompacted consistency, due to the slow downslope movement of the material.

Overall, there appears to be an abundant supply of materials suitable for reclamation on the east island.

- Most of the organic, organic over glaciolacustrine, and glaciolacustrine deposits occur on large level plains and could be easily salvaged for stockpiling.
- Other materials suitable for reclamation occur in small, sometimes confined areas, and will need to be selectively salvaged from the less suitable reclamation materials, such as the stony morainal deposits and bedrock.
- The reclamation plan for the mine should include a detailed salvage and stockpiling procedure to ensure that these valuable reclamation materials are not lost by lack of effort during salvage, inappropriate stockpiling, or sterilisation by stockpiling granite over this resource.

TABLE 1

TABLE 1 LANDSCAPE AND SOIL PROFILE CHARACTERISTICS

SITE	LANDSCAPE	HOR	DEPTH (cm)	COLOUR	TEXT	RECL RATING	STRUCT	CONS	RECL RATING	ROCKS (%)	RECL RATING
1	Topography: Depressional Slope: 0% Slope Position: n/a Surface Stoniness: Nonstony Drainage: Poor Parent Material: Glaciolacustrine UTM Coordinates: E530000 N7150242	Om smooth Bm wavy Cg	0 - 6 6 - 20 20 - 99+	 10YR4/3 10YR5/3	 fSL fSL	 good good	 GR MA	 MVFR MFR	 good good	0 10 10	 good good
2	Topography: Depressional Slope: 0% Slope Position: n/a Surface Stoniness: Nonstony Drainage: Poor Parent Material: Organic/Glaciolacustrine UTM Coordinates: E529902 N7150375	Of wavy Om wavy Cg wavy Cz	0 - 33 33 - 41 41 - 53 53 - 99+	 10YR4/4 10YR4/4	 SiL SiL	 good good	 MA MA	 MFR frozen	 good n/a	0 0 0 0	 good good
3	Topography: Level Slope: 0% Slope Position: n/a Surface Stoniness: Slightly Stony Drainage: Poor Parent Material: Organic/Glaciolacustrine UTM Coordinates: E529992 N7150393	Om wavy Cg	0 - 20 20 - 99+	 10YR5/1	 fSL	 good	 MA	 MVFR	 good	0 10	 good
4	Topography: Moderately Rolling Slope: 14% Slope Position: Lower Surface Stoniness: Exceedingly Stony Drainage: Moderately Well to Well Parent Material: Morainal UTM Coordinates: E529620 N7151500	Ah irreg. Bm irreg. C1 wavy C2	0 - 4 4 - 24 24 - 35 35 - 99+	10YR3/3 10YR4/4 10YR5/3 10YR5/3	SL SL SL SL	good good good good	GR GR MA MA	DS MFR MFR ML	good good good fair	10 30 30 60	good fair fair poor

SITE	LANDSCAPE	HOR	DEPTH (cm)	COLOUR	TEXT	RECL RATING	STRUCT	CONS	RECL RATING	ROCKS (%)	RECL RATING
5	Topography: Gently Sloping Slope: 5% Slope Position: Middle Surface Stoniness: Nonstony Drainage: Moderately Well Parent Material: Glaciolacustrine UTM Coordinates: E530146 N7151481	Ah irreg. Bm irreg. C1 wavy C2	0 - 4 4 - 26 26 - 45 45 - 99+	10YR3/3 10YR4/4 10YR5/3 10YR3/2	SL SL SL L	good good good good	GR GR MA MA	DS MFR MFR MFR	good good good good	10 10 10 5	good good good good
6	Topography: Moderately Rolling Slope: 17% Slope Position: Middle Surface Stoniness: Exceedingly Stony Drainage: Moderately Well Parent Material: Morainal UTM Coordinates: E529738 N7151752	Of irreg. Oh irreg. C1 wavy C2	0 - 6 6 - 12 12 - 43 43 - 99+	 10YR4/3 10YR4/3	 grSL grSL	 good good	 MA MA	 MVFR MVFR	 good good	0 0 40 80	 fair unsuit
7	Topography: Moderately Sloping Slope: 8% Slope Position: Lower Surface Stoniness: Slightly Stony Drainage: Moderately Well Parent Material: Colluvial UTM Coordinates: E530159 7152293	Of irreg. C	0 - 13 13 - 99+	 10YR3/3	 grLS	 poor	 SGR	 ML	 fair	0 10	 good
8	Topography: Strongly Sloping Slope: 14% Slope Position: Lower Surface Stoniness: Nonstony Drainage: Moderately Well Parent Material: Organic/Colluvial UTM Coordinates: E530528 N7152393	Of wavy Om irreg. Cz	0 - 14 14 - 34 34 - 99+	 10YR4/3	 SL	 good	 MA	 frozen	 n/a	0 0 20	 fair

SITE	LANDSCAPE	HOR	DEPTH (cm)	COLOUR	TEXT	RECL RATING	STRUCT	CONS	RECL RATING	ROCKS (%)	RECL RATING
9	Topography: Steeply Sloping Slope: 18% Slope Position: Middle Surface Stoniness: Slightly Stony Drainage: Well Parent Material: Colluvial UTM Coordinates: E530948 N7152459	Ahy irreg. Cy	0 - 33 33 - 99+	10YR3/1 10YR4/4	SiL SL	good good	GR MA	DS DL	good fair	10 40	good poor
10	Topography: Level Slope: 0% Slope Position: n/a Surface Stoniness: Nonstony Drainage: Imperfect Parent Material: Glaciolacustrine UTM Coordinates: E533232 N7151987	Oh irreg. Cg	0 - 8 8 - 99+	 10YR6/2	 fSL	 good	 MA	 DS	 good	0 0	 good
11	Topography: Level Slope: 0% Slope Position: n/a Surface Stoniness: Nonstony Drainage: Poor Parent Material: Glaciolacustrine UTM Coordinates: E531349 N7150545	Of wavy Bm wavy Cg wavy Cz	0 - 7 7 - 30 30 - 95 95 - 99+	 10YR6/3 10YR6/1 10YR6/1	 S S S	 poor poor poor	 SGR SGR SGR	 ML ML frozen	 fair fair n/a	0 0 0 0	 good good good
12	Topography: Depressional Slope: 0% Slope Position: n/a Surface Stoniness: Slightly Stony Drainage: Very Poor Parent Material: Organic/Morainal UTM Coordinates: E531742 N7150638	Of irreg. Cg	0 - 38 38 - 99+	 10YR6/1	 grS	 poor	 SGR	 WNS	 good	0 90	 unsuit

SITE	LANDSCAPE	HOR	DEPTH (cm)	COLOUR	TEXT	RECL RATING	STRUCT	CONS	RECL RATING	ROCKS (%)	RECL RATING
13	Topography: Undulating Slope: 5% Slope Position: Lower Surface Stoniness: Slightly Stony Drainage: Moderately Well Parent Material: Morainal UTM Coordinates: E531621 N7151022	Om wavy Bm irreg. Cgy	0 - 2 2 - 9 9 - 99+	 10YR4/4 10YR5/2	 SiL grSiL	 good good	 GR MA	 DS MFR	 good good	0 5 30	 good fair
14	Topography: Gently Undulating Slope: 2% Slope Position: Upper Surface Stoniness: Very Stony Drainage: Moderately Well Parent Material: Morainal UTM Coordinates: E532387 N7150469	Om wavy Cgy	0 - 4 4 - 99+	 10YR6/3	 grfSL	 good	 GR	 MVFR	 good	0 40	 poor
15	Topography: Level Slope: 0% Slope Position: n/a Surface Stoniness: Nonstony Drainage: Imperfect to Poor Parent Material: Organic/Glaciolacustrine UTM Coordinates: E532629 N7150681	Of wavy Bm irreg. Cgy wavy Cz	0 - 20 20 - 46 46 - 60 60 - 99+	 10YR4/4 10YR5/2 10YR5/2	 fSL grLS grLS	 good poor poor	 GR SGR SGR	 MFR ML frozen	 good fair n/a	0 0 10 10	 good good good
16	Topography: Gently Undulating Slope: 2% Slope Position: Middle Surface Stoniness: Very Stony Drainage: Moderately Well Parent Material:Glaciolacustrine/Morainal UTM Coordinates: E533373 N7150301	Of irreg. Bmy irreg. Cgy irreg. Cz	0 - 2 2 - 24 24 - 88 88 - 99+	 10YR4/4 10YR6/3 10YR6/3	 grSL grSL grSL	 good good good	 MA MA MA	 MFR MFR frozen	 good good n/a	0 10 30 30	 good fair fair

SITE	LANDSCAPE	HOR	DEPTH (cm)	COLOUR	TEXT	RECL. RATING	STRUCT	CONS	RECL. RATING	ROCKS (%)	RECL. RATING
17	Topography: Level Slope: 0.5% Slope Position: Middle Surface Stoniness: Nonstony Drainage: Imperfect to Poor Parent Material: Glaciolacustrine UTM Coordinates: E533884 N7150213	Of wavy Bmy irreg. Cgy irreg. Cz	0 - 10 10 - 18 18 - 86 86 - 99+	 10YR4/4 10YR6/2 10YR6/2	 fSL SL SL	 good good good	 GR MA MA	 MFR MFR frozen	 good good n/a	0 0 0 0	 good good good
18	Topography: Level Slope: 0% Slope Position: n/a Surface Stoniness: Slightly Stony Drainage: Poor Parent Material: Organic/Bedrock UTM Coordinates: E533740 N7150822	Of wavy Om irreg. R	0 - 39 39 - 53 53 - 99+								
19	Topography: Very Gently Sloping Slope: 1.5% Slope Position: Middle Surface Stoniness: Very Stony Drainage: Imperfect Parent Material: Colluvial UTM Coordinates: E534179 N7151165	Of irreg. Cgy	0 - 3 3 - 99+	 10YR5/3	 fSL	 good	 MA	 MFR	 good	0 5	 good
20	Topography: Very Gently Sloping Slope: 1.5% Slope Position: Middle Surface Stoniness: Slightly Stony Drainage: Imperfect Parent Material: Organic/Colluvial UTM Coordinates: E533657 N7151393	Of irreg. Cz	0 - 45 45 - 99+	 10YR4/4	 SL	 good	 MA	 frozen	 n/a	0 10	 good

SITE	LANDSCAPE	HOR	DEPTH (cm)	COLOUR	TEXT	RECL RATING	STRUCT	CONS	RECL RATING	ROCKS (%)	RECL RATING
21	Topography: Gently Sloping Slope: 4% Slope Position: Middle Surface Stoniness: Nonstony Drainage: Imperfect Parent Material:Colluvial/Glaciolacustrine UTM Coordinates: E533714 N7151625	Of wavy Cgy wavy Cz	0 - 2 2 - 76 76 - 99+	 10YR6/3 10YR6/3	 fSL fSL	 good good	 MA MA	 MFR frozen	 good n/a	0 5 5	 good good
22	Topography: Level Slope: 0.5% Slope Position: n/a Surface Stoniness: Nonstony Drainage: Imperfect Parent Material: Glaciolacustrine UTM Coordinates: E533845 N7151751	Of wavy Cgy wavy Cz	0 - 23 23 - 42 42 - 99+	 10YR6/3 10YR6/3	 fSL fSL	 good good	 MA MA	 MFR frozen	 good n/a	0 5 5	 good good
23	Topography: Depressional Slope: 0% Slope Position: n/a Surface Stoniness: Nonstony Drainage: Poor Parent Material: Organic/Glaciolacustrine UTM Coordinates: E532147 N7153737	Of wavy Cz	0 - 35 35 - 99+	 10YR4/4	 LS	 poor	 SGR	 frozen	 n/a	0 0	 good
24	Topography: Level Slope: 0% Slope Position: n/a Surface Stoniness: Nonstony Drainage: Poor to Very Poor Parent Material: Organic/Glaciofluvial UTM Coordinates: E532937 N7153414	Of wavy Cgy wavy Cz	0 - 37 37 - 62 62 - 99+	 10YR4/4 10YR4/4	 S S	 poor poor	 SGR SGR	 ML frozen	 fair n/a	0 0 0	 good good

SITE	LANDSCAPE	HOR	DEPTH (cm)	COLOUR	TEXT	RECL RATING	STRUCT	CONS	RECL RATING	ROCKS (%)	RECL RATING
25	Topography: Level Slope: 0% Slope Position: n/a Surface Stoniness: Moderately Stony Drainage: Imperfect Parent Material: Organic/Morainal UTM Coordinates: E532257 N7152978	Of irreg. Cgy	0 - 26 26 - 35+	10YR4/4	grSL	good	GR	MFR	good	0 60	unsuit
26	Topography: Gently Sloping Slope: 4% Slope Position: Middle Surface Stoniness: Nonstony Drainage: Imperfect Parent Material:Colluvial/Glaciolacustrine UTM Coordinates: E532626 N7152654	Of wavy Cgy wavy Cz	0 - 4 4 - 75 75 - 99+	10YR5/3 10YR5/3	fSL fSL	good good	MA MA	MFR frozen	good n/a	0 0 0	good good
27	Topography: Very Gently Sloping Slope: 2% Slope Position: Middle Surface Stoniness: Moderately Stony Drainage: Moderately Well Parent Material: Colluvial/Glaciofluvial UTM Coordinates: E533717 N7152857	Of irreg. Bmy wavy Cy wavy Cz	0 - 4 4 - 30 30 - 87 87 - 99+	10YR4/3 10YR5/3 10YR5/3	grLS grLS grSL	poor poor good	SGR SGR MA	ML ML frozen	fair fair n/a	0 30 30 30	fair fair fair
28	Topography: Level Slope: 0% Slope Position: n/a Surface Stoniness: Nonstony Drainage: Poor Parent Material: Organic/Glaciolacustrine UTM Coordinates: E534269 N7152503	Of irreg. Om wavy Cz	0 - 12 12 - 50 50 - 99+	10YR4/3	LS	poor	SGR	frozen	n/a	0 0 5	good

SITE	LANDSCAPE	HOR	DEPTH (cm)	COLOUR	TEXT	RECL RATING	STRUCT	CONS	RECL RATING	ROCKS (%)	RECL RATING
29	Topography: Gently Sloping Slope: 3% Slope Position: Middle Surface Stoniness: Slightly Stony Drainage: Well Parent Material: Glaciolacustrine UTM Coordinates: E534894 N7152262	Of irreg. Om wavy Cy1 wavy Cy2 wavy Cz	0 - 5 5 - 10 10 - 43 43 - 78 78 - 99+	 10YR6/6 10YR3/3 10YR3/3	 S S S	 poor poor poor	 SGR SGR SGR	 ML ML frozen	 fair fair n/a	0 0 5 5 5	 good good good
30	Topography: Level Slope: 0% Slope Position: n/a Surface Stoniness: Moderately Stony Drainage: Well Parent Material: Glaciolacustrine UTM Coordinates: E534905 N7151602	Of wavy Cy wavy Cgy wavy Cz	0 - 2 2 - 40 40 - 85 85 - 99+	 7.5YR4/4 10YR6/3 10YR6/3	 S S S	 poor poor poor	 SGR SGR SGR	 ML ML frozen	 fair fair n/a	0 0 0 0	 good good good
31	Topography: Level Slope: 1% Slope Position: n/a Surface Stoniness: Nonstony Drainage: Imperfect Parent Material: Glaciolacustrine UTM Coordinates: E535247 N7152015	Of wavy Om wavy Cgy wavy Cz	0 - 5 5 - 10 10 - 93 93 - 99+	 10YR6/3 10YR6/3	 S fS	 poor good	 SGR SGR	 ML frozen	 fair n/a	0 0 5 10	 good good
32	Topography: Gently Sloping Slope: 3% Slope Position: Middle Surface Stoniness: Very Stony Drainage: Imperfect Parent Material: Colluvial/Morainal UTM Coordinates: E535254 N7153635	Of wavy Bmy wavy Cy wavy Cz	0 - 5 5 - 24 24 - 68 68 - 99+	 10YR5/4 10YR5/3 10YR5/3	 grSL grSL grSL	 good good good	 GR MA MA	 MFR MFR frozen	 good good n/a	0 20 20 20	 fair fair fair

SITE	LANDSCAPE	HOR	DEPTH (cm)	COLOUR	TEXT	RECL RATING	STRUCT	CONS	RECL RATING	ROCKS (%)	RECL RATING
33	Topography: Level Slope: 0% Slope Position: n/a Surface Stoniness: Slightly Stony Drainage: Imperfect Parent Material: Organic/Glaciofluvial UTM Coordinates: E535092 N7153858	Of irreg. Cgy wavy Cz	0 - 32 32 - 95 95 - 99+	 10YR6/2 10YR6/2	 grSL grSL	 good good	 MA MA	 MFR frozen	 good n/a	0 10 10	 good good
34	Topography: Gently Sloping Slope: 3% Slope Position: Middle Surface Stoniness: Slightly Stony Drainage: Imperfect Parent Material: Organic/Colluvial UTM Coordinates: E534692 N7154000	Of irreg. Cgy wavy Cz	0 - 32 32 - 39 39 - 99+	 10YR5/2 10YR5/2	 SiL SiL	 good good	 MA MA	 WSS frozen	 good n/a	0 5 5	 good good
35	Topography: Gently Sloping Slope: 2% Slope Position: Middle Surface Stoniness: Moderately Stony Drainage: Moderately Well Parent Material: Colluvial/Morainal UTM Coordinates: E534590 N7153767	Om wavy Bmy wavy Cy wavy Cz	0 - 5 5 - 26 26 - 77 77 - 99+	 10YR4/3 10YR5/3 10YR5/3	 grSL grSL grSL	 good good good	 GR MA MA	 MFR MFR frozen	 good good n/a	0 40 20 20	 poor fair fair
36	Topography: Level Slope: 0.5% Slope Position: n/a Surface Stoniness: Slightly Stony Drainage: Poor Parent Material: Organic/Glaciolacustrine UTM Coordinates: E534137 N7153956	Of wavy Om wavy Cz	0 - 18 18 - 33 33 - 99+	 10YR4/3	 SL	 good	 MA	 frozen	 n/a	0 0 10	 good

SITE	LANDSCAPE	HOR	DEPTH (cm)	COLOUR	TEXT	RECL RATING	STRUCT	CONS	RECL RATING	ROCKS (%)	RECL RATING
37	Topography: Gently Sloping	Of	0 - 3							0	
	Slope: 3%	wavy									
	Slope Position: Lower	Cgy	3 - 98	10YR6/2	fSL	good	MA	MFR	good	5	good
	Surface Stoniness: Moderately Stony	wavy									
	Drainage: Moderately Well to Imperfect	Cz	98 - 99+	10YR6/2	fSL	good	MA	frozen	n/a	5	good
	Parent Material:Colluvial/Glaciolacustrine										
	UTM Coordinates: E534253										
	N7154355										
38	Topography: Gently Sloping	Of	0 - 15							0	
	Slope: 2.5%	wavy									
	Slope Position: Middle	Om	15 - 43							0	
	Surface Stoniness: Slightly Stony	wavy									
	Drainage: Imperfect	Cz	43 - 99+	10YR6/2	fSL	good	MA	frozen	n/a	5	good
	Parent Material: Organic/Glaciolacustrine										
	UTM Coordinates: E533917										
	N7154544										
39	Topography: Gently Sloping	Of	0 - 14							0	
	Slope: 3%	wavy									
	Slope Position: Lower	Bmy	14 - 22	10YR5/3	grSL	good	SGR	MVFR	good	80	unsuit
	Surface Stoniness: Slightly Stony	irreg.									
	Drainage: Moderately Well to Imperfect	Cgy	22 - 68	10YR6/2	grSL	good	MA	MFR	good	20	fair
	Parent Material: Colluvial/Morainal	irreg.									
	UTM Coordinates: E533475	Cz	68 - 99+	10YR6/2	grSL	good	MA	frozen	n/a	20	fair
	N7154571										
40	Topography: Gently Sloping	Of	0 - 10							0	
	Slope: 4%	irreg.									
	Slope Position: Middle	Om	10 - 18							0	
	Surface Stoniness: Very Stony	irreg.									
	Drainage: Moderately Well	Cy	18 - 68	10YR5/3	grSL	good	MA	MFR	good	40	poor
	Parent Material: Organic/Colluvial	wavy									
	UTM Coordinates: E533195	Cz	68 - 99+	10YR5/3	grSL	good	MA	frozen	n/a	40	poor
	N7154265										

SITE	LANDSCAPE	HOR	DEPTH (cm)	COLOUR	TEXT	RECL RATING	STRUCT	CONS	RECL RATING	ROCKS (%)	RECL RATING
41	Topography: Depressional Slope: 0% Slope Position: n/a Surface Stoniness: Slightly Stony Drainage: Poor Parent Material: Organic/Morainal UTM Coordinates: E533410 N7153277	Of irreg. Om irreg. Cz	0 - 13 13 - 45 45 - 99+	 10YR4/3	 grSL	 good	 MA	 frozen	 n/a	0 0 20	 fair
42	Topography: Level Slope: 0% Slope Position: n/a Surface Stoniness: Nonstony Drainage: Poor Parent Material: Organic/Glaciolacustrine UTM Coordinates: E534116 N7153338	Of wavy Om irreg. Cz	0 - 17 17 - 38 38 - 99+	 10YR4/3	 fSL	 good	 MA	 frozen	 n/a	0 0 5	 good
43	Topography: Depressional Slope: 0% Slope Position: n/a Surface Stoniness: Slightly Stony Drainage: Poor Parent Material: Organic/Glaciolacustrine UTM Coordinates: E534207 N7153351	Of irreg. Om irreg. Cy wavy Cz	0 - 13 13 - 29 29 - 68 68 - 99+	 7.5YR4/2 7.5YR4/2	 fSL fSL	 good good	 MA MA	 MFR frozen	 good n/a	0 0 5 5	 good good
44	Topography: Strongly Sloping Slope: 15% Slope Position: Middle Surface Stoniness: Very Stony Drainage: Well Parent Material: Colluvial/Morainal UTM Coordinates: E534924 N7153054	Of wavy Bmy wavy Cy wavy Cz	0 - 9 9 - 22 22 - 59 59 - 99+	 10YR4/3 10YR5/3 10YR5/3	 grSL grLS grLS	 good poor poor	 SGR SGR SGR	 DS ML frozen	 good fair n/a	0 80 40 40	 unsuit poor poor

SITE	LANDSCAPE	HOR	DEPTH (cm)	COLOUR	TEXT	RECL RATING	STRUCT	CONS	RECL RATING	ROCKS (%)	RECL RATING
45	Topography: Very Gently Sloping Slope: 2% Slope Position: Upper Surface Stoniness: Nonstony Drainage: Imperfect Parent Material: Organic/Glaciolacustrine UTM Coordinates: E535308 N7152559	Of wavy Om wavy Bmy wavy Cgy wavy Cz	0 - 10 10 - 19 19 - 26 26 - 58 58 - 99+	 10YR4/4 10YR6/2 10YR6/2	 LS LS LS	 poor poor poor	 SGR SGR SGR	 MVFR WSS frozen	 good good n/a	0 0 0 0 0	 good good good
46	Topography: Depressional Slope: 0% Slope Position: n/a Surface Stoniness: Slightly Stony Drainage: Very Poor Parent Material: Organic/Glaciolacustrine UTM Coordinates: E535921 N7151929	Of irreg. Om wavy Cg wavy Cz	0 - 12 12 - 35 35 - 58 58 - 99+	 10YR5/2 10YR5/2	 SL SL	 good good	 MA MA	 WSS frozen	 good n/a	0 0 5 5	 good good
47	Topography: Very Gently Sloping Slope: 1% Slope Position: n/a Surface Stoniness: Slightly Stony Drainage: Imperfect Parent Material: Glaciolacustrine UTM Coordinates: E535521 N7151989	Of irreg. Om irreg. Bmy wavy Cgy wavy Cz	0 - 7 7 - 14 14 - 30 30 - 90 90 - 99+	 10YR4/4 10YR6/2 10YR6/2	 S fLS fLS	 poor fair fair	 SGR SGR SGR	 ML ML frozen	 fair fair n/a	0 0 5 5 5	 good good good

TABLE 1 LEGEND:

Texture

SL	sandy loam
fSL	fine sandy loam
grSL	gravelly sandy loam
SiL	silt loam
grSiL	gravelly silt loam
LS	loamy sand
grLS	gravelly loamy sand
L	loam
S	sand
grS	gravelly sand
fS	fine sand

Structure

GR	granular
SGR	single grained
MA	massive

Consistence

MVFR	moist very friable
MFR	moist friable
ML	moist loose
DS	dry soft
DL	dry loose
WNS	wet nonsticky
WSS	wet slightly sticky

Reclamation Ratings

Texture	Good	fine Sandy Loam, very fine Sandy Loam, Loam, Silty Loam, Sandy Loam
	Fair	Clay Loam, Sandy Clay Loam, Silty Clay Loam
	Poor	Sand, Loamy Sand, Silty Clay, Clay, Heavy Clay
	Unsuitable	Bedrock
Consistence	Good	Very Friable, Friable
	Fair	Loose, Firm
	Poor	Very Firm
	Unsuitable	Extremely Firm
Stone Content	Good	<11%
	Fair	11 to 30%
	Poor	31 to 60%
	Unsuitable	>60%

FIGURES

7 155 000 N
7 154 500 N
7 154 000 N
7 153 500 N
7 153 000 N
7 152 500 N
7 152 000 N
7 151 500 N
7 151 000 N
7 150 500 N
7 150 000 N
7 149 500 N
7 149 000 N
7 148 500 N

529 000 E
529 500 E
530 000 E
530 500 E
531 000 E
531 500 E
532 000 E
532 500 E
533 000 E
533 500 E
534 000 E
534 500 E
535 000 E
535 500 E
536 000 E
536 500 E
537 000 E
537 500 E
538 000 E

FIGURE 13
FIGURE 12
FIGURE 11
FIGURE 5
FIGURE 6
FIGURE 7
FIGURE 8
FIGURE 10
FIGURE 4
FIGURE 3
FIGURE 9
FIGURE 2

N

LEGEND

- CONTOUR ELEVATION 420m
- CONTOUR ELEVATION 425m
- CONTOUR ELEVATION 430m
- CONTOUR ELEVATION 435m
- CONTOUR ELEVATION 440m
- CONTOUR ELEVATION 445m
- CONTOUR ELEVATION 450m
- CONTOUR ELEVATION 455m
- CONTOUR ELEVATION 460m
- CONTOUR ELEVATION 465m

SCALE 1:30,000

0 500 1000 1500 2000

NO	DATE	REVISION	BY	CHK.
A	97/X/X	X	X	X

DIAVIK DIAMOND MINES INC.

Golder Associates

SURFICIAL MATERIALS EAST ISLAND

DRAWN: RFM	DATE: 17 JAN 97	SCALE: AS SHOWN	
CHECKED: TB	ACAD FILE:	DRAWING No.	REV
REVIEWED: TB	a:\1996\2309\5551\FIGLOCS.dwg	1	A

N

LEGEND

R Bedrock
Rf Felsenmeer
Tg Glacial Till
Gl Glaciolacustrine
Gf Glaciofluvial
O Organic
S Solifluction
C Cryoturbation

NOTE

FOR LOCATION OF FIGURE 2
REFER TO FIGURE 1.

REFERENCE

GEOGRAPHIC AIR SURVEY LTD. AIR PHOTO G9508039-11-17
ORIGINAL SCALE 1:10,000

0 100 200 300 400 500 metres
SCALE 1:10000

NO	DATE	REVISION	BY	CHK.
A	97/X/X	X	X	X

DIAVIK DIAMOND MINES INC.

Golder Associates

SURFICIAL MATERIALS EAST ISLAND

DRAWN: RFM	DATE: 17 JAN 97	SCALE: AS SHOWN	
CHECKED TB	ACAD FILE: d:\1996\2309\5551\SURF1.dwg	DRAWING No. 2	REV A
REVIEWED TB			

LEGEND

P31 Photo Location and Direction

R Bedrock
Rf Felsenmeer
Tg Glacial Till
Gl Glaciolacustrine
Gf Glaciofluvial
O Organic
S Solifluction
C Cryoturbation

NOTE

FOR LOCATION OF FIGURE 3
REFER TO FIGURE 1.

REFERENCE

GEOGRAPHIC AIR SURVEY LTD. AIR
PHOTO G9508038–10–211
ORIGINAL SCALE 1:10,000

0 100 200 300 400 500 metres

SCALE 1:10000

NO	DATE	REVISION	BY	CHK.
A	97/X/X	X	X	X

DIAVIK DIAMOND MINES INC.

Golder Associates

SURFICIAL MATERIALS EAST ISLAND

DRAWN: RFM	DATE: 17 JAN 97	SCALE: AS SHOWN	
CHECKED: TB	ACAD FILE: J:\1996\2309\5501\SURF1.dwg	DRAWING No. 3	REV A
REVIEWED: TB			

N

LEGEND

P1 Photo Location and Direction

R Bedrock
Rf Felsenmeer
Tg Glacial Till
Gl Glaciolacustrine
Gf Glaciofluvial
O Organic
S Solifluction
C Cryoturbation

NOTE

FOR LOCATION OF FIGURE 4
REFER TO FIGURE 1.

REFERENCE

GEOGRAPHIC AIR SURVEY LTD. AIR PHOTO G9508038–10–209
ORIGINAL SCALE 1:10,000

0 100 200 300 400 500 metres

SCALE 1:10000

NO	DATE	REVISION	BY	CHK.
A	97/X/X	X	X	X

DIAVIK DIAMOND MINES INC.

Golder Associates

SURFICIAL MATERIALS EAST ISLAND

DRAWN: RFM	DATE: 17 JAN 97	SCALE: AS SHOWN	
CHECKED: TB	ACAD FILE:	DRAWING No. 4	REV A
REVIEWED: TB	J:\1996\2309\5551\SURF1.dwg		

LEGEND

P6 Photo Location and Direction

R Bedrock
Rf Felsenmeer
Tg Glacial Till
Gl Glaciolacustrine
Gf Glaciofluvial
O Organic
S Solifluction
C Cryoturbation

NOTE

FOR LOCATION OF FIGURE 5
REFER TO FIGURE 1.

REFERENCE

GEOGRAPHIC AIR SURVEY LTD. AIR PHOTO G9508038-9-160
ORIGINAL SCALE 1:10,000

0 100 200 300 400 500 metres

SCALE 1:10000

NO	DATE	REVISION	BY	CHK.
A	97/X/X	X	X	X

DIAVIK DIAMOND MINES INC.

Golder Associates

SURFICIAL MATERIALS EAST ISLAND

DRAWN: RFM	DATE: 17 JAN 97	SCALE: AS SHOWN	
CHECKED: TB	ACAD FILE: a:\1996\2309\5551\SURF1.dwg	DRAWING No. 5	REV A
REVIEWED: TB			

LEGEND

P12 Photo Location and Direction

R Bedrock
Rf Felsenmeer
Tg Glacial Till
Gl Glaciolacustrine
Gf Glaciofluvial
O Organic
S Solifluction
C Cryoturbation

NOTE

FOR LOCATION OF FIGURE 6
REFER TO FIGURE 1.

REFERENCE

GEOGRAPHIC AIR SURVEY LTD. AIR PHOTO G9508038-9-161
ORIGINAL SCALE 1:10,000

0 100 200 300 400 500 metres

SCALE 1:10000

NO	DATE	REVISION	BY	CHK.
A	97/X/X	X	X	X

DIAVIK DIAMOND MINES INC.

Golder Associates

SURFICIAL MATERIALS EAST ISLAND

DRAWN: RFM	DATE: 17 JAN 97	SCALE: AS SHOWN	
CHECKED: TB	ACAD FILE:	DRAWING No. 6	REV A
REVIEWED: TB	d:\1996\2309\5551\SURFL.dwg		

LEGEND

P17 Photo Location and Direction

R Bedrock
Rf Felsenmeer
Tg Glacial Till
Gl Glaciolacustrine
Gf Glaciofluvial
O Organic
S Solifluction
C Cryoturbation

NOTE

FOR LOCATION OF FIGURE 7
REFER TO FIGURE 1.

REFERENCE

GEOGRAPHIC AIR SURVEY LTD. AIR
PHOTO G9508038-9-162
ORIGINAL SCALE 1:10,000

0 100 200 300 400 500 metres

SCALE 1:10000

NO	DATE	REVISION	BY	CHK.
A	97/X/X	X	X	X

DIAVIK DIAMOND MINES INC.

Golder Associates

SURFICIAL MATERIALS EAST ISLAND

DRAWN: RFM	DATE: 17 JAN 97	SCALE: AS SHOWN	
CHECKED: TB	ACAD FILE: J:\1996\2309\5551\SURF1.dwg	DRAWING No. 7	REV A
REVIEWED: TB			

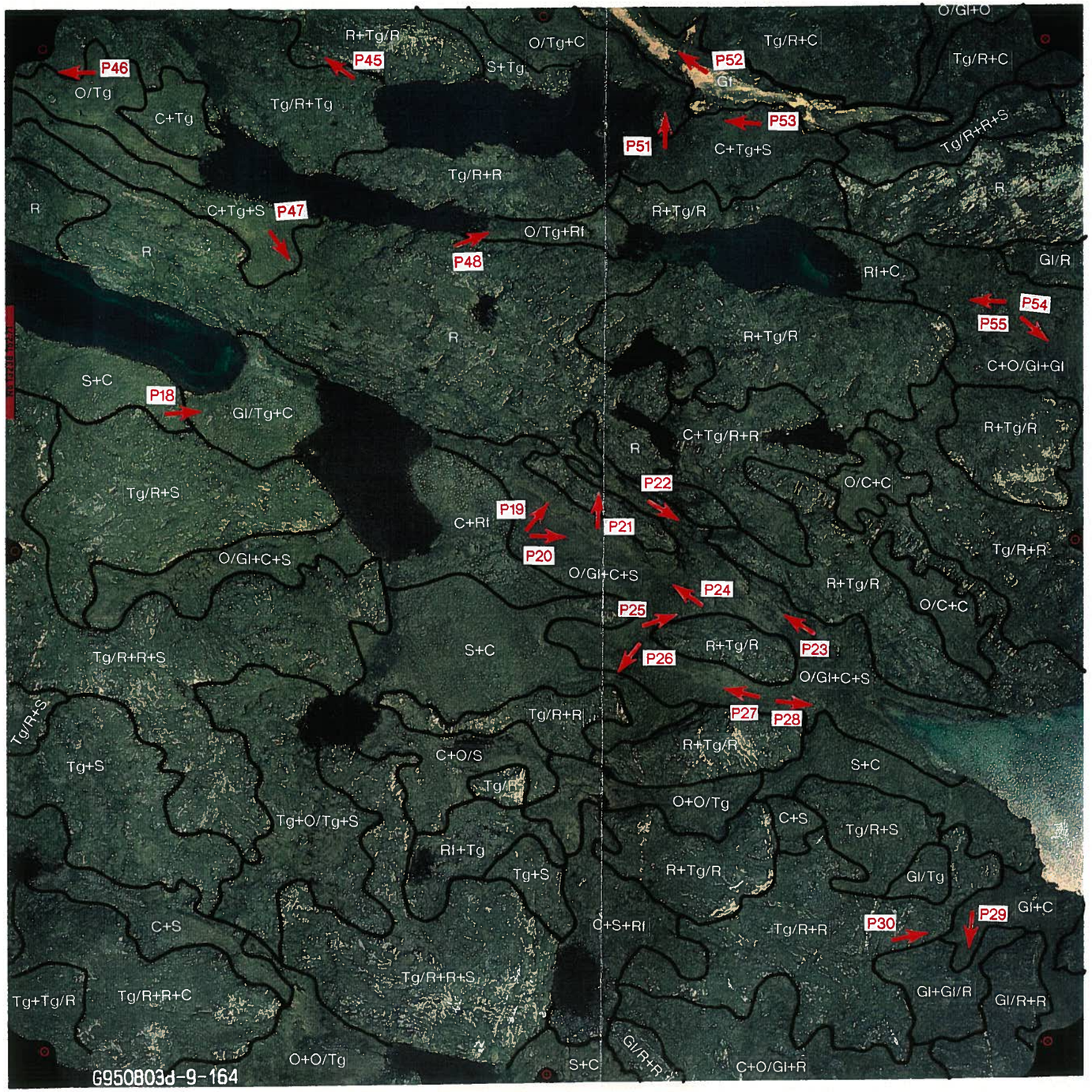

LEGEND

P20 Photo Location and Direction

- R Bedrock
- Rf Felsenmeer
- Tg Glacial Till
- Gl Glaciolacustrine
- Gf Glaciofluvial
- O Organic
- S Solifluction
- C Cryoturbation

NOTE

FOR LOCATION OF FIGURE 8
REFER TO FIGURE 1.

REFERENCE

GEOGRAPHIC AIR SURVEY LTD. AIR PHOTO G9508038-9-164
ORIGINAL SCALE 1:10,000

0 100 200 300 400 500 metres

SCALE 1:10000

NO	DATE	REVISION	BY	CHK
A	97/X/X	X	X	X

DIAVIK DIAMOND MINES INC.

Golder Associates

SURFICIAL MATERIALS EAST ISLAND

DRAWN: RFM	DATE: 17 JAN 97	SCALE: AS SHOWN	
CHECKED: TB	ACAD FILE: J:\1998\2309\5551\SURF1.dwg	DRAWING No. 8	REV A
REVIEWED: TB			

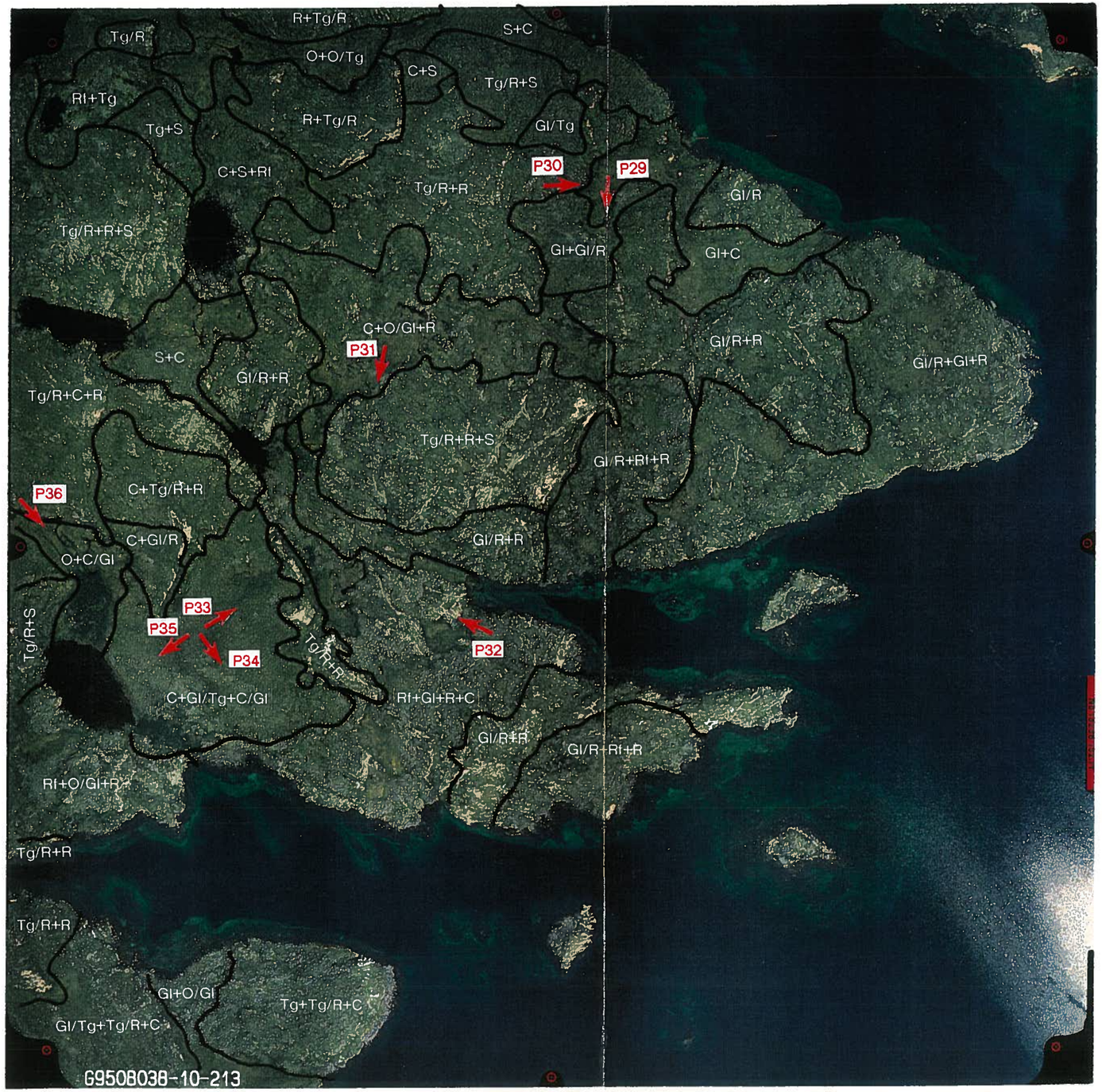

LEGEND

P32 Photo Location and Direction

R	Bedrock
Rf	Felsenmeer
Tg	Glacial Till
Gl	Glaciolacustrine
Gf	Glaciofluvial
O	Organic
S	Solifluction
C	Cryoturbation

NOTE

FOR LOCATION OF FIGURE 9
REFER TO FIGURE 1.

REFERENCE

GEOGRAPHIC AIR SURVEY LTD. AIR PHOTO G9508038–10–213
ORIGINAL SCALE 1:10,000

0 100 200 300 400 500 metres

SCALE 1:10000

NO	DATE	REVISION	BY	CHK.
A	97/X/X	X	X	X

DIAVIK DIAMOND MINES INC.

Golder Associates

SURFICIAL MATERIALS EAST ISLAND

DRAWN: RFM	DATE: 17 JAN 97	SCALE: AS SHOWN	
CHECKED: TB	ACAD FILE:	DRAWING No. 9	REV A
REVIEWED: TB	z:\1998\2309\5551\SURF1.dwg		

LEGEND

P59 Photo Location and Direction

R Bedrock
Rf Felsenmeer
Tg Glacial Till
Gl Glaciolacustrine
Gf Glaciofluvial
O Organic
S Solifluction
C Cryoturbation

NOTE

FOR LOCATION OF FIGURE 10
REFER TO FIGURE 1.

REFERENCE

GEOGRAPHIC AIR SURVEY LTD. AIR PHOTO G9508038-9-166
ORIGINAL SCALE 1:10,000

0 100 200 300 400 500 metres

SCALE 1:10000

NO	DATE	REVISION	BY	CHK.
A	97/X/X	X	X	X

DIAVIK DIAMOND MINES INC.

Golder Associates

SURFICIAL MATERIALS EAST ISLAND

DRAWN: RFM	DATE: 17 JAN 97	SCALE: AS SHOWN	
CHECKED TB	ACAD FILE: J:\1996\2309\5551\SURF1.dwg	DRAWING No. 10	REV A
REVIEWED TB			

LEGEND

P78 Photo Location and Direction

R Bedrock
Rf Felsenmeer
Tg Glacial Till
Gl Glaciolacustrine
Gf Glaciofluvial
O Organic
S Solifluction
C Cryoturbation

NOTE

FOR LOCATION OF FIGURE 11
REFER TO FIGURE 1.

REFERENCE

GEOGRAPHIC AIR SURVEY LTD. AIR PHOTO G9508038-8-118
ORIGINAL SCALE 1:10,000

0 100 200 300 400 500 metres

SCALE 1:10000

NO	DATE	REVISION	BY	CHK.
A	97/X/X	X	X	X

DIAVIK DIAMOND MINES INC.

Golder Associates

SURFICIAL MATERIALS EAST ISLAND

DRAWN: RFM	DATE: 17 JAN 97	SCALE: AS SHOWN	
CHECKED: TB	ACAD FILE:	DRAWING No. 11	REV A
REVIEWED: TB	J:\1956\2309\55511\SURF1.dwg		

LEGEND

P74 Photo Location and Direction

R Bedrock
Rf Felsenmeer
Tg Glacial Till
Gl Glaciolacustrine
Gf Glaciofluvial
O Organic
S Solifluction
C Cryoturbation

NOTE

FOR LOCATION OF FIGURE 12
REFER TO FIGURE 1.

REFERENCE

GEOGRAPHIC AIR SURVEY LTD. AIR PHOTO G9508038-8-116
ORIGINAL SCALE 1:10,000

0 100 200 300 400 500 metres
SCALE 1:10000

NO	DATE	REVISION	BY	CHK.
A	97/X/X	X	X	X

DIAVIK DIAMOND MINES INC.

Golder Associates

SURFICIAL MATERIALS EAST ISLAND

DRAWN: RFM	DATE: 17 JAN 97	SCALE: AS SHOWN	
CHECKED TB	ACAD FILE:	DRAWING No. 12	REV A
REVIEWED TB	J:\1996\2309\5551\SURF1.dwg		

LEGEND

P70 Photo Location and Direction

R Bedrock
Rf Felsenmeer
Tg Glacial Till
Gl Glaciolacustrine
Gf Glaciofluvial
O Organic
S Solifluction
C Cryoturbation

NOTE

FOR LOCATION OF FIGURE 13
REFER TO FIGURE 1.

REFERENCE

GEOGRAPHIC AIR SURVEY LTD. AIR
PHOTO G9508038-8-114
ORIGINAL SCALE 1:10,000

0 100 200 300 400 500 metres
SCALE 1:10000

NO	DATE	REVISION	BY	CHK.
A	97/X/X	X	X	X

DIAVIK DIAMOND MINES INC.

Golder Associates

SURFICIAL MATERIALS EAST ISLAND

DRAWN: RFM	DATE: 17 JAN 97	SCALE: AS SHOWN	
CHECKED TB	ACAD FILE:	DRAWING No. 13	REV A
REVIEWED TB	J:\1995\2309\55551\SURF1.dwg		

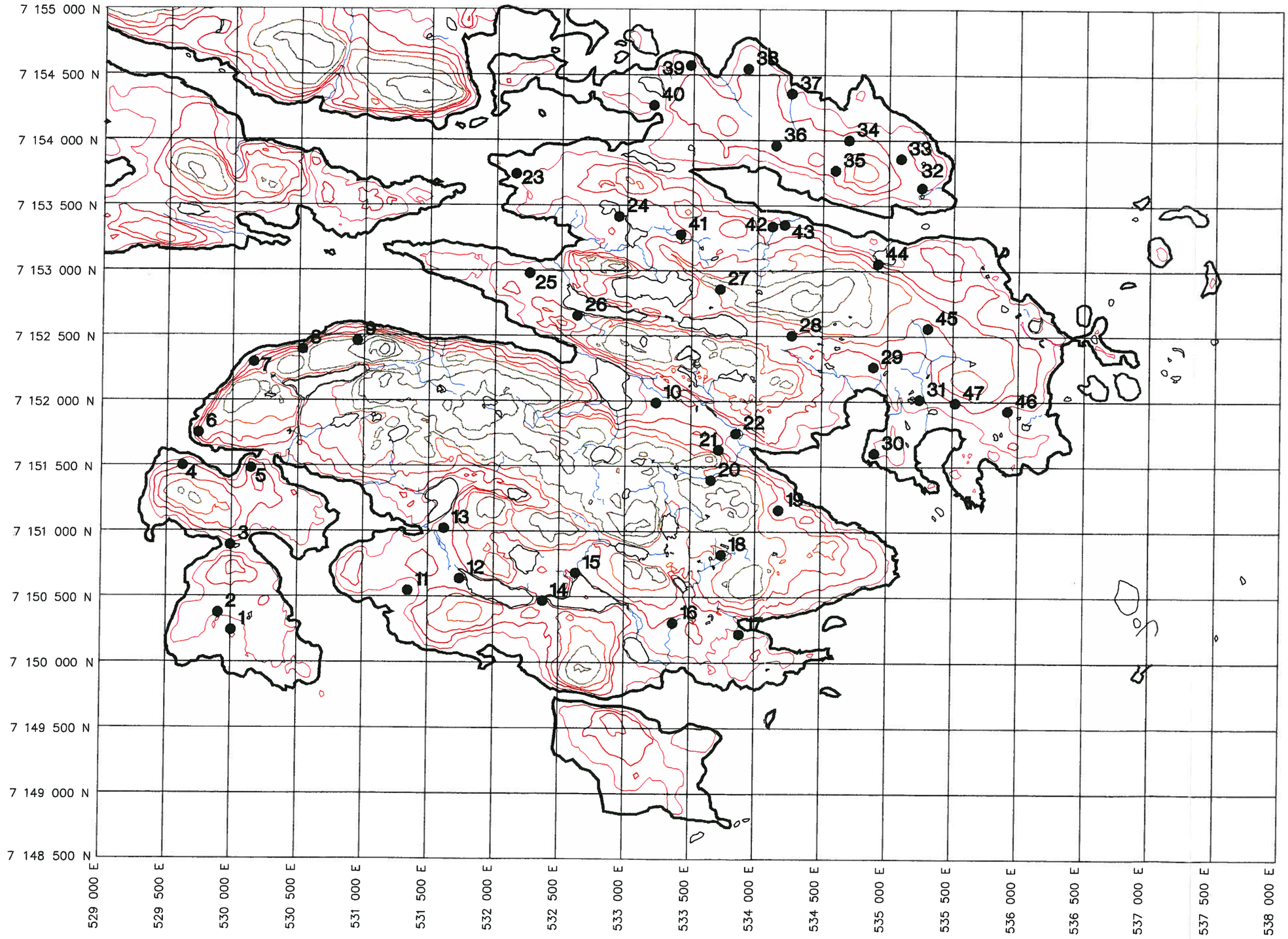

LEGEND

- 11 SOIL INSPECTION SITE
- CONTOUR ELEVATION 420m
- CONTOUR ELEVATION 425m
- CONTOUR ELEVATION 430m
- CONTOUR ELEVATION 435m
- CONTOUR ELEVATION 440m
- CONTOUR ELEVATION 445m
- CONTOUR ELEVATION 450m
- CONTOUR ELEVATION 455m
- CONTOUR ELEVATION 460m
- CONTOUR ELEVATION 465m

SCALE 1:30,000

0 500 1000 1500 2000

NO	DATE	REVISION	BY	CHK
A	97/X/X	X	X	X

DIAVIK DIAMOND MINES INC.

Golder Associates

SOIL INSPECTION SITES EAST ISLAND

DRAWN: RFM	DATE: 17 JAN 97	SCALE: AS SHOWN	
CHECKED RFM	ACAD FILE: d:\1998\23091\5551\SOILPNTS.dwg	DRAWING No. 14	REV A
REVIEWED TB			

PLATES

Plate 1 Looking north from Soil Inspection Site #1. Organic over glaciolacustrine in the foreground, and glacial till and glacial till over bedrock in the background.

Plate 2 Looking north-west from Soil Inspection Site #2. Organic over glaciolacustrine in foreground and extending to lake, and glacial till on each side of photo.

Plate 3 Looking north from Soil Inspection Site #3. Organic over glaciolacustrine in foreground, and very stony glacial till over bedrock in background. Note vegetation in areas protected from the wind on leeward slope, and where snow would accumulate.

Plate 4 Looking south from Soil Inspection Site #3. Very stony glacial till, with some areas of exposed bedrock.

Plate 5 Looking east from Soil Inspection Site #3. Organic over glaciolacustrine. These types of areas are the best source of materials for reclamation.

Plate 6 Looking north-east from Soil Inspection Site #4. Glaciolacustrine over glacial till in foreground, and glacial till and bedrock in background. Note frost boils in foreground. These features provide a good source of materials for reclamation.

Plate 7 Looking north-west towards Soil Inspection Site #5. Glaciolacustrine over glacial till in middle of photo, and very stony glacial till in foreground and background.

Plate 8 Looking north-east at a south aspect (leeward) slope. Shrubs are protected from the wind. Frost boils (foreground) provide a good source of reclamation materials.

Plate 9 Looking east at an area of extensive frost boiling and solifluction. These materials should be salvaged and stockpiled for later use during reclamation.

Plate 10 Looking west from small inland lake at an area of frost boiling. These areas are valuable sources for reclamation materials and should be selectively salvaged prior to stockpiling of the granite.

Plate 11 Looking north at a narrow canyon. The reclamation of the granite stockpile should include features such as this to add diversity to the landscape, as well as promoting proper surface drainage.

Plate 12 Looking south-west towards Soil Inspection Site #4. Note lower density of surface stones on lower slope (glaciolacustrine) compared to upper slope and foreground of photo (glacial till).

Plate 13 Looking south-south-east from Soil Inspection Site #7. The soils are frost boiled (cryoturbated) and slowly moving downslope (soliflucted). These types of materials should be salvaged for reclamation purposes.

Plate 14 Looking east towards Soil Inspection Site #8. Toe of solifluction lobe.

Plate 15 Looking south-south-east from Soil Inspection Site #8 (toe of solifluction lobe). These materials should be salvaged for reclamation purposes prior to stockpiling of the granite.

Plate 16 Looking south-south-west towards Soil Inspection Site #9. This is a relatively recent solifluction lobe, judging from the lack of vegetation cover. This is a good source of reclamation material.

Plate 17 Looking south from shore of lake inlet. Most of the material is moving slowly downslope (solifluction), with some frost boils (foreground).

Plate 18 Looking east at glaciolacustrine deposit at end of lake inlet. This material should be selectively removed for use during reclamation. Bedrock ridge in background.

Plate 19 Looking north-north-east from Soil Inspection Site #10. Organic over glaciolacustrine, with some frost boils. This is the best type of material for reclamation, since it contains organic material and moderately fine-textured mineral material.

Plate 20 Looking east-south-east from Soil Inspection Site #10. This is an extensive deposit of organic over glaciolacustrine material.

Plate 21 Looking north from a bedrock ridge at an organic over glaciolacustrine deposit. This material is of value for reclamation.

Plate 22 Looking south-east at an extensive deposit of organic over glaciolacustrine. A lot of the area is frost boiled.

Plate 23 Looking west-north-west from Soil Inspection Site #22 at an extensive deposit of organic over glaciolacustrine. The organics are between 20 to 40 cm thick in this area.

Plate 24 Looking west-north-west from Soil Inspection Site #21 at an extensive glaciolacustrine deposit. These deposits have been extensively frost boiled.

Plate 25 Looking east-north-east down a frost boiled, soliflucted slope towards Soil Inspection Site #21. Bedrock and very stony glacial till over bedrock in background.

Plate 26 Looking south-west at an organic over glaciolacustrine deposit. Bedrock ridge in background.

Plate 27 Looking west from Soil Inspection Site #20. Organic over frost boiled glaciolacustrine material. This material should be salvaged prior to stockpiling the granite, so as not to sterilise this valuable reclamation material.

Plate 28 Looking east from Soil Inspection Site #20. Organic over glaciolacustrine material right to shore of lake. Glacial till over bedrock in background. Note camp on horizon.

Plate 29 Looking south from Soil Inspection Site #19. Primarily frost boiled glaciolacustrine material. These types of areas are important sources for reclamation materials.

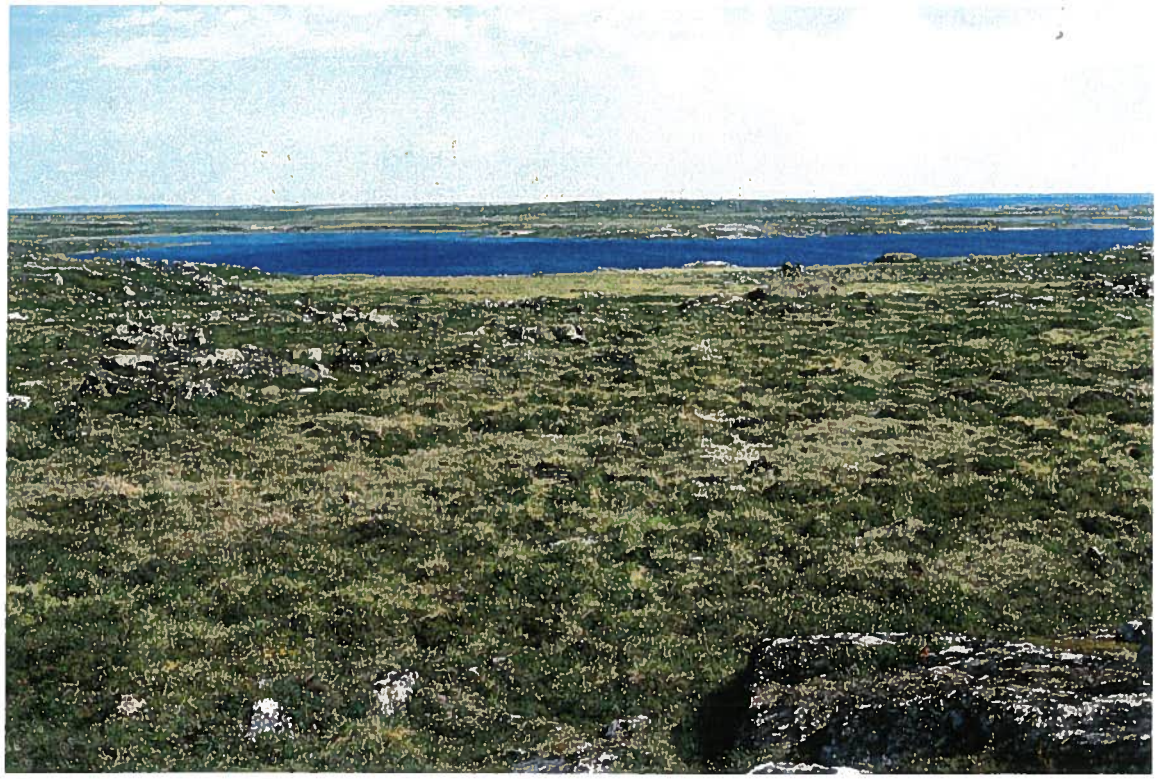

Plate 30 Looking east-north-east toward Soil Inspection Site #19. Glaciolacustrine over glacial till in foreground and glaciolacustrine in middle of photo. Note camp on horizon.

Plate 31 Looking south from Soil Inspection Site #18. Frost boiled glaciolacustrine material in foreground, and glacial till over bedrock in background.

Plate 32 Looking west-north-west from Soil Inspection Site #17. Glaciolacustrine in foreground, and bedrock ridge in background.

Plate 33 Looking east-north-east from Soil Inspection Site #16. Glaciolacustrine and organic over glaciolacustrine deposits. Most of this area is frost boiled. Bedrock ridge in background.

Plate 34 Looking south-east from Soil Inspection Site #16. The frost boiled glaciolacustrine material should be salvaged prior to granite stockpiling, for later use during reclamation.

Plate 35 Looking south-west from Soil Inspection Site #16. Frost boiled glaciolacustrine material in foreground, and bedrock ridge in right background. Note solifluction lobes on ridge.

Plate 36 Looking south-east across small creek at organic area. Surface drainage channels, similar to this one, will need to be established on the reclaimed surface.

Plate 37 Looking north-east towards Soil Inspection Site #15. Organic over glacial till deposit. These materials should be salvaged prior to granite stockpiling, for later use during reclamation. Bedrock ridge in background.

Plate 38 Looking north-west at a small organic deposit. Even these small deposits should be salvaged prior to granite stockpiling, so as not to sterilise them from use during reclamation.

Plate 39 Looking south-west from Soil Inspection Site #14. Mainly frost boiled glacial till in this area. Even though the material has numerous stones (40%) throughout the profile, it may still be worth salvaging for reclamation.

Plate 40 Looking west-south-west at organic area (light green tone). Bedrock in immediate foreground, and glacial till over bedrock in foreground to shore of lake.

Plate 41 Looking south-east (upslope) from Soil Inspection Site 13. Frost boiled glacial till. This material may have some value for reclamation.

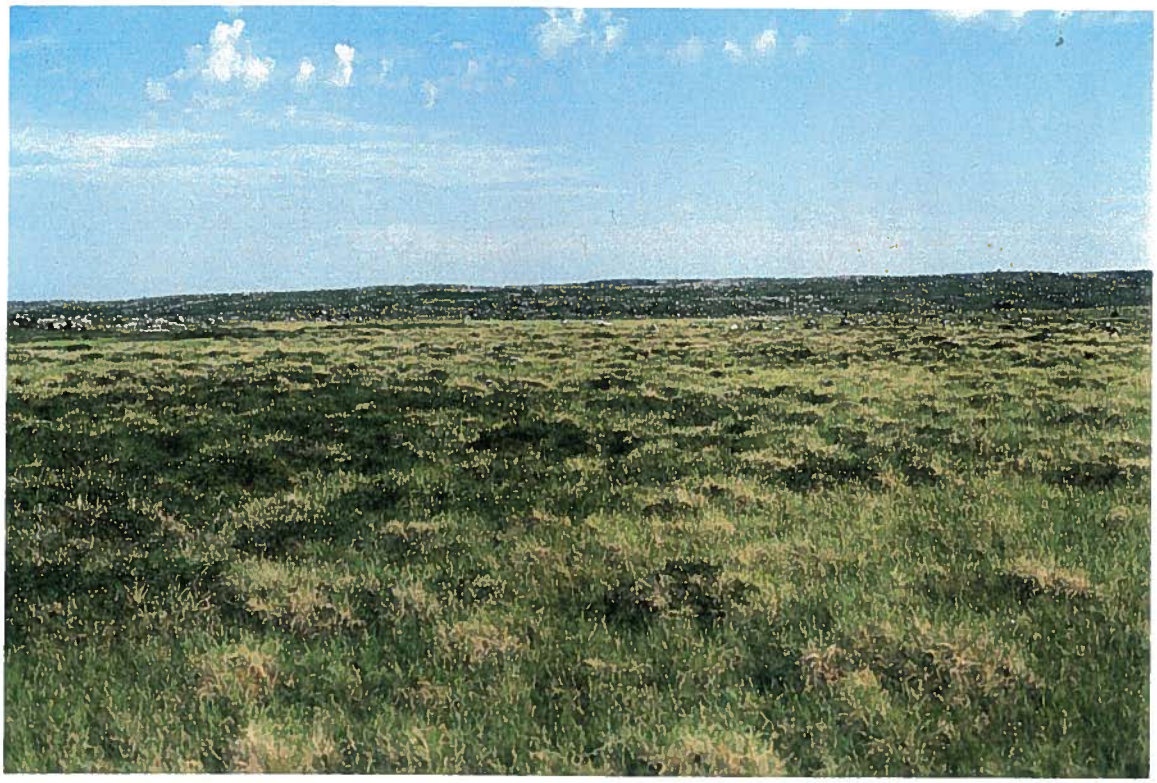

Plate 42 Looking north-west from Soil Inspection Site #12. Organic and organic over glacial till deposits. This area is an important source of reclamation materials.

Plate 43 Looking east-north-east from Soil Inspection Site #11. Organic over glaciolacustrine deposits in foreground, and frost boiled glaciolacustrine deposits in background. Note absense of surface stones in glaciolacustrine deposit.

Plate 44 Looking south-west from Soil Inspection Site #11. These organic and glaciolacustrine materials are valuable for reclamation and should be salvaged prior to granite stockpiling.

Plate 45 Looking west-north-west toward Soil Inspection Site #25. Mainly glacial till, however, numerous small patches of organic over glacial till (light green areas). These small deposits should be selectively salvaged for later use during reclamation.

Plate 46 Looking west from Soil Inspection Site #25. Organic over glacial till. Most of the materials in these depressional areas are suitable for reclamation purposes.

Plate 47 Looking south-south-east from Soil Inspection Site #26. Frost boiled glaciolacustrine on lower slopes and frost boiled glacial till on upper slopes. The glaciolacustrine deposits are slightly stony to nonstony and are valuable reclamation materials.

Plate 48 Looking east-north-east at an organic over glacial till deposit between two inland lakes. Although small in area, it contains an abundant supply of good quality reclamation material.

Plate 49 Looking north-west from bedrock ridge at a large organic and glaciolacustrine deposit. This area is an important source of reclamation materials.

Plate 50 Looking northeast at a large organic and glaciolacustrine deposit. Note glaciofluvial feature (esker) in upper right of photo.

Plate 51 Looking north at a major glaciofluvial feature (esker). The esker is primarily sand and fine gravel and would be of limited use for reclamation.

Plate 52 Looking north-west from esker at a large organic and frost boiled deposit. These materials would be a valuable resource for reclamation.

Plate 53 Looking west from Soil Inspection Site #27. Primarily frost boiled glacial till.

Plate 54 Looking east-south-east from Soil Inspection Site #28. Organic over glaciolacustrine deposits. This is an excellent source of good quality reclamation materials.

Plate 55 Looking west from Soil Inspection Site #28 at organic over glaciolacustrine deposit.

Plate 56 Looking east-south-east at organic (light green tones), glaciolacustrine and glaciofluvial (light tan tones) deposits. This is an excellent source area for reclamation materials.

Plate 57 Looking east at organic (light green tones) and glaciolacustrine deposits. Note camp on horizon.

Plate 58 Looking north from Soil Inspection Site #29. This glaciolacustrine deposit is an excellent source of good quality reclamation material.

Plate 59 Looking north from Soil Inspection Site #31. Frost boiled glaciolacustrine material. This material could be used for reclamation. The surface organic layer is an important source of native seed and stolons.

Plate 60 Looking south-east toward Soil Inspection Site #46. The organic and glaciolacustrine deposits, and frost boiled materials in this area can be selectively salvaged from the stony glacial tills for use as reclamation materials.

Plate 61 Looking south from Soil Inspection Site #45. Frost boiled and soliflucted glaciolacustrine material. This slightly stony to nonstony material is very suitable for reclamation.

Plate 62 Looking north from Soil Inspection Site #45. Organic over glaciolacustrine in foreground, and frost boiled and soliflucted material in background.

Plate 63 Looking east-south-east from Soil Inspection Site #44. Frosted boiled and soliflucted glacial till on this 15% slope. This material is of little to no value for reclamation.

Plate 64 Looking north-west at glaciolacustrine deposit (lower slope). This material is a valuable resource for reclamation.

Plate 65 Looking north-east from Soil Inspection Site #42. Organic over glaciolacustrine.

Plate 66 Looking south-west from Soil Inspection Site #42. Organic over glaciolacustrine.

Plate 67 Looking south-east from Soil Inspection Site #41. Organic and organic over glacial till. The organic materials should be salvaged from the stony glacial tills for use during reclamation. Note esker in background.

Plate 68 Looking west towards large organic deposit (light green tone). Note esker beyond organic deposit.

Plate 69 Looking north-north-west from Soil Inspection Site #24. Organic over glaciofluvial. The organic material contains a reserve of native seeds and stolons, and is therefore of value for reclamation.

Plate 70 Looking east from Soil Inspection Site #23. Organic over glaciolacustrine. These deposits are a valuable source for reclamation materials.

Plate 71 Looking north-east from Soil Inspection Site #40. Frost boiled glaciofluvial. This material is of limited value for reclamation.

Plate 72 Looking south-south-west from Soil Inspection Site #39. Frost boiled glaciolacustrine over glacial till on lower slopes and frost boiled glacial till on upper slopes. This material would be of limited value for reclamation.

Plate 73 Looking north-west from Soil Inspection Site #38. Knobs are part of an outwash (esker) complex. Organic over glaciolacustrine.

Plate 74 Looking south-south-west from Soil Inspection Site #38. Frost boiled glaciolacustrine on lower slopes, and frost boiled glacial till on upper slopes.

Plate 75 Looking south-south-west from Soil Inspection Site #37. Frost boiled glaciolacustrine on lower slopes and frost boiled glacial till on upper slopes.

Plate 76 Looking north-east from Soil Inspection Site #36. Organic and organic over glaciolacustrine. This area is a valuable source for reclamation materials.

Plate 77 Looking north-east from Soil Inspection Site #35. Frost boiled glacial till. This material is of limited value for reclamation.

Plate 78 Looking north from Soil Inspection Site #34. Organic over frost boiled glacial till. The organic material is of value for reclamation as it contains a reserve of native seeds and stolons.

Plate 79 Looking north-west from Soil Inspection Site #33. Organic over glaciofluvial.

Plate 80 Looking south from Soil Inspection Site #32. Frost boiled glacial till. This material is of limited value for reclamation.

TP-8-11-0

1. PURPOSE

This technical procedure describes the methodology to be used for the investigation and sampling of surficial soils. Contained within are detailed investigation and sampling instructions.

2. APPLICABILITY

This technical procedure is applicable to any person involved in the investigation and manual sampling of surficial soils.

3. DEFINITIONS

3.1 Chain-of Custody Forms

Standardised forms are used as a means of keeping close track of soil samples taken from the field and transported to laboratories for analysis. Whenever the samples are transported from the field, the custody is relinquished from the delivery person to the receiver by signatures on the forms. These forms substantially decrease the risk of losing samples because they provide a clear record of the chain of transport and handling of the samples.

3.2 Surficial Soil

Refers to the unconsolidated material on the ground surface that serves as a natural medium for the growth of plants, and that has been subjected to or influenced by parent material, climate, macro and microorganisms, and topography over time producing a material that differs physically, chemically, biologically and morphologically from the material from which it was derived.

4. REFERENCES AND SUGGESTED READING

Agriculture Canada Expert Committee on Soil Survey. 1987. The Canadian System of Soil Classification. 2nd ed. Agric. Can. Publ. 1646. 164pp.

5. DISCUSSION

5.1 General Safety

Refer to Golder Associates Ltd. Safety Manual.

5.2 Methods

Soils will be investigated based on a visual examination of excavated pits, with information gathered being recorded on Soil Inspection Sheets (see attached example). Certain soils are sampled from the various horizons identified during the soil investigation. Samples are taken using a shovel, trowel, or auger. Each sample is individually bagged and labeled to location and analysis to be performed. Each sample is also indicated on the appropriate soil inspection sheet as a cross reference.

5.3 Site Location

Samples are taken from the various soil horizons exposed in the excavated pits used for soil characterisation. Sites will be pinpointed on air photos and maps in the field, and marked using the global positioning system.

5.4 Sample Handling

Soil samples are placed in ziploc type plastic bags. The bagged soil samples are stored in cardboard boxes to protect the plastic bags from ripping during transport to the lab.

5.5 Cleaning Sampling Equipment

The shovel, trowel, or auger used to take each sample is wiped clean of any soil residue after each sample is taken to minimise contamination of other samples.

5.6 Field Records and Logbook

For proper interpretation of field survey results, thorough documentation of all field investigation and sample collection activities is required. All logbooks should be perfect-bound and waterproof, forms should be preprinted on waterproof paper, and only indelible ink and pencil (if form or paper is wet) should be used.

Characteristics of the soils being investigated are recorded on Soil Inspection Sheets (see attached example). Soil samples are also recorded on these sheets. Basic information from each site investigated or sampled, such as site number and GPS location, will be recorded in a logbook.

All pertinent information on field activities and sampling must be recorded in an appropriate (i.e. waterproof) bound logbook. The field crew leader is responsible for ensuring that sufficent detail is recorded in the logbook. The logbook must be complete enough to enabel someone unfamiliar with the project to completely reconstruct field activity without relying on the memory of the field crew. All entries must be made in indelible ink, with each page numbered, signed and dated by the author, and a line drawn through the remainder of any partly used page. All corrections are made by a single-line cross-out of the error, entering the correct information, dating and initialing the change. Upon return to the office, all field notes must be photocopied and placed in the appropriate project files.

Entries in the field logbook must include:

- Purpose of proposed sampling effort
- Date and time (24 hour clock) of sampling
- Names of field crew leader an tema members
- Description of each sampling site, including information on any photographs that may be taken.
- Location of each sampling site, name and number, applicable navigational coordinates, waterbody name/segment numbers.
- Details of sampling method and effort, particularly deviations from Specific Work Instructions.
- Clear identification of site names and sample numbers.
- Field observations.
- Field measurements taken (recorded on Soil Inspection Sheets)

Sample shipping information.

The field logbook should also be used to document any additional information on sample collection activities or any unusula activities observed or problems encountered that would be useful to the project manager when evaluating the quality of the soil and terrain data.

To document field activities, sample identification labels, Chain-of-Custody forms, field logbooks, field record sheets (Appendix A) should be used. This will serve as an overall "Chain-of-Custody" documenting all field samples and field events beginning with sample collection through, preservation and shipment to the laboratory.

6. EQUIPMENT

6.1 Sampling and Investigation Equipment

Soils will be investigated and sampled with a shovel, trowel and auger.

6.2 Field Location Equipment and Logs

The following pieces of equipment are required to properly investigate and sample soils.

- perfect bound, water-proof field logbook
- soil inspection sheets (sample attached)
- maps and aerial photographs of the site
- indelible ink pens and felt tip markers, and pencils
- munsell colour chart
- 12 metre tape measure
- bottle of clean water
- bottle of 10% hydrochloric acid
- clean rags
- clinometre

- compass
- shovel
- trowel
- soil auger
- penetrometer
- plastic ziploc type storage bags
- pH meter
- metre wheel

SWI-150

SOIL INSPECTION SHEET

Diavik Diamond Mines Inc. Project

Project # 962-2309 (Task 5551) **SITE** _____

Inspectors:_____ **GPS #**_____

Inspection Date:_____**(day),** _____**(month),** _____**(year)**

Inspection Time:_____**(24 hour clock)**

Slope:_____ **Apect:**_____ **Topography:**_____

Drainage:_____ **Surface Stoniness:**_____

Slope Position:_____ **Parent Material:**_____

HORIZON	DEPTH (cm)	BDY	COLOUR	TEXTURE	STRUCTURE	STONES (%)	CONS	EFF	SAMPLE #
	-								
	-								
	-								
	-								
	-								

NOTES

_____

_____

_____

_____

_____

Photographs: Numbers_____ **Roll**_____

SPECIFIC WORK INSTRUCTIONS

SPECIFIC WORK INSTRUCTIONS **SWI No.:** SWI-15.0

Project: Diavik Dimond Mines Inc. Baseline Summer Survey (SOIL INVESTIGATION AND SAMPLING)

Date: JULY 11 1996

Author:

To:

cc: Kym Holley **File No.:**

Subject: SUMMER 1996 SOIL INVESTIGATION AND SAMPLING **Job/Task No.:** 962-2309/5551

Scope of Work/Specific Instructions:

Soil Investigation: Soil investigation sites will be located using maps and aerial photographs of the local study area. The location and number of sites may be relocated or increased/decreased to ensure all soil types are represented. Each site will be pinpointed using a global positioning system, with the location being recorded. A photographic record will be kept of the existing terrain at each site. Terrain characteristics will also be recorded. At each site a soil pit will be excavated using a track shovel, trowel and auger. Soil profile characteristics (including drainage and parent material) will be investigated based on a visual examination of the excavated pits. Information will be recorded on Soil Inspection Sheets (see attached). Certain soils will be sampled from the various horizons identified during the soil investigation. Samples will be taken using the shovel or trowel. Each sample will be individually bagged and labeled with site location for analysis.

All health and safety procedures for Golder and Kennecott must be strictly adhered to during the work period.

Crew is to telephone the Golder office in Calgary a minimum of once every three days. If problems in the field arise, phone the project manager at once.

Technician: n/a

Discipline Leader: Tim Bossenberry

Technical Supervisor: David Kerr

Project Manager: Gordon Macdonald

Work Product(s) Due By: 03 September 1996

Allocated Man-hours: Task 5551

Subcontractor (as applicable): n/a

Special Handling Requirements: Forms to use: Soil Inspection Sheets (see attached), Chain of Custody Forms, Analytical Request Forms.

Applicable Specs. and Procedures: Golder T.P. 8.10-0

Project Manager Approval/Date: **QA Manager/Date:**

Appendix X-8

Climate Change Adaption Project

Climate Change Adaptation Project

Rio Tinto

Climate Change Impacts in the Diavik Region of Northern Canada

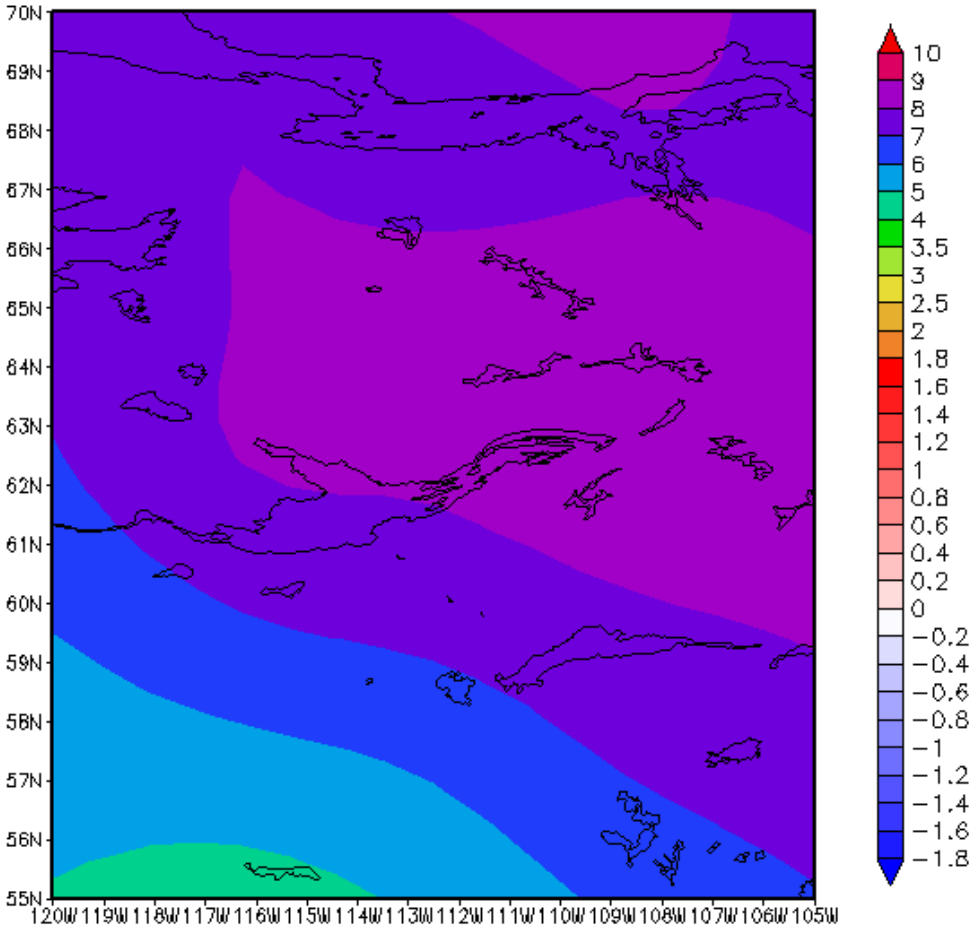

Future climate mean minimum temperature change predictions for Diavik for December 2060-2069

4 July 2008

Executive Summary

Caveat: Climate modelling is still an emerging science with practical constraints imposed by limitations on supercomputing and data processing of terabytes of data. Although the analyses that follow are based upon the best currently available science, there are inherent limitations on the skill of the techniques used. Due care should be exercised when interpreting these results.

Future climate analyses, spanning the period out to 2060, were conducted for Rio Tinto's Diavik Diamond Mine Incorporated (DDMI) operations in the Northwest Territories Province of northern Canada. The mine site at Diavik (latitude 64º 30'N, longitude 110º 20' W), is located approximately 300 km northeast of Yellowknife and is connected to this location by a 350km long ice road that is constructed annually, 75% of which is built over frozen lakes. The analyses and data provided can be used to assess what the future climate impacts are likely to be upon this ice road, as well as at the mine site itself.

The data for the analyses was from a suite of climate models especially configured and run to meet Rio Tinto's global climate change requirements which was completed in May 2007. The northern Canadian region has high resolution data (notionally a grid box size 20km x 20km, although the narrowing of the longitudes at these locations improves the effective resolution closer to 15km) available across the entire region and for the offshore waters from a suite of 12 individual century-long Coupled Ocean – Atmosphere Climate Model runs from the Oklahoma University. The numerical scheme used in the climate models means that meteorological features are able to be resolved down to an effective resolution of close to 12km.

The future climate models used a mix of mathematical and physical climate model schemes as used in the leading climate modeling centres of the world, including the Hadley Centre in the United Kingdom, and the National Center for Atmospheric Research in the USA, combined with refined versions developed by Prof. Lance Leslie at the Oklahoma University. These models have been used and verified extensively in other climate studies focused upon future climate severe weather in widely separated parts of the world for the insurance and mining industries, and have very high long term atmospheric energy stability, a critical feature of climate models.

The climate models were run in two sets of six model members, one set of which simulated the historical climate of the world, and the other set simulated the future climate using an up-to-date adjustment, valid as at early 2007 to the IPCC's A2 scenario, making the prediction most closely resembling the A1B greenhouse gas/aerosol forcing scenario (referred to as the future greenhouse gas climate, or simply "future climate" throughout this report). This approach is undertaken to identify the best performing climate model and to allow the mean of all six model members to be calculated, thereby providing future climate predictions that possess a higher level of confidence than can be achieved from a single climate model run. An analysis of all of the ensemble model runs demonstrated that the ensemble mean of the six member future Coupled Global Climate Model runs is most likely to be the best predictor of the future climate for the northern Canadian region. The analyses that are provided in the detailed report contain a mix of results from the average of the six ensemble model members and the more detailed results from the model closest to the ensemble mean.

The preliminary investigations of the future climate impacts on the northern Canadian region, under what is currently considered to be the most likely IPCC future greenhouse gas / aerosol emission scenario for the period from the present out to the year 2060, are summarized in the following paragraphs.

Temperature

The ensemble mean climate model predictions of minimum, mean and maximum temperatures were validated against those observed at Environment Canada's weather stations at Lupin A and Ekati and the limited Rio Tinto Canada data from the Diavik mine site for the period through to 2007. There are warm model biases evident for the period from January through to June, greatest in April for Diavik, Ekati and Lupin A data but not for the longer period Fort Reliance data. These biases are not thought to affect the predicted trends and bias corrections were applied to the future climate predictions to account for these differences. There are also warming trends through the model validation period (1970 to 2007) that fit the overall trends observed in the various observational data, although some months in the observational dataset were subject to

multi-decadal oscillations that have the effect of producing transient cooling trends when viewed in isolation and over a limited period of record. Attachments 4a and b North that show the spatial distributions of minimum and maximum temperature across the northern Canadian region should be consulted for further information.

Using the bias corrected linear trends, the predicted annual temperature rises for Diavik, from 1970 to 2060, were as follows:

- Maxima: from -8.3^{o}C to -2.8^{o}C, a rise of 5.5^{o}C over the 90 year period. This equates to an annual maximum temperature increase of 0.061^{o}C.
- Mean temperature: from -11.0^{o}C to -6.0^{o}C, a rise of 5.0^{o}C over the 90-year period. This equates to an annual mean temperature increase of approximately 0.056^{o}C.
- Minima: from -14.7^{o}C to -9.3^{o}C, a rise of 5.4^{o}C over the 90-year period. This equates to an annual minimum temperature increase of approximately 0.060^{o}C.

The predicted temperature changes can be applied to the historical daily air temperature data to determine likely changes to the Freezing Index at any given time through the future climate period. The predicted changes in surface temperature can also be applied in the same way to historical surface temperature data to determine expected changes in the Surface Freezing Index into the future. Although it is outside the scope of this project to determine the Freezing Index, the future climate model predictions clearly show a marked reduction in the number of below-freezing days are to be expected in the future climate, with this reduction accelerating through the future climate period.

Other changes identified were:

- The greatest predicted warming is through the winter to spring period, meaning the length of the snow season, and hence the duration when the ice road is likely to be viable, are likely to be greatly shortened in the future climate period.
- The greatest predicted warming was forecast for January minima with the forecast bias-corrected change from -33.6^{o}C in 1970 up to -25.4^{o}C by the year 2060, a very large rise of 8.2^{o}C over the 90-year period.
- The predicted warming through the summer months, typified by those for the month of July, were much smaller with rises of around 2^{o}C predicted for the

minimum, mean and maximum temperatures out to the year 2060. However, the hottest of the climate models indicated one-off much warmer years could be expected with the potential for temperature jumps in the future of up to 5^{o}C for individual summer months. This should also apply to the maximum temperatures at Diavik.

- July is predicted to remain the hottest month.
- By the year 2060, the average monthly temperatures are very likely to be hotter than the hottest months recorded in the historic record for most months of the year.
- Maximum temperatures were predicted to rise fastest through the winter and spring months.
- The predicted warming was forecast to continue well beyond the end of the analysis period.

Precipitation

It must be noted that the climate modelling technique produces rainfall predictions across a 20km x 20km grid, or an area of 400km^2, whereas the observations from Diavik are from point locations with the diameter of the precipitation gauges used being typically around 10cm. The precipitation received is inherently highly variable in space and time and snow is a particularly difficult phenomenon to accurately measure. It is almost impossible to separate wind driven snow from freshly fallen snow. There are also strong topographic influences that affect the distributions and intensities of the precipitation producing weather systems. Hence the uncertainty in future climate predictions for precipitation must be considered to be higher than those for temperature. The climate models are less likely to predict extremely heavy or light precipitation events that would completely match the observed extreme spot snow and rainfalls. There are also strong multi-decadal signals evident in the precipitation record with trends over the full length of the observational record being markedly different to those over the shorter validation period. It was also discovered that the way in which the historically measured snowfall was converted into equivalent liquid precipitation changed from month to month and year to year at Ekati, producing spurious trends and biases for many of the months

in which snowfall dominates the precipitation record. Therefore there are inherent uncertainties in the observational records to consider.

The predicted trends in precipitation were more complex than for temperature. For most months of the year the climate models predicted increases in precipitation, although the magnitudes of these increases varied markedly from month to month. The predicted annual increase in precipitation went from an average of near 310mm in 1970 to near 360mm by 2060, which equates to a rise of around 16% over 90 years.

In the winter months the quantity of precipitation received at Diavik is relatively small due to the very cold conditions. The climate model predictions for the mean monthly December precipitation ranges from around 18mm in 1970 up to 25.5mm by the year 2060, an increase of 7.5mm, which equates to a very large, in percentage terms, rise of near 42% for the month. A large increase in precipitation, in percentage terms, was predicted for the mid winter month of January with an increase of 24% forecast. The actual quantity of snow involved is small, being only 4mm in liquid precipitation terms, or roughly4cm of snow. The intensity of the heavier snowfalls are also expected to increase for many of the coolest months of the year with most of the months, but not all, expected to also experience an increase in the frequency of these heavier precipitation events.

Looking at the summer precipitation, the ensemble mean model prediction for Diavik varies from month to month. In June the predictions are for no appreciable change through the future climate period although the wettest months are forecast to increase from around 65mm up to 83mm. For July the climate models predict a slight decline in rainfall, from an average of near 38mm in 1970 to near 35mm by 2060, or a decline of approximately 8%. The climate model predictions indicate a decreasing frequency of extreme heavy rainfall events, although the two heaviest July rainfall predictions lie in the future climate period, indicating new extremes of heavy rainfall are possible in the future climate period, even if the heaviest falls become less frequent than they currently are. In August the climate models return to predicting increases in precipitation, a trend that continues through the remainder of the year.

There is a marked multi-decadal oscillation in the future climate predictions, indicating these changes will not be steady increases but rather a general increasing trend interrupted by large excursions from the mean. There is a marked leveling off of the precipitation increases indicated through the future climate period beyond around model year 2025. The predictions indicate there will be fewer dry years in the future and a trend towards gradually increasing extremely wet years, by Diavik standards, although this region will still only have relatively modest precipitation through the future climate period in comparison to warmer regions of the world. The wettest years tend to occur as lone events, as are the predicted driest years.

Extreme Precipitation Events

The climate model predictions for Diavik vary from month to month. In general the predictions favour increases in both the intensity and frequency of heavy precipitation events through the future climate period. December was predicted to have a particularly large increase in extreme precipitation, jumping from 45mm for the year through the validation period to 65mm in the future climate. Although heavy by local standards, the climate models do not predict falls through the future climate period as great as for other parts of Canada.

The predictions at the lowest end of the precipitation spectrum (the dry years) are for either no change through the future climate period or for a gradual increase in the quantities of precipitation to be expected in the driest months and years.

Snowfall and Accumulation

A set of four attachments have been prepared that show the decadal monthly average snow cover, snow cover anomaly, snow depth and snow depth anomaly charts for the northern Canadian region (Attachments 3b, c, d and e North) and these should be consulted for details on the changes in the amount and depth of snowfall through the Diavik to Yellowknife region. There are also monthly decadal surface temperate average and anomaly charts that map the changes in the temperature of the ground across this

region through the future climate period (Attachments 4, 4a North), which help to quantify the changes in the ground surface that affect snow and ice accumulations.

The anomaly charts for the month of January, representative of the mid winter months, show an interesting transition in the predicted snow cover. The initial predictions show an increase in snow cover over most of the region with the greatest increases centred over and southeast of the Great Slave Lake, reaching a peak of around 7.5% in the 2020-2029 decade. This anomaly pattern then generally changes to one where decreasing snow cover dominates from the decades from 2040 onwards and particularly the 2060-2069 decade. For the onset period of the snow season, the November predictions for Diavik it is likely the snow cover would vary significantly along the access road to Diavik from year to year in the expected future climate. Although this would be positive in some years, the model tends to slightly favour the years of reduced snow cover overall.

The month of April is one where the snow cover is still relatively high in the Diavik region but is rapidly declining in the Great Slave Lake region. The climate model predictions show a very interesting and unusual sequence of anomaly charts. For the first three decades – from 2010 out to 2039, the climate models predict a general increasing trend for snow cover with a strong increase predicted for the 2030-2039 decade over the north and east of the Great Slave Lake, including an area where the snow cover is predicted to increase by over 25%. The increases in cover over the Diavik region during this period are slight, given that this region has a high snow cover to begin with. However, the climate models then predict a sudden and strong reversal in this trend, particularly in the region just north of the Great Slave Lake where snow cover is predicted to decline by over 15% in the 2040-2049 decade increasing to over 22.5% by the 2060-2069 decade. The changes in snow cover at Diavik itself are not shown to be great being within +/- 2.5% for all the decades apart from the 2050-2059 decade when a 7.5% decline in coverage is predicted.
Overall the predictions show a shortening of the length of the season which has snow accumulations on the ground with a general reduction of the depth of the snow, particularly during the months of onset and cessation of the snowfall.

Wind Speeds and Directions

Attachments 5 and 5a North provides analyses of the expected average monthly wind speeds and directions and the corresponding anomalies across northern Canada out to 2060 relative to the 1970-1999 reference period. The future changes in winds are quite variable from season to season and decade to decade. Strong multi-decadal oscillations are evident in the wind anomaly predictions for each month, indicating the changes will not be simple progressions of a trend, but rather complex changes to the weather patterns throughout the future climate period.

For the mid winter month of January the climate model predictions are for initial reversals of the wind anomalies, starting with a southeasterly wind anomaly in the 2000-2009 decade but turning to a northwesterly anomaly for the following one. Then the trend is for a progressive clockwise swing in the wind anomalies. Initially in the 2010-2019 decade the wind anomalies are predicted to be from the northwest. By the 2020-2029 decade the model predicts a swing back to the north to northeast, continuing around to the northeast by the 2030-2039 decade. Then there is an abrupt reversal of the wind anomalies predicted for the 2040-2049 decade with wind anomalies forecast to change to a south southwesterly. Speeds throughout this period of time are generally within the 0.5 to 1.0m/s range for most of the region. This then settles in as the dominant wind anomaly through the remainder of the future climate analysis period, strengthening through the 2060-2069 decade.

During April the predictions are for a general increase in the easterly wind anomalies, which would serve to increase the wind speeds to the north of Diavik and decrease them to the south of the Great Slave Lake.

In July there is a predominant trend towards a strengthening of the westerly wind anomalies across much of the region to the north of the Great Slake Lake with the strength of the anomalies increasing northwards and reaching close to 1m/s in regions near the Coronation Gulf. There is a more erratic increase in the westerlies to the south of the Great Slave Lake.

During October the climate model predictions highlight a move into a future climate regime with growing variability of the weather patterns, with these variations having signatures that last a decade or more at a time.

With increased energy predicted in the summer time wind regimes and marked multi-decadal oscillations predicted in the weather systems throughout the future climate period, it is likely there will be an intensification of some of the associated weather systems. Although a detailed investigation of individual weather systems is required to quantify this, it is likely that some of these systems will have the potential to increase the severe wind storm risk for the Diavik region.

Relative Humidity

Attachment 6 North provides an analysis of the expected changes in the relative humidity over the northern Canadian region, including the Diavik to Yellowknife area. During the cold winter months there are only small changes in relative humidity predicted. The relative humidity anomalies begin to increase as temperatures rise in April. For this month a band of decreased relative humidity, mostly in the 1-2% range but with a small area of over 2%, develops with an orientation from the west northwest towards the east southeast, centred just north of the Great Slave Lake and hence across the region between Yellowknife and Diavik. Bands of increasing relative humidity, mostly only around 1%, simultaneously form over the eastern parts of the Coronation Gulf and to the southwest of the Great Slave Lake. Diavik itself tends to remain in a region of little change in relative humidity.

In the mid summer month of July the predicted changes in relative humidity become relatively large with a reasonably significant amount of variability from decade to decade. During this time of the year a region of decreasing relative humidity can be seen to become established in a west to east oriented band roughly centred over or along the northern shore-line of the Great Slave Lake. For most of the future climate decades this decrease peaks around 3% although through the 2060-2069 a decrease of over 8% is predicted, including the Yellowknife region. There tends to be a countering increase in

relative humidity across the northern parts of the region, particularly near Coronation Gulf where the humidity is predicted to rise by 4-5% for several of the future climate decades, and further north. Diavik itself tends to experience little change or slight increases in humidity through to the end of the 2050-2059 decade. After this the relative humidity starts to decline.

In October the changes in relative humidity become insignificant once more.

Evaporation

Attachments 7 and 7a North provides analyses of the expected changes in the environmental evaporation for the northern Canadian region, including the Diavik to Yellowknife region. This is a measure of the actual quantity of water evaporated from the environment and not potential evaporation, which only applies to open water surfaces. The evaporation anomalies are derived based upon changes relative to the current decade (2000-2009). For the mid winter months, typified by January, the change in the evaporation rates remain low due to the continuing very cold temperatures at this time of the year. The evaporation anomaly rates remain low until the warmer months of the year, particularly north of the Great Slave Lake.

The trends in evaporation become far more significant as temperatures rise from May through to August. The trends are bimodal in nature with decreases in evaporation rates predicted across the northern parts of this region with a corresponding increase in evaporation rates to the south. There is a marked increase in evaporation rate through the central region in a band that lies across the Great Slave Lake through the 2020-2029 decade with a corresponding decrease in evaporation through the Coronation Gulf and further northwards. The 2030-2039 decade marks a transition period with the evaporation rates then accelerating over the Great Slave Lake and areas southwards, particularly to the southeast near Lake Athabasca where evaporation rates climb to over 0.4mm/day. Diavik remains in a region of slightly reduced evaporation through this period of time although at Yellowknife the evaporation rates are predicted to start to increase. Through the 2050-2059 and 2060-2069 decades the strengths of the evaporation rate anomalies tends to increase with greatest increases over and southeast

of the Great Slave Lake, again peaking to the southeast over and beyond Lake Athabasca. There are opposing decreases in evaporation across the north of this region. Diavik is predicted to remain in a region where slight decreases in evaporation rate dominate, although the Yellowknife region is predicted to experience increases of around 0.25mm/day by the 2060-2069 decade.

The evaporation anomaly rates again become small from October onwards as temperatures fall.

Solar Radiation

Attachments 8 and 8a North provides analyses of the expected changes in solar radiation across northern Canada out to 2060 relative to the 1970-1999 reference period. Given there is little incident solar radiation during the winter months the anomalies are small through out the region for these months, although what trend there is indicates a reduction in incoming solar radiation due to increased cloud cover. For the mid spring month of April, both Diavik and Yellowknife tend to lie close to the no change line through the future climate period and fluctuate between increases and decreases in solar radiation through the future climate period in the order of 6 Watts/m^2.

During the mid summer month of July very strong decreases in solar radiation, in excess of 30 Watts/m^2, are predicted for the northern part of the northern Canadian domain for the period beyond 2050, as well as slightly lower reductions in solar radiation over the regions south of Lake Athabasca. However, in the area from Diavik down to Yellowknife tends to be in an area where the solar radiation anomalies oscillate from increases to decreases with the size of the anomalies remaining generally below 6 Watts/m^2.

Overall the larger solar radiation anomalies are predicted to occur during the warmer months of the year and reach a peak during the months of June and July. Although the solar radiation anomaly patterns show considerable variability from decade to decade, there is a marked move towards decreases in solar radiation across this region as a whole, although Diavik and Yellowknife are expected to remain away from the largest changes.

Climate Change Impacts in the Diavik Region of Northern Canada

1. The Current Climate

This report covers the key location of Diavik and its' access road to Yellowknife, both of which form a part of Rio Tinto's DDMI operations. The mine site at Diavik (64º 30'N, 110º 20'W) is located in the Northwest Territories of northern Canada, approximately 300km to the northeast of Yellowknife. A 350km long ice road connects the two locations that is constructed annually, with 75% built over frozen lakes. The future response of the frozen lakes to a changing climate is therefore a key concern. Although the authors of this report do not have a sufficient understanding of the response rates of these ice lakes to changing weather conditions, it is hoped that the data and analyses provided here will enable those with this knowledge to be able to determine how the ice lakes will fare in the future.

The Google Earth image in Figure 1 shows the relative positions of Diavik and Yellowknife and the general topography of the region. The climate data used to validate the climate models' performance near Diavik is from a combination of the data measured near the Diavik mine site and from the Environment Canada weather stations at Ekati and Lupin A. Obviously is it preferable to have historical climate data from the same location as the climate model data but the length of the climate data for Diavik is too short for proper climate analysis. This is the reason why historical data from relatively climate stations is also included.

Diavik's inland location protects it from the more extreme stormy weather conditions that affect coastal parts of Canada, although the intense polar low pressure systems bring recurring blizzards during the cooler months of the year. Its' northern latitude and high elevation (Ekati is at an elevation of 470m and it is assumed Diavik has a similar elevation) means it has very cold winters with minima having dropped as low as -47.0^{o}C, although the average winter temperature during the coldest month of January is -33.4^{o}C (both figures for Ekati). The high elevation and northern latitude of the Diavik to

Yellowknife region also allows its snow pack to last well through the spring months. The mean monthly temperatures climb through the 0^{o}C during the month of May (average temperature -3.7^{o}C) then drop below zero again early in the month of October (average temperature -9.1^{o}C). The summers are cool to mild with temperatures rising to an average minimum of 10.2^{o}C during its warmest month, July, with a mean monthly temperature near 14.2^{o}C and an average maximum a mild 18.2^{o}C. Infrequent relatively warm days can occur in this location with the all time record maximum temperature reaching 28.0^{o}C. Being very cold through winter, little precipitation falls through the winter months, almost all of it falling as snow. The precipitation rapidly increases during the warmer months, August being the wettest month of the year with an average of 64mm. The precipitation is almost entirely rain at this time of the year.

The prevailing wind regime across the Diavik to Yellowknife region tends to be westerly winds through much of the year. However they do become quite changeable through certain months and particularly during the April to June period. At this time of the year the centres of the polar lows that dominate the regions weather tend to track eastwards between Diavik and Yellowknife. The complete set of long term average wind speed and direction charts are to be found in the report entitled “Wind average charts Canada – 2”.

The weather tends to be dominated by the passage of sometimes intense polar low pressure systems separated by transient highs. As a result of this there can be very abrupt changes in the weather from mild and sunny conditions to heavy rain or snow within a short space of time. The passage of warm and cold fronts brings the heaviest rain and snow falls. There are few thunderstorms at this high latitude and any that do occur are likely to be experienced in summer.

Diavik’s temperature and precipitation climate will be discussed in more detail in the following sections.

Figure 1: Location map showing Rio Tinto DDMI's Diavik operations and Yellowknife with the location of the climate model data extraction location shown as the Diavik yellow marker. Map courtesy of Google Earth.

1.1 Precipitation

The available climate data is from the Diavik mine site supplemented by the Ekati and Lupin A data from Environment Canada's records. Some long term data is also used for Fort Reliance, although this is a little further away from Diavik than is desirable. The

Environment Canada climate records are relatively complete, although there are small numbers of missing months or months when the data is estimated. The historical records can be considered comparatively good quality datasets, although there appear to be problems with the Ekati total precipitation data for months when snow falls. Diavik's precipitation is summarized in Figures 2a and b and in Table 1, although the data is actually from nearby stations. The total precipitation refers to the sum of melted snow together with any rainfall that occurred during the same month. It should be noted at this point that it is very difficult to accurately measure snowfall as the catch efficiency of snow gauges decreases rapidly with increasing exposure to wind, and it is also virtually impossible to separate out wind-driven snow that fell elsewhere and then was blown across the snow gauge from freshly fallen snow. The broader climate records shows the Diavik region has moderate to fresh average wind speeds throughout the year but with bouts of very strong winds. Hence it is to be assumed there is a large degree of uncertainty in the underlying accuracy of the snowfall records at all of the locations used in this study caused by the difficulty in measuring snowfall, not by the quality of the underlying observations program. The measurement of liquid rainfall should be considered more accurate, although the efficiency of rain gauges also declines significantly with increasing wind speed.

Diavik, being an elevated inland location with a northerly latitude, has an Arctic-type of precipitation climate with relatively low quantities of snow falling during the very cold winter months but relatively good falls of rain being received through the few warmer months of the year. There are no long term Climate Normals available for Diavik, Ekati or Lupin A from Environment Canada and so, as a general guide to the long term climate of the region, data from the nearest station with long term data, Fort Reliance (62^{o} 34'N, 109^{o} 10'W), is shown in Table 1, and graphically in Figure 2a. As Table 1 shows, from November through to March the precipitation falls almost entirely as snow. Then there is a rapid transition in the snow/rain mix from April, when snow still dominates, to May when most of the precipitation falls in liquid form. The period from June to August inclusive is almost all rain with the reverse transition occurring during the months of October and November. The greatest amount of snow is shown to fall in the month of November (29.9cm) with the greatest amount of rainfall (50mm) falling in August, which also has the greatest total precipitation. The driest month is March with around 9.6mm of

total precipitation, followed closely by February with 9.9mm. The annual total precipitation is a modest 272mm, concentrated in the warmer months of the year from June to October.

	Jan	Feb	Mar	Apr	May	Jun	Jul	Aug	Sep	Oct	Nov	Dec	Year
Rainfall (mm)	0	0	0	2.5	13.9	29.3	33.2	50	29.9	13.1	0.4	0	172.3
Snowfall (cm)	17.8	16.6	15.2	15.9	5	1.1	0	0	2.6	20.3	29.9	22.4	146.8
Precipitation (mm)	11	9.9	9.6	14.5	19.2	30.5	33.2	50	32.2	28.5	19.7	13.7	272
Ave Snow Depth	32	38	41	36	9	0	0	0	0	2	14	25	16
Median Snow Depth	31	38	41	37	7	0	0	0	0	1	15	25	16
Snow Depth End Mth	36	40	42	25	0	0	0	0	0	6	19	29	N/A

Table 1: Average monthly rainfall (mm), snowfall (cm), total precipitation (mm, average snow depth, median snow depth and snow depth at end of month (cm) for Fort Reliance from 1971 to 2000. Data courtesy of Environment Canada.

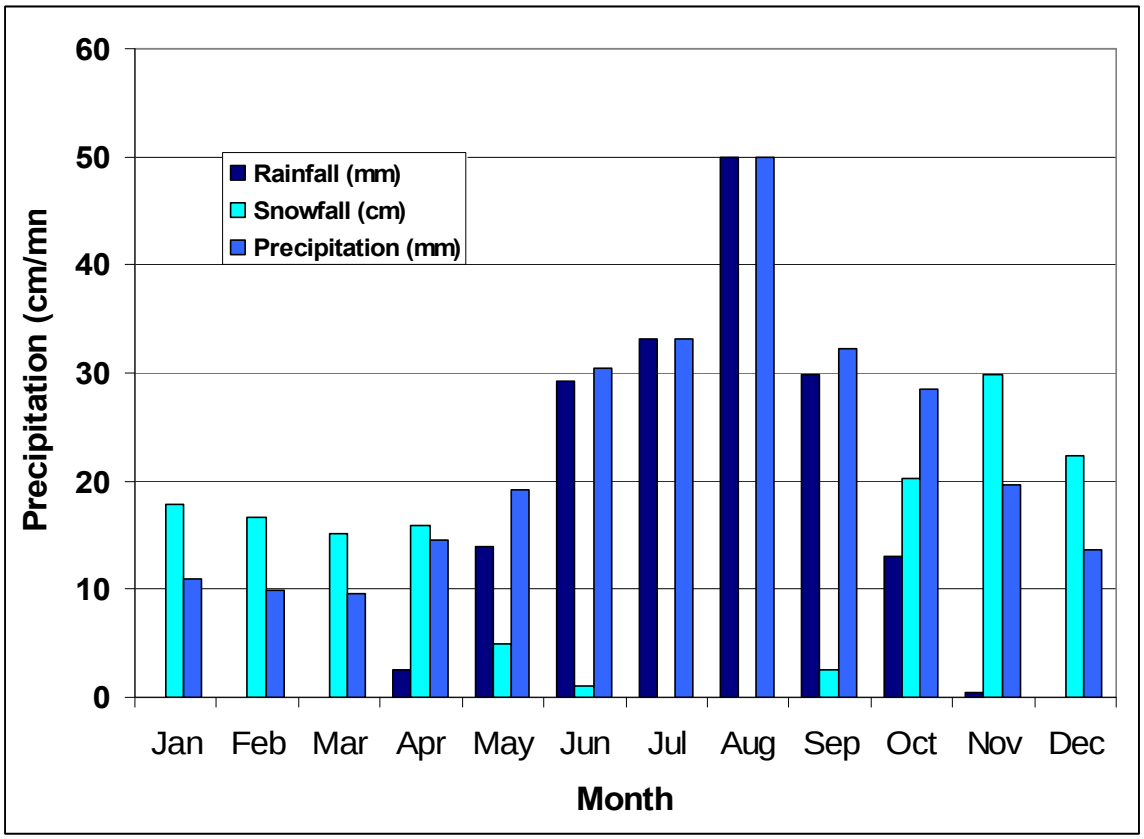

Figure 2a: Average monthly rainfall, snowfall and total precipitation graph for Fort Reliance. Data courtesy of Environment Canada.

Although the mix of snow and rainfall for the Fort Reliance area is generally indicative of that to be expected at Diavik, there are localised differences from one place to another across this region. This can be seen by comparing the longer term data in Figure 2a with the shorter length of total precipitation data from Ekati in Figure 2b. August is still the wettest month although Ekati has a larger average rainfall. The driest month shifts to April followed by January at Ekati, rather than March, although the late winter to early spring period is still the driest time of the year. The shorter period of records for Ekati means the individual months are likely to have been biased by anomalously wet and dry months within the available period of record and hence they should not be considered true long term averages. The conversion of snowfall into liquid precipitation is also an issue here. None-the-less, they do provide a useful guide of the likely climate at Diavik.

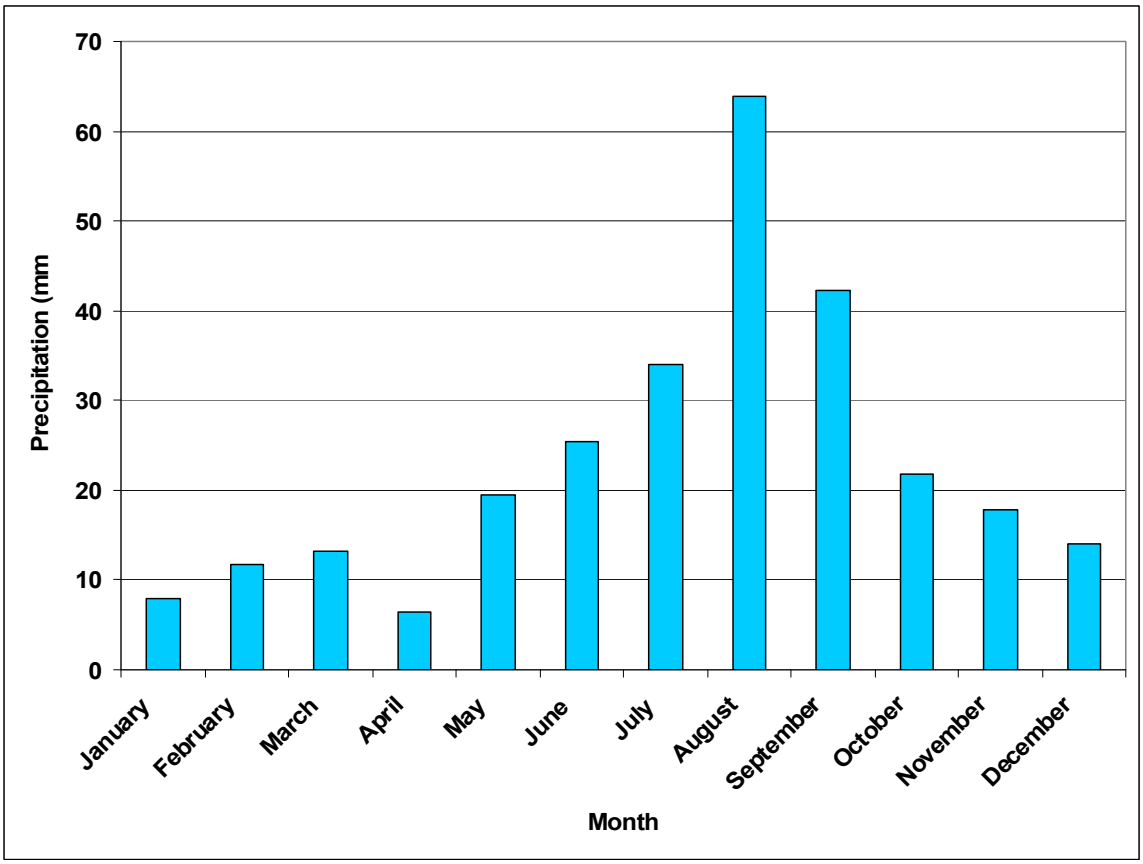

Figure 2b: Average monthly total precipitation graph for Ekati. Data courtesy of Environment Canada.

There is, unfortunately, insufficient length of observations from Diavik or Ekati to prepare a long term trend analysis. Some indications of the trends in the climate variables can be gained from viewing the time series data plotted in the model validation section that follows, although it must be noted that the trends in the observational data must be treated with extreme caution as they are prone to be heavily affected by naturally occurring multi-decadal climate variability.

The original rainfall records show the annual totals are significantly affected by one-off heavy rainfall or snowfall events in only one or two months of the year, highlighting the fact that the rainfall regime in this part of Canada are quite variable from month to month and year to year. It can be concluded that the magnitude of any long term changes in precipitation at Diavik are smaller than the magnitude of the naturally occurring multi-decadal oscillations.

1.2. Temperature

The temperature regime for the Diavik region is characterized by relatively mild summers and very cold winter days and nights, as can be seen in Table 2 and Figure 3 where the historical minimum, mean and maximum temperature records for Fort Reliance, in lieu of the limited data available for Diavik, for the period from 1971 to 2000 are shown on a monthly basis. The diurnal range ranges from around 12.1^{o}C in the spring months of March and April to a small 5.6 ^{o}C in the mid-fall month of October. January is the coldest month for both maximum and minimum temperatures with a rapid rise in temperatures during the March to May period. July is the warmest month, again for both maximum and minimum temperatures, with the decline in temperatures during the October to December period being more rapid than the rate of the transition out of the winter period.

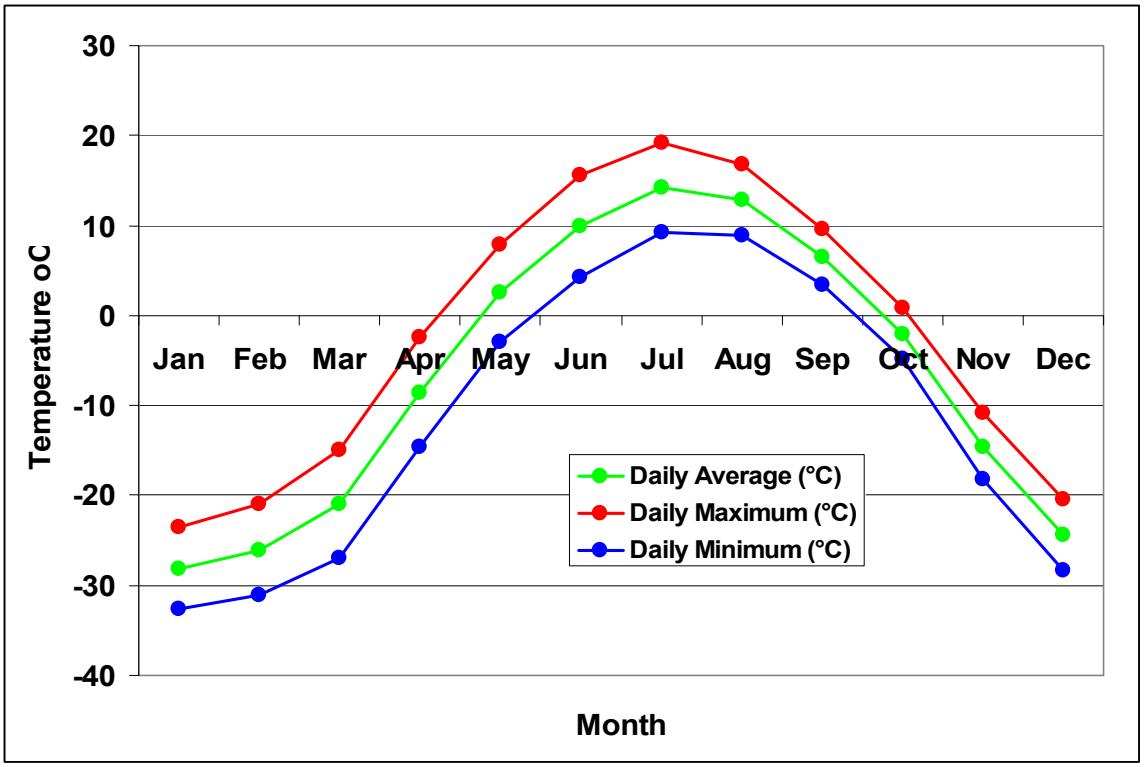

Figure 3: Average monthly maximum, mean and minimum temperature graph for Fort Reliance, in lieu of Diavik. Data courtesy of Environment Canada.

	Jan	Feb	Mar	Apr	May	Jun	Jul	Aug	Sep	Oct	Nov	Dec	Year
Daily Ave (°C)	-28.1	-26.1	-21	-8.6	2.5	9.9	14.3	12.9	6.5	-2	-14.6	-24.4	-6.6
Std Devn	4	5.3	3.4	3.6	3.4	1.6	1.5	1.8	1.8	2.1	3.3	4.1	5.2
Daily Max (°C)	-23.5	-21	-14.9	-2.5	7.9	15.6	19.2	16.8	9.6	0.8	-10.9	-20.4	-2
Daily Min (°C)	-32.7	-31.1	-27	-14.6	-2.9	4.2	9.3	8.9	3.4	-4.8	-18.2	-28.4	-11.2

Table 2: Monthly maximum, mean and minimum temperature (^{o}C), together with the standard deviation for the mean daily temperature for Fort Reliance, in lieu of data for Diavik, from 1971 to 2000. Data courtesy of Environment Canada.

In Diavik Attachment 2 in Figures DT1a, b and c the time series of minimum, mean and maximum temperatures are shown for the very limited period of record from 1997 through to 2008. From the data it can be seen that there is typically a variation in the monthly temperatures of around +/-1.5^{o}C from the mean monthly values from one year to the next, although there are one-off large variations of up to 10^{o}C for individual months, notably February. It is not possible to determine whether these larger

excursions from the mean are true or errors in the dataset. The winter time temperatures, both maximum and minimum, can be seen to experience the greatest inter-annual variations with February being the most variable month of all. The summer months, in contrast to this, have a relatively stable temperature regime from year to year. The trends will be discussed in the model comparison section that follows.

2. Future Climate Simulations of the Diavik Region of Northern Canada

The analysis that follows utilizes the results from a suite of 12 ensemble Coupled Atmosphere-Ocean Climate model runs. The modeling procedure used is described in simple terms earlier in this report. Six of the ensemble model members were run with the observed historical greenhouse gas forcing through to 2000, after which time the greenhouse gas and aerosol concentrations were held at a constant level. This represents the historical climate. The other six model members were subject to a modified IPCC A2 scenario, similar to the A1B scenario, greenhouse gas / aerosol forcing from 2000 onwards. The ensemble means were then calculated for each suite of model runs and these are considered most likely to provide the most reliable information on future climate trends. The model member closest to the ensemble mean was then selected as being the model with both the greatest likelihood of representing the future climate and as the model that is likely to provide the most accurate detailed information on variability associated with climate change. The fields from either of the ensemble mean or of the model closest to the ensemble mean, form the basis of most of the analyses that follow, with all ensemble members used for some of the analyses.

2.1 Future Temperature Changes

In the following section the modelled changes in mean monthly air temperatures for the Diavik region will be discussed. Firstly the model validation will be discussed, followed by the future climate predictions. The model validation data is available for each month of the year. However, in order to reduce the size of the report, the comparisons between the historical observations of air temperature and the climate model predictions are discussed primarily for the middle month for each of the four seasons, namely January,

April, July and October, as well as annually, although interesting aspects of the other months are also covered..

2.1.1 Model Validation

In Figures DT2a, b and c, the mean of the six climate model member predictions, the predictions from the warmest climate model member and the predictions from the coldest climate model member for the period from 1970 through to 2007 are shown for the coldest month of the year, January, against the available observations from Diavik, Ekati and Lupin A for the minimum, mean and maximum temperatures. Linear trend lines are included for the ensemble mean of the models for maximum, mean and minimum temperatures and also for the coldest of the model members. It must be remembered that the climate model predictions are for the air temperature at 2m above the ground for the 20km square grid point centred upon Diavik, whereas the comparison observations are from the temperatures measured inside a temperature screen at a point location. Hence the two datasets are not exactly the same, but are as close as the current state of the science will allow.

From the comparisons it can be seen that the ensemble mean modelled maximum, minimum and mean temperatures have a warm bias of approximately 2-3^{o}C against the observed Diavik minimum temperature data, based upon observations from Lupin A, Ekati and Diavik, which grows to around 4^{o}C for the maximum temperatures. This bias is much smaller if the long term Fort Reliance data is used (se Table 2). The coldest of the model members is, in general able to reproduce the observed temperature records best. It is likely this is also the model that is best able to predict snowfall and hence is the most skillful at these latitudes at this time of the year. The observed, ensemble mean model and coldest ensemble model member trends are very close to each other, with the linear trend lines showing very similar rates of warming through the 1970 to 2007 model validation period. This warming is predicted to affect both minimum and maximum temperatures. The observed mean temperatures show greater year to year variability, which is to be expected as the ensemble mean is an average of six models, which reduces the amount of inter-annual variability. The variability in the coldest of the model members is quite similar o that of the observations showing the individual climate model

members are able to replicate the prevailing weather conditions at this location quite well.

The observed maximum temperatures, shown in Figure DT2c, tend have mean values close to those of the coldest ensemble model. The variability of maximum temperatures is greater than the climate model mean but similar to the coldest model member's variability. The hottest observed maxima remain within the envelope described by the hottest of the climate model members throughout the validation period and generally lie in the region between the ensemble mean and the coldest model member. The observed extreme low monthly maximum temperatures are very close to the coldest of the climate model member's predictions. This means that the coldest model member replicates the observed mean maxima well, with the observed extremes of temperature lying within the bounds of the range of predictions from the ensemble of model predictions. Overall the mean model bias is around 4^{o}C and this should be considered when the future climate model predictions are being considered.

The observed minimum temperatures, shown in Figure DT2b, tend have mean values mid way between those of the ensemble mean model and the coldest of the model members. The variability of observed minimum temperatures is greater than the climate model mean but is similar to that of the coldest model member. The warmest observed minima remain within the envelope described by the warmest of the climate model members throughout the validation period and, for the most part, lie below the predicted values of the ensemble mean of the models. The coldest minimum temperatures tend to be very similar to the coldest minima predicted by the coldest of the ensemble of model members. It can be concluded that the climate model predictions are quite well calibrated for minimum temperatures at Diavik for this time of the year, although the ensemble mean model has a warm bias of approximately 2^{o}C at this time of the year.

The comparisons for Diavik for February similar skill with the climate model again having a similar warm bias. It is noted the observed mean temperatures for February for Diavik and Ekati are too short to be able to identify any trend. However the longer period of record from Lupin A does show a rising trend similar o that of the climate models. Once

again the observed temperatures generally sit within the envelope of predictions provided by the climate model members.

In Figures DT5a, b and c the mid-spring month of April temperature comparisons are shown for Diavik. For this month the observed temperatures from Diavik, Ekati and Lupin A continue to be cooler than the ensemble mean of the climate models with the warm bias growing to around 6^{o}C. This bias is greater than preferred but it should be noted that in complex terrain such as that around Diavik, naturally occurring variations over short distances can be of this magnitude. It should be noted that the longer term record for Fort Reliance matches the ensemble mean model values almost exactly with a monthly mean value of -8.6^{o}C. The same applies to both the maximum and minimum data with Fort Reliance matching the ensemble model mean data very well.

These local biases can be exacerbated by differential accumulations of snow and ice that can dramatically affect the temperatures over small distances. As the climate model is providing an average over an area while the observations are for point locations, differences are inevitable. Bias corrections need to be applied to the future climate model temperature predictions at Diavik to account for this warm bias, although it should also be noted that no bias correction at all is required if the Fort Reliance data is considered representative. As was the case for the preceding months, the longer period of record from Lupin A shows a warming trend comparable to that of the ensemble mean of the climate models. The observed minimum and maximum temperatures tend to show similar warm model biases with the coldest of the model members being most similar to the coldest of the climate model members. At this time of the year the observed coldest minima and maxima are lower than the lowest modelled minima and maxima and so this needs to be borne in mind when the future climate model predictions are interpreted.

In Figures DT8a, b and c the same comparisons are made for Diavik for the mid summer month of July, which is the warmest month of the year for this location. It can be seen that the climate model has a reduced warm bias for this month of the year with the warm bias for the mean temperature being around 2^{o}C. The trend for Lupin A's observational record shows a rise of similar magnitude to the climate models mean. The observed minima and maxima for Diavik also show a similar bias of around 2^{o}C. The coldest of the

observed minimum temperatures is only marginally below the coldest predictions from the coldest model member for this month with the coldest maxima being similar to the model predicted coldest maxima. The warmest of the observed temperatures are all below the highest predicted temperatures from the warmest model member.

In Figures DT11a, b and c the comparisons for the mid-fall month of October are shown for the climate models and the available observations for the Diavik region. For this month the observed minimum, mean and maximum temperature matches the climate model extremely well, with the observations being almost identical to the modelled values in both magnitude and trend. No bias correction is required at this time of the year. The minimum and maximum temperatures again sit well inside the envelope of predictions of the climate model. Hence there can be a high level of confidence in the ability of the climate model to represent the temperature regime for the Diavik region at this rapidly changing time of the year.

It should be noted that the ensemble mean model predictions require very little in the way of bias corrections for the months from August through to December inclusive. Hence the warm bias of the ensemble mean models is a seasonal feature of the climate model that applies to the period from mid winter through to mid summer, peaking in mid spring.

The annual comparisons between the climate models and the Diavik observations are shown in Figure DT14. The maximum, minimum and mean temperatures, at an annual level, are between 2 and 2.5^{o}C cooler than the ensemble mean climate model, which is considered good for an Arctic location in complex terrain such as Diavik. The modelled trend over the 38 years of this comparison for the annual data shows a 2.5^{o}C increase for the mean temperature, which is comparable to the observed warming trend at Lupin A of 2^{o}C over the period since 1982. The trend lines show that this increase is a fairly constant feature throughout the 38 years of the validation period, although there are multi-decadal oscillations present, more obvious in individual model runs. From all of the comparisons it can be concluded that the ensemble mean model temperature data recreates the observed Diavik temperature record to an acceptable degree with the application of bias corrections thought to be a suitable way of adjusting for the

differences between model and observations as the trends and observed variability are similar between the datasets.

2.1.2 Future Climate Model Predictions

Next the future climate temperature predictions are analyzed for the grid box centred upon Diavik. The model predictions for Diavik for all twelve months are shown in Diavik Attachment D2 as Figures DT15 a, b and c (mean, minimum and maximum temperatures respectively) through to DT26 a, b and c with the annual predictions shown in DT27a (ensemble mean of the climate models) and DT27b (the model closest to the ensemble mean). The predictions from the hottest and the coldest of the six climate model predictions are also shown for maximum and minimum temperatures. These serve to provide an estimate of the range of possibilities for the more extreme hot or cold periods. The ensemble mean of the six models will, in general, provide the best estimate of the long term trends in the minimum, mean and maximum temperatures. The future climate temperature prediction discussions that follow are based upon the ensemble mean of the climate models. Comments on inter-annual and decadal scale oscillations, and likely changes in the frequency of more extreme events, will generally be based upon the results of the model closest to the ensemble mean. For brevity, only the months in the middle of the four seasons and the annual trends will be discussed in any detail.

The predicted temperature changes can be applied to the historical daily air temperature data to determine likely changes to the Freezing Index at any given time through the future climate period. The predicted changes in surface temperature can also be applied in the same way to historical surface temperature data to determine expected changes in the Surface Freezing Index into the future. Although it is outside the scope of this project to determine the Freezing Index, the future climate model predictions clearly show a marked reduction in the number of below-freezing days are to be expected in the future climate, with this reduction accelerating through the future climate period.

January

In Figures DT15a, b and c the ensemble mean model predictions of minimum, mean and maximum temperatures for Diavik are shown from 1970 through to 2060 for the mid-winter month of January, together with linear trend lines for the ensemble mean of the model predictions. The climate models show an ongoing, almost linear increasing trend in the minimum, mean and maximum temperatures through to at least 2060, although there is a definite multi-decadal signal in the rate at which the temperatures rise. This can be seen as a series of steps in the graphs of temperature with the temperatures remaining relatively constant for a decade or more followed by a sudden rise, then another period of relatively constant temperature before the next rapid rise occurs. The warming trends are quite significant for both minima and maxima, with the rate of rise of minimum temperatures predicted to be slightly greater than for maximum temperatures. Both are predicted to warm relatively rapidly.

Using the linear trend lines as the reference, the predicted temperature changes, from 1970 to 2060, are as follows:

- Maxima: from -23.4^{o}C to -15.8^{o}C, a rise of 7.6^{o}C over the 90-year period. This equates to an annual maximum temperature increase of 0.084^{o}C.
- Mean temperatures: from -27.3^{o}C to -19.6^{o}C, a rise of 7.7^{o}C over the 90-year period. This equates to an annual mean temperature increase of 0.086^{o}C.
- Minima: from -31.6^{o}C to -23.4^{o}C, a rise of 8.2^{o}C over the 90-year period. This equates to an annual minimum temperature increase of 0.091^{o}C.

Applying bias corrections to these datasets based upon the observations shown in Figures DT2a, b and c, adjusts the predicted temperature changes for the month of January for the period from 1970 to 2060 to the following values (bias correction not required for Fort Reliance data):

- Maxima: from -27.4^{o}C to -19.8^{o}C, a rise of 7.6^{o}C over the 90-year period.
- Mean temperatures: from -30.3^{o}C to -22.6^{o}C, a rise of 7.7^{o}C over the 90-year period.
- Minima: from -33.6^{o}C to -25.4^{o}C, a rise of 8.2^{o}C over the 90-year period.

Looking at the variability of the year to year temperature variations at Diavik it can be seen that there are likely to be decades in the future when the temperature rise plateaus for a period of time, followed by an accelerated rise. Also there are predictions of one-off years when there are spikes in the temperatures predicted – either hot or cool spikes, One key thing to note concerns the transition into a consistently warmer climate beyond the 1990-1999 decade. In the period from 1970 through to around 2000 there are occasional years when there are relatively cold years – when the January minima drop to around -32^{o}C, well below the long term average. However, beyond 2015 these colder years become less frequent or severe, with the coldest of the years predicted to drop only as far as -27^{o}C. The minimum temperatures predicted for the period from 2050-2060 are all shown to be higher than the warmest minimum temperature during the 1970s and 1980s.

April

For the spring month of April, the predicted changes in maximum, mean and minimum temperatures for Diavik are shown in Figures DT18a, b and c. The future climate predictions are based upon the mean of the ensemble of models. However, it must be noted that the ensemble mean model has a warm bias of approximately 4-5^{o}C at this time of the year, based upon the Diavik, Ekati and Lupin A data but not the Fort Reliance data, and this bias correction can be applied to better match the available Diavik observations. The coldest of the model members appears to replicate Diavik's temperature regime more closely during this month. Again there are multi-decadal oscillations in the temperature predictions for both maximum and minimum evident. However, over the full 90 years of the climate model predictions the linear trend line provides a good estimate of the predicted long term trend in the temperatures.

Using the linear trend lines for the analysis, the predicted temperature changes, from 1970 to 2060, are as follows:

- Maxima: from -4.5^{o}C to -0.9^{o}C, a rise of 3.6^{o}C over the 90-year period. This equates to an annual maximum temperature increase of 0.040^{o}C.
- Mean temperatures: from -9.7^{o}C to -5.0^{o}C, a rise of 4.7^{o}C over the 90-year period. This equates to an annual mean temperature increase of 0.052^{o}C.

- Minima: from -14.8^{o}C to -9.2^{o}C, a rise of 5.6^{o}C over the 90-year period. This equates to an annual minimum temperature increase of 0.062^{o}C.

Applying bias corrections to these datasets based upon the observations, which are at their greatest at this time of the year and are shown in Figures DT5a, b and c, adjusts the predicted temperature changes for the month of January for the period from 1970 to 2060 to the following values (bias correction not required for Fort Reliance data):

- Maxima: from -11.5^{o}C to -7.9^{o}C, a rise of 3.6^{o}C over the 90-year period.
- Mean temperatures: from -15.7^{o}C to -11.0^{o}C, a rise of 4.7^{o}C over the 90-year period.
- Minima: from -19.3^{o}C to -13.7^{o}C, a rise of 5.6^{o}C over the 90-year period.

These predictions show the April period to have a slightly slower rate of warming but still one that is considered rapid in a global context. The minima are expected to rise at a faster rate than for the maxima, although this rate is a slightly slower rate than for the mid winter months. The climate model predictions for both the minimum and maximum temperatures show a relatively large amount of variability from one year to another, indicating there can be expected to be abrupt jumps in the temperature followed by equally rapid falls the following year. The rise in mean temperature of 4.7^{o}C over the period of the future climate predictions would amount to a much earlier and more rapid thaw of the accumulated snow in the future climate regime. With a similar rate of warming predicted for the month of May, this would also mean the ice road connecting Diavik and Yellowknife would be expected to disintegrate much earlier in the future climate regime. The climate model predictions still show outlying abnormally cool and warm years but there is clear evidence in these predictions for a move into a consistently significantly warmer climate.

July

The predicted changes in maximum, mean and minimum temperatures for the warmest time of the year at Diavik, July, are shown in Figures DT21a, b and c. The ensemble mean of the model predictions can be seen to go through cycles of increased then decreased inter-annual variability through the future climate period, indicating the nature

of the climate variability is not expected to be uniform through the future climate period. This variability appears to affect both maximum and minimum temperature predictions. There are also marked multi-decadal signals in the temperature predictions, as illustrated by the series of step-like increases in temperature predicted through to the year 2060.

Using the linear trend lines for the analysis, the predicted temperature changes, from 1970 to 2060, are as follows:

- Maxima: from 18.2^{o}C to 20.0^{o}C, a rise of 1.8^{o}C over the 90-year period. This equates to an annual maximum temperature increase of 0.020^{o}C.
- Mean temperatures: from 13.6^{o}C to 15.7^{o}C, a rise of 2.1^{o}C over the 90-year period. This equates to an annual mean temperature increase of 0.023^{o}C.
- Minima: from 9.0^{o}C to 10.9^{o}C, a rise of 1.9^{o}C over the 90-year period. This equates to an annual minimum temperature increase of 0.021^{o}C.

Again applying bias corrections to these datasets based upon the observations, which have reduced to a modest 1.5^{o}C (minimum) to 2.5^{o}C (maximum) for this month, as shown in Figures DT8a, b and c, adjusts the predicted temperature changes for the month of January for the period from 1970 to 2060 to the following values:

- Maxima: from 15.7^{o}C to 17.5^{o}C, a rise of 1.8^{o}C over the 90-year period.
- Mean temperatures: from 11.6^{o}C to 13.7^{o}C, a rise of 2.1^{o}C over the 90-year period.
- Minima: from 7.5^{o}C to 9.4^{o}C, a rise of 1.9^{o}C over the 90-year period.

From these predictions it can be seen that the ensemble mean climate model forecasts a relatively uniform increase in maximum and minimum temperatures through the summer period, although the rate of increase in temperatures are predicted to be very slow in comparison to the winter and spring months. Although the predictions are for ongoing warming, there continue to be a reasonably number of years, sometimes several years in succession as for the period from 2022-2025, when there are Julys with maximum temperatures a couple of degrees cooler than the long term average trend would indicate as being the normal conditions. The variability is predicted to similar for both maximum and minimum temperatures.

October

The predicted changes in maximum, mean and minimum temperatures for Diavik for the central month of fall, October, are shown in Figures DT24a, b and c. October represents the start of the transition from the mild to warm season into the time of year when snowfalls become more frequent. Hence it is an inherently changeable time of the year and one when the accumulation of snow on the ground can be expected to commence as the mean daily temperatures historically drops below freezing during this month.

Once again the linear trend lines are used to quantify the expected changes in the temperature for this time of the year. On this basis, the predicted temperature changes, from 1970 to 2060, are as follows:

- Maxima: from -3.8^{o}C to 0.4^{o}C, a rise of 4.2^{o}C over the 90-year period. This equates to an annual maximum temperature increase of 0.047^{o}C.
- Mean temperatures: from -6.9^{o}C to -2.0^{o}C, a rise of 4.9^{o}C over the 90-year period. This equates to an annual mean temperature increase of 0.054^{o}C.
- Minima: from -9.9^{o}C to -4.4^{o}C, a rise of 5.5^{o}C over the 90-year period. This equates to an annual minimum temperature increase of 0.061^{o}C.

Again applying bias corrections to these datasets based upon the observations, which have reduced to very small values of zero ^{o}C (minimum) to 1.0^{o}C (maximum) for this month, as shown in Figures DT11a, b and c, adjusts the predicted temperature changes for the month of January for the period from 1970 to 2060 to the following values:

- Maxima: from -4.8^{o}C to -0.6^{o}C, a rise of 4.2^{o}C over the 90-year period.
- Mean temperatures: from -7.4^{o}C to -2.5^{o}C, a rise of 4.9^{o}C over the 90-year period.
- Minima: from -9.9^{o}C to -4.4^{o}C, a rise of 5.5^{o}C over the 90-year period.

The climate models show an important shift in the temperature regime at this time of the year as the warming becomes significantly faster than for the summer months. The climate model indicates there would be significant delays in the starting time for snow accumulations and for the lakes to start to freeze. Although the modelling does show

there will still be some years in the future when the mean monthly temperature is close to the current values, they become increasingly less common. By around the year 2020 there are indications that the mean monthly temperature could be within 1^{o}C of freezing, which is a significant warming within only just over a decade. It would become increasingly likely that less snow would accumulate on the ground during this month through the future climate period due to these rapid rises in temperature. The predicted rises in minimum temperature are also faster than those forecast for the maximum temperatures which would exacerbate this effect. Towards the end of the future climate period, mean monthly temperatures are no longer expected to drop below -3^{o}C and are likely to start to be above zero for some years.

Based upon the predicted temperature rises, the expectation would be for fewer snow events with more precipitation falling as rain, which is also harmful for snow and ice formation.

Annual

Finally, the trends in the annual minimum, mean and maximum temperatures for Diavik are shown in Figure DT27a for the ensemble mean of the models and in Figure DT27b for the model closest to the ensemble mean. Both of these approaches give very similar trends for this location. These are the trends normally used to quantify, in the simplest of terms, the effects of climate change at a given location. Smoothed over an entire year, the predictions show a relatively constant rate of increase in temperature over the coming decades, although periods of climate variability are evident throughout the climate predictions. The inter-annual and multi-decadal oscillations are not as pronounced as they are for the individual months as they are not aligned throughout the entire year and tend to cancel each other out over time. On almost all occasions the annual temperatures (maximum, mean and minimum) lie within 2^{o}C of the expected temperature, as indicated by the linear trend line.

The linear trend line provides a good estimate of the long-term warming trend. Using this trend line, the predicted temperature changes, from 1970 to 2060, can be quantified as follows:

- Maxima: from -4.8^{o}C to 0.7^{o}C, a rise of 5.5^{o}C over the 90-year period. This equates to an annual maximum temperature increase of 0.061^{o}C.
- Mean temperatures: from -8.0^{o}C to -3.0^{o}C, a rise of 5.0^{o}C over the 90-year period. This equates to an annual mean temperature increase of approximately 0.056^{o}C.
- Minima: from -12.2^{o}C to -6.8^{o}C, a rise of 5.4^{o}C over the 90-year period. This equates to an annual minimum temperature increase of approximately 0.060^{o}C.

Applying the annualized bias corrections to these dataset, again based upon the observations, shown in Figures DT14a, b and c, adjusts the predicted temperature changes for the month of January for the period from 1970 to 2060 to the following values:

- Maxima: from -8.3^{o}C to -2.8^{o}C, a rise of 5.5^{o}C over the 90-year period.
- Mean temperatures: from -11.0^{o}C to -6.0^{o}C, a rise of 5.0^{o}C over the 90-year period.
- Minima: from -14.7^{o}C to -9.3^{o}C, a rise of 5.4^{o}C over the 90-year period.

These temperature rises are likely to have a significant impact upon the way of life and ecology of the Diavik Yellowknife region as this still amounts to a significant warming, one of the highest in the world, and one that would greatly reduce the length of the very cold snow season. The length of time that the lakes would be frozen to sufficient depth to be used as ice roads would almost certainly be greatly reduced. Someone more familiar with ice roads should be consulted to quantify the extent of these reductions based upon the data provided here.

It should be emphasized that, as marked as these temperature rises are, these are not the end points of climate change. Beyond this period of time, the temperatures would be expected to continue to rise, although the rate at which they rise will be determined, to a large extent, by what happens to the global rate of greenhouse gas and aerosol emissions over the next couple of decades. For the future climate scenario used in this series of climate predictions, which is the one considered to be the most likely future climate outcome, the region surrounding Diavik are showing a marked trend towards

increasing temperatures, particularly for minimum temperatures, with sustained and increasing impacts to be expected upon the communities and ecology of the region.

Climate Periodicities – Wavelet Analysis

The periodicities and oscillations in the temperature record for Diavik have been analyzed through the use of wavelet analyses. These analyses and their interpretations are to be found in the document entitled Diavik Wavelet (Appendix A).

2.2 Future Precipitation Changes

In the following sections the results of a series of analyses using data from all six of the ensemble members are presented, covering precipitation predictions from 1970 through to 2060. In the first section the results of the models are validated against the observed rainfalls for the Diavik area using Environment Canada's climatological data for the Ekati and Lupin A weather stations, and the limited Rio Tinto Diavik weather station data. In the following section the future climate predictions are presented.

2.2.1 Precipitation Validation

In this section the ensemble control mean rainfall for the period 1970-2006 for the Diavik grid box is used as the principle reference precipitation for trend analysis purposes. The precipitation used is the total precipitation from liquid rainfall and the water equivalent of snow fall and is the values obtained from across the grid box, rather than being a point measurement, which is the observed precipitation. Results from all six of the model members are also shown in the form of the driest and the wettest of the climate model predictions in order to provide an indication of the variability of the rainfall at this location and the potential extreme precipitation events, both wet and dry, on monthly time scales.

The lowest line shows the predictions from the driest of the six models for each of the model validation years with one graph for every month of the year. The lowest predicted precipitation for any given year could come from any one of the six models and is almost certain to change from one model to another from one year to the next. The lowest

precipitation, labeled “Driest Model” on the graphs, therefore identifies what is likely to be the lower bounds for the rainfall regime for that month in any given year. It can be seen from the plots that there can be a large separation between the highest and lowest precipitation for many of the model years, indicating the Diavik area experiences a quite variable precipitation regime with very large fluctuations possible from one year to the next. The highest line on the graphs, labeled “Wettest Model”, shows the heaviest predicted precipitation for that month and year from the six ensemble model members. Again the highest precipitation could be from any one of the six climate models and the highest predictions could and does vary from one model member to another from one year to the next and from one month to the next. A detailed analysis of the model outputs shows that some of the climate model members are better able to predict the precipitation climate of this region than the others. The heaviest precipitation is normally predicted best by those models with the cloud physics that is best able to simulate frontal precipitation processes that produce the heaviest precipitation at this location. Conversely, the models that predict the lightest rainfall (for example drizzle, snow and ice crystals) would be from a different set of climate models. The area between the highest and lowest model predictions is shaded light blue in order to show the model spread of the rainfall predictions.

In the earlier section on observed precipitation for the Diavik area, the precipitation regime was shown to be highly seasonal with considerable variability from month to month and year to year. The difficulty in accurately measuring snowfall in a location exposed to wind was also noted. The mean values of the models and the spread of the six model members are used to quantify the rainfall regime throughout the validation periods. Ideally the observed precipitation would lie within the envelope of predictions from the wettest to the driest of the climate model members and the mean of the two distributions would be identical. Precipitation is a highly variable quantity in both space and time, subject to geographically-produced very localised enhancements or reductions (rain shadow and lake snow enhancement effects). Hence it is to be expected that the simplified physics employed within the climate model would not be able to replicate the finer detail of the precipitation climate. However, the trends identified by the climate model predictions should serve as a useful guide as to the likely future nature of the

precipitation regime in this region, with bias corrections applied to the model data where these can be identified with confidence.

In Figures D2 to D14 comparisons are presented in graphical form between the modelled precipitations for the 20km square grid box surrounding Diavik against the corresponding observed precipitation, where there are sufficient observational records available, for each of the twelve months of the year and annually. The Ekati precipitation data is shown as the red dots connected by red lines, Lupin A as the purple lines and dots and the Ekati data as orange lines and dots. The ensemble mean model data represented in dark green dots on the graph. The spread between the highest and lowest model predictions is coloured pale blue. Linear trend lines are also included for both the observed Lupin A precipitation, being the only station of the three with a reasonable length of climate record, and the data from the ensemble mean of the climate model runs.

The heaviest observed precipitation at Diavik would be expected to generally lie below a curve connecting the highest points from the wettest of the climate models, with the exception that the one or two most extreme precipitation events could be expected to lie above this curve. This is because the precipitation measured at the three observation stations used in this comparison are from point locations whereas the model produces rainfall across a region 20km x 20km, or over approximately 400km^2. Running the model at very high horizontal resolution (e.g. 500m) and with complex cloud physics would better define the true nature of the potential rainfall extremes but this is computationally too expensive at the present time.

The best way to quantify the model predictions of precipitation is through the use of the ensemble mean rainfall or, in cases where one of the climate model members is very well configured to represent the precipitation regime experienced at Diavik, the model closest to the ensemble mean. The ensemble mean precipitation is the average precipitation from the six climate models, calculated on a monthly basis throughout the entire period of the climate model runs. Although the ensemble means smoothes out the variability caused by the heavy and light precipitation events that are a feature of the climate of this region, experience has shown that it normally provides a very good

estimate of the typical precipitation of the region under investigation on monthly and annual bases. The middle month of each season will now be discussed in detail, although there will be a little discussion of some of the intermediate months as well.

In January, the comparisons between the climate models and the Diavik region (i.e. Ekati, Diavik and Lupin A) precipitation observations are shown in Figure D2. From the graph it can be seen that the ensemble mean quantity of total precipitation tends to be above the Lupin A and Ekati precipitation records but is closer to the limited data available for Diavik itself. Of the 8 Januarys of data available there are three years above the average and five below. The lowest Diavik precipitation record is similar to the lowest precipitation of the driest climate model and the highest precipitation matches the wettest model well. Lupin A tends to be consistently drier, as does Ekati. This could be a feature of the precipitation regime of the area or it could be related to the catch efficiency of the snow gauges at this time of the year. The trend line for Lupin A shows a decline although with heavier rainfalls indicated in the Diavik data for 2007 and 2008 (no data available for Lupin A for these two years) the trend line would most likely flatten out and possibly increase if there was a corresponding increase in precipitation. There is also a change from rapidly fluctuating relatively high then low then high precipitation values at Lupin A through to 1993 after which time the plot changes to one of remarkably small year to year fluctuations. This is often a sign of changing instrumentation exposure or a site change rather than a true climate change. However, the siting and exposure history for these stations are unknown and hence this cannot be confirmed. There is insufficient data for Ekati and Diavik for any form of trend analysis, although it is interesting to note Diavik has had a run of relatively wet Januarys in recent years, noting that this is a very dry month overall. The climate model predicts a gradual increase in precipitation from near 17mm in 1970 up to 19mm in 2008, a rise of 10.5%, with similar increases for both the wettest and driest of the climate models. The observed total precipitation in the graph, which is the recorded quantity of melted snow from the Environment Canada records, needs to be treated with caution, partially for the reasons mentioned previously, but also due to the way in which recorded snow fall is converted into equivalent precipitation.

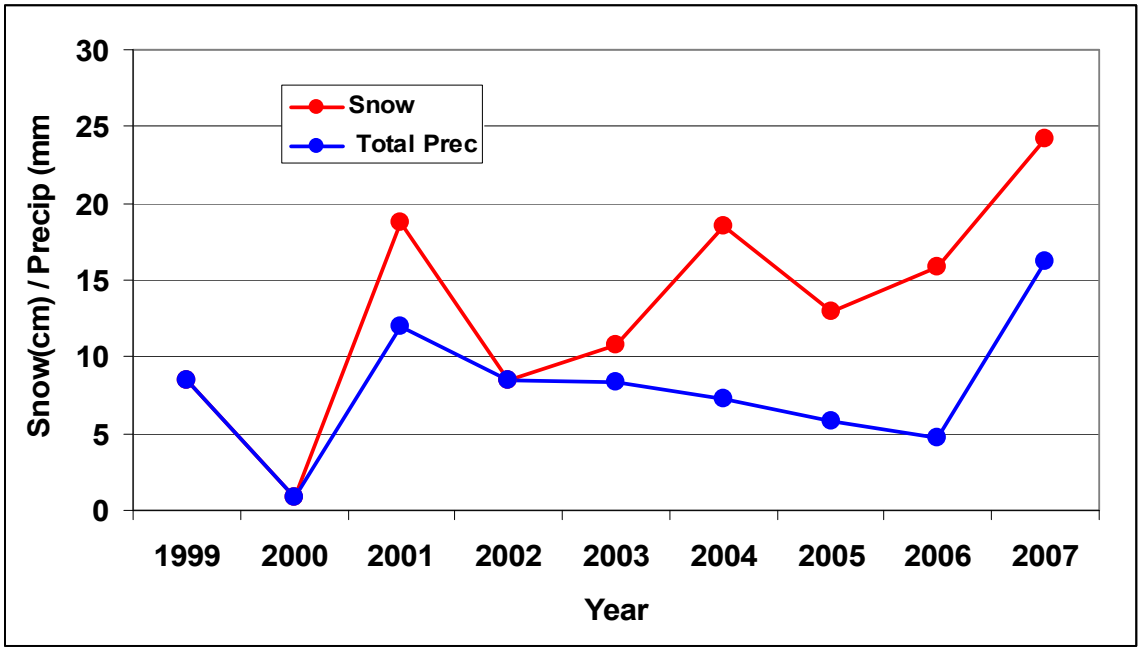

Figure 5: Observed snow and the corresponding melted snow (total precipitation) for January for Ekati from 1999 to 2007. Data courtesy of Environment Canada.

At Ekati, for example, this conversion has been handled differently from month to month and year to year, as the graph in Figure 5 and the data in Table 3 shows. Although the technique could make allowances for changes in snow density, it is more likely there have been a variety of techniques used in the way the snow is gathered and melted through the observational record through to the current time. The original snow measurements show a marked increasing trend in snowfall whereas the snow converted into liquid precipitation shows a much lower trend. The snow to liquid precipitation ratio has a remarkably large range, from 1.0 up to 3.4 (in January 2006). The same issues were noted at some other locations across Canada and for other months. It should be noted the climate model does not suffer from altered observational practices as do the original observations. Hence the trends and model biases based upon precipitation measurements which include a snowfall component have to be treated very cautiously. From this information it would be concluded the climate model replicates the Diavik January total precipitation very well.

Year	Snow	Total Precipitation	Ratio
1999	8.5	8.5	1.0
2000	0.8	0.8	1.0
2001	18.7	12	1.6
2002	8.5	8.5	1.0
2003	10.8	8.4	1.3
2004	18.5	7.2	2.6
2005	13	5.8	2.2
2006	15.9	4.7	3.4
2007	24.2	16.2	1.5

Table 3: Observed snowfall and subsequently derived total liquid precipitation for Ekati for January, together with the snow to liquid precipitation ratio. Data courtesy of Environment Canada.

For the month of February the limited Diavik total precipitation record fits in well with the ensemble mean modelled precipitation with the wettest and driest months also fitting within the range of ensemble model predictions. It is apparent that Lupin A tends to have more dry months than the other two locations. The Ekati data continues to be affected by an inconsistent approach to the conversion of snow into liquid precipitation. For this month, arguably the driest time of the year, the climate model predicts a smaller increase in precipitation, being a rise of just under 1 mm over the 38 years of the validation period. The reliability of the trend from Lupin A is still subject to an insufficient length of good quality data as the trend is reversed for the following month of March. Diavik data is again well calibrated to the model mean data for the month of March. The heaviest recorded precipitation events for Lupin A and Ekati appear to match the predictions from the wettest climate model well.

The same issues affect the Ekati comparisons for April with most of the precipitation falling as snow. Table 4 shows how great the variations are in the conversion of snow into liquid precipitation for this month, which makes the Ekati plot in the graph open to question as a conversion rate close to 1.0 would have removed the apparent low bias in this dataset. The limited Diavik data fits in well with the ensemble mean and spread once more. For this month the trend for the Lupin A data is almost identical to that of the driest

of the climate model members, indicating there could be a believable trend starting to emerge from the observational data at this time of the year. The heaviest Lupin A and Diavik falls also match those of the wettest climate model well.

Year	Snow	Total Precipitation	Ratio
1999	11.8	11.8	1.0
2000	5.4	5.1*	1.1
2001	8.7	2.4	3.6
2002	5.0	4.4	1.1
2003	21.1	8.8	2.4
2004	9.2	2.5	3.7
2005	10.7	9.9*	1.1
2006	17.5	7.3*	2.4
2007	10.9	9.2*	1.2

Table 4: Observed snowfall and subsequently derived total liquid precipitation for Ekati for April, together with the snow to liquid precipitation ratio. Data courtesy of Environment Canada. * indicates rain has been added to this total for consistency purposes.

For the month of May the precipitation at Diavik is becoming dominated by liquid rainfall with the problems associated with snowfall becoming less of an issue. The Diavik observations show a high level of year to year variability, including one fall heavier than anything recorded at Ekati and Lupin A for this month. It is also slightly higher, around 4mm, than the highest precipitation predicted by the wettest of the climate model members. The Lupin A data continues to be consistently drier than Diavik and the ensemble mean model with little trend through the future climate period. Of significance are the large variations between the observed precipitations for the three stations at times when there is an overlap of their observations, confirming the inherently variable nature of the precipitation in the Diavik region at this time of the year. Overall the ensemble mean provides a realistic representation of the likely precipitation for this area, although probably with a slight wet bias.

For June the available Lupin A data more closely matches the ensemble mean, wettest and driest rainfall data and shows a similar trend of little change in precipitation over the

available length of record. In contrast to the Lupin A data, the limited Diavik rainfall record indicates the development of a dry bias with Ekati also generally being drier than the ensemble mean model, apart from a lone very heavy rainfall event. If the Diavik data is considered a true indication of the long term average then a bias correction should be applied to the ensemble mean model data. However, the ensemble mean average precipitation is relatively close to that of Lupin A (30mm) and Fort Reliance (30.5mm) and so the difference between the two datasets could be a function of natural climate variability or a localised micro-climatic effect at Diavik.

For the mid summer month of July the ensemble mean of the climate models appears to be quite close to the mean of the observed Diavik rainfall with the wettest and driest models also matching the available observations well. The Lupin A mean rainfall also agrees well with the model data although the linear trend line is unrealistic, biased by the combination of three wet years near the start of the observational record and three dry ones at the end. This trend is markedly different to that seen in June and August. The Ekati data also seems close to both the Diavik and model data for this month, one in which snowfall plays no role.

In August the model data appears to have a dry bias of approximately 15mm when compared to the Diavik rainfall data. Lupin A appears to be even wetter, although it is interesting to note that the Lupin A data appears to be markedly different to both Diavik and Ekati for many of the years where the datasets overlap, indicating this location may not truly represent the Diavik region’s precipitation regime.

There is a reduced dry bias in the model data for the month of September, down to around 10mm for the three observation stations. The observations also show greater variability than the wettest and driest climate models, indicating the model is likely to underestimate the magnitude of extreme precipitation events at this time of the year. Both the model and Lupin A data show an almost horizontal trend, or no change in the rainfall regime for this month through the validation period.

October is the month when snowfall once again dominates the precipitation figures. The model bias appears to vanish at this time of the year with the ensemble mean

precipitation close to that of the observed Diavik precipitation, slightly below that of Lupin A and above that of Ekati, which appears to have problems with conversion into liquid precipitation for months when snowfall is a significant part of the record. The Lupin A trend is again almost flat, although it shows an increase in November. The ensemble mean model data indicates a gradually increasing trend, primarily due to greater amounts of precipitation predicted through the 2000's. This trend returns to one of little change in November, indicating this could be a function of natural climate variability rather than a true long term rise.

It is difficult to determine if there is a model bias at Diavik for the month of November. The limited observations at Diavik show good agreement with the ensemble mean precipitation until three wet years appear from 2005 through to 2007. Ekati and Lupin A remain well below Diavik for months where there is data and either match or are below the ensemble mean model data, raising a question as to whether these were atypical very heavy falls, local effects or a true reflection of the Diavik climate. These extremes of rainfall do not appear in the Diavik December precipitation record with all three observing stations tending to be around 5mm drier than the modelled precipitation. This could be considered a wet model bias for this month of the year. The trends and the observed extremes in precipitation match those of the climate models to a pleasing extent. The problems associated with increasing quantities of snowfall have to be considered at this time of the year, of course.

The annual climate model predictions of total precipitation for Diavik and the observed rainfalls for the three observing stations are shown in Figure D14, together with linear trend lines for the model and Lupin A data. The climate model predictions are for very slightly increasing precipitation, in good agreement with the annual trend for Lupin A. The limited Diavik data is in very good agreement with the ensemble mean model data with a minor dry bias evident in the Lupin A data. Ekati appears drier than the model but this could be attributed to the inconsistent conversion procedure used for snowfall.

So it can be concluded that, provided the observational record is treated correctly and with appropriate caution, the historical precipitation data and the climate model data agree to a satisfying degree. Bias corrections improve the correlations between the

climate model data and individual months, although these bias corrections change in sign and magnitude from month to month with several months requiring no bias correction at all. The level of agreement between the observations and the climate models is best when viewed on seasonal and annual time scales as the effects of natural climate variability on time scales as short as a month can provide misleading trends, even when twenty five years of records are used.

2.2.2 Future Climate Precipitation Predictions

Next the future climate rainfall predictions out to the year 2060 are analyzed. Once again the data from the six ensemble models and the ensemble mean were used. The time series of modelled monthly rainfalls from 1970 through to 2060 are shown in Figures D15a (model closest to the ensemble mean) and D15b (ensemble mean, wettest and driest of the climate models) through to D27 for Diavik. Both sets of graphs have linear and polynomial trend lines included for the model mean data. The same colour schemes are used for these future climate predictions as were used for the validation period. No bias corrections have been applied to these datasets to adjust them to match the observed data precisely as some of the values to use for the bias corrections are subject to interpretation and also it is the trends that are important.

The data shows strong evidence of inter-annual and decadal variability with the sixth order polynomial trend line highlighting the multi-decadal oscillations in the rainfall climate. The wavelet analysis discussions for Diavik should also be consulted when looking at trends in the climate oscillations. Overall, despite the presence of these oscillations, the linear trend line appears to represent the long-term changes in the monthly total precipitation well, even though the linear trend lines have been shown to be misleading even over periods of close to 40 years duration in some circumstances. The climate model predictions for all twelve months are shown in the Attachments and spreadsheets. For brevity, the discussions that follow will again focus on the middle month of each season, with references to the other months where these illustrate a point of particular interest.

January

The climate model predictions for Diavik show a continuation of a highly variable, though relatively low, rainfall regime for the winter months with an identifiable multi-decadal signal, illustrated by the polynomial trend line. This oscillation continues through to the end of the future climate prediction period and is super-imposed upon the linear trend. The linear trend line from the ensemble mean model shows an increasing trend although the polynomial trend line shows a plateauing of the precipitation from around 2020 onwards with a very minor decline towards the end of the prediction. The ensemble minimum rainfall predictions show a slight upwards trend as well with the largest change indicated by the wettest of the model members with more frequent heavier falls predicted. The driest year of all is a predicted fall of near 5mm in climate model year 1970 and it is not until model year 2026 when this low precipitation prediction is approached with a fall of 5.5mm forecast.

Using the linear trend line as the reference for the long-term trend in precipitation, it can be seen that the mean monthly precipitation is predicted to be around 17 mm in the year 1970, increasing to around 21 mm by the year 2060. This represents a rise of 4 mm per January by the year 2060, which equates to an increase in the mean precipitation by the year 2060 of close to 24%, compared to that of the years near 1970. In average terms this is a very slow increase of around 0.04mm for each successive January. The climate models show an increase in the quantity of the heaviest precipitation events through the future climate period from around 32mm for the validation period out to 2007 up to 41mm for the future climate period. There is also a predicted increase in their frequency. For example, looking at the events where 30mm or more precipitation is predicted by the wettest of the climate models, only three events are indicated for the first 30 years of the predictions, nine events are predicted for the next 30 years and ten events of 30mm or more are predicted from 2030 onwards. The differences in their magnitudes are considered to be modest in modelling terms but with some confidence in the increasing trend. This indicates the future climate regime will support heavier snowfalls than does the current climate regime for January, with an increasing frequency of these heavier snowfalls in the future climate.

For the month of February, the predicted increases in Diavik's mean and extreme precipitation is similar to that for January whereas in March the slight increasing trend continues for the mean precipitation but the changes in the extreme snowfalls are less compelling.

April

April is still in a precipitation regime dominated by snowfall but one where rainfall starts to become more important for the Diavik region. With the predicted warming of the temperatures through the future climate period rainfall can be expected to increase in frequency and intensity as time progresses. The driest of the climate model members indicates little change in the lowest of the precipitation events with predictions in the future equal to, even slightly less than, those for the validation period. The linear trend line for the ensemble mean model predictions shows a gradual increase from around 19.5 mm in the year 1970 to around 22.5 mm by the year 2060. This represents a rise of 3 mm per April by the year 2060, which, due to the low precipitation quantities involved, equates to an increase in the mean precipitation by the year 2060 of close to 15%, compared to that of the years near 1970. The wettest of the ensemble model members does predict a heavier precipitation event in the future (44mm) than those for the model validation period (37mm) with a slight increase in the frequency of these more extreme events.

These trends appear to accelerate for May, the first month there liquid precipitation dominates at Diavik with the climate models predicting a future climate of gradually increasing mean and extreme precipitation totals. The mean precipitation is predicted to rise from near 26mm in 1970 up to around 34mm in 2060, an increase of 8mm or 31% over the length of the climate prediction. The extreme monthly rainfall is predicted to climb from around 57mm through the validation period to around 65mm in the future climate environment with a corresponding increase in frequency.

For June the long term mean is not predicted to change significantly through the future climate period although the wettest months are forecast to increase from around 65mm up to 83mm into the future.

July

The future climate model predictions for July for Diavik reverse the trends of the earlier months with a gradual decline in mean precipitation forecast. The climate model predictions are for a decrease in rainfall from an average of near 38mm in 1970 to near 35mm by 2060. This 3mm decrease in rainfall amounts to an 8% decline in precipitation over 90 years, an annual rate of decrease of a very small 0.03mm/year. The climate model predictions indicate a decreasing frequency of extreme heavy rainfall events, although the two heaviest July rainfall predictions lie in the future climate period, indicating new extremes of heavy rainfall are possible in the future climate period. The wettest of the climate models predicts a fall of near 95mm in the future climate period near model year 2052 compared to 84mm in the validation period. Although not a major trend, the driest of the climate model predictions tend to indicate dry months slightly drier than those of the historical past are likely in the future climate regime.

This reduction in future rainfall appears to be confined to the month of July as in August the ensemble mean model predictions return to one of increasing mean and heavier rainfalls.

October

October is one of the transition months back into a regime where snowfall becomes increasingly important. At Diavik the driest of the climate models predicts a gradual increase in the lowest rainfalls, indicating extremely dry Octobers are likely to become less frequent than those experienced in the past. The linear trend is for a gradual increase in total precipitation with the average rising from near 30mm in 1970 to around 40mm by the year 2060. This 10mm increase amounts to a significant 33% change in mean monthly precipitation over 90 years, or an annual rise of 0.11mm/year. The wettest of the climate models predicts an increase in the frequency of the wettest Octobers in the future although the quantity of precipitation is not shown to rise. The change in driest Octobers is predicted to be slight through the future climate period.

In November a similar increasing trend is predicted with the extreme wet years also forecast to increase in both frequency and intensity.

December is predicted to have one of the greatest change with the ensemble mean precipitation forecast to rise from around 18mm in 1970 up to 25.5mm by the year 2060, an increase of 7.5mm, which equates to a very large, in percentage terms, rise of near 42% for the month. The wettest December is also predicted to jump from around 45mm through the validation period up to around 65mm in the future climate.

Annual Precipitation

The Diavik annual precipitation trends from the ensemble mean of the climate models is shown in Figure D27. The ensemble mean model prediction is for an increase in precipitation from around 310mm in the year 1970 up to around 360mm by the year 2060, an increase in annual precipitation of around 50mm, or approximately 16%. There is a marked multi-decadal oscillation in the future climate predictions, indicating this change will not be a steady increase but rather one interrupted by large excursions from the mean. There is a marked leveling off of the precipitation increases indicated through the future climate period beyond around model year 2025. The predictions indicate there will be fewer dry years in the future and a trend towards gradually increasing extremely wet years, by Diavik standards, although this region will still only have relatively modest precipitation through the future climate period in comparison to warmer regions of the world. The wettest years tend to occur as lone events, as are the predicted driest years.

2.2.3 Precipitation Periodicities

A separate appendix has been prepared that summarizes the periodicities in the precipitation climate record for Diavik. This should be referred to in order to identify climate model predicted changes to the variability of this record.

3.0 Conclusions

An ensemble of six future Coupled Global Climate Model runs were analyzed and the mean used for determining likely future trends in the climate for the northern Canadian region, specifically Diavik and the ice road connecting it to the Great Slave Lake. The results of these analyses are detailed in the body of this report and its' attachments. The Executive Summary contains a summary of the more important findings of these analyses.

Appendix X-9

Diavik Underground Backfill

Diavik Diamond Mines Inc.
P.O. Box 2498
5007 – 50th Avenue
Yellowknife, NT X1A 2P8
Canada
T (867) 669 6500
F (867) 669 9058

Dr. Kathleen Racher
Regulatory Director (Mining)
Wek'èezhíi Land and Water Board
Box 32
Wekweeti, NT X0E 1W0

Ms. Jennifer Potten
Resource Management Officer III
South Mackenzie District
#16 Yellowknife Airport
Yellowknife, NT X1A 3T2

October 8, 2010

Re: Diavik Underground Backfill

Diavik Diamond Mines Inc. (DDMI) would like to advise you of our immediate plans for underground backfilling. As you are aware different underground mining methods and different kimberlite pipes have different geotechnical requirements for backfilling mine openings in the kimberlite ore. The specific composition of each type of backfill will be determined based on the specific geotechnical requirements. A large component of backfill is mine wasterock.

For the next 12-18 months DDMI is planning to use the wasterock, from underground development work, to prepare a cemented rock fill (CRF). DDMI has identified possible concerns with cement curing when mixed with low temperature wasterock. To eliminate the need to warm the wasterock from the open-pit or wasterock pile, and the associated energy consumption, use of wasterock from underground that is already above 0^{o}C has been proposed. To meet the tonnage requirements both Type I and Type III underground wasterock will be required.

DDMI has previously evaluated the geochemical implications of using Type III wasterock in underground backfill. These evaluations were conducted because over the long term it is preferable geochemically to encapsulate Type III material in cement and place it underground as compared with having it exposed on the surface. However, DDMI also wanted to ensure there would not be any significant impacts on operational water quality.

The evaluation consisted of two phases; a) geochemical testing, and b) water quality modeling.

Geochemical Testing

Wasterock samples were taken from the Type I and Type III dump areas, crushed to < 2" diameter and mixed with 5% cement. After 28 days of curing the samples were sent to CEMI in Vancouver B.C for the following analysis:

- Acid-Base Accounting (ABA)

- Whole rock and Bulk metal Analysis on Solids
- Short Term Leach Testing
- Mineralogical Analysis

The short term leach testing results were used in the water quality modeling.

Water Quality Modeling

A mass-balance geochemical model was used to estimate the mine water quality once the seepage water from underground workings and the water from the open pit sumps have been mixed to produce a final mine water. The model consists of a number of source components (i.e. underground seepage, open-pit sumps, etc.) that are linked together to define a mass transport system. Each source component was assigned a flow (based on flow modeling) and water chemistries that together define the load contribution from each component.

The following Tables provide the model inputs used to define each source component. These inputs remained constant in all model scenarios.

Table 2 – Flow rates assumed for open-pits, ramps, vents and drainage drifts and the water origin (groundwater versus lake water).
Table 3C – Groundwater quality assumed for groundwater inflows.
Table 3D – Lake water quality assumed for lake water inflows.
Table 4 – Pit sump water quality assumed for open-pit sump inputs

Numerous scenarios were run using the inputs as defined above but varying the quality of the leach water from the backfill material. Table 1 lists all the backfill scenarios that were modeled. Several different types of backfill were modeled using both a high seepage rate from the backfill and a low seepage rate. Of relevance here are Scenarios 2, 9, and 18. Scenarios 9 and 18 use the leaching rates from the geochemical testing of the cemented rock fills (CRF) made with material from the Type I and Type III stockpiles respectively (see above) and the higher seepage rates (worst-case).

As it turns out, results of the out whole rock testing of the samples collected from the Type I and Type III stockpiles both had sulphur contents of 0.06%S meaning they are both actually representative of Type II rock using DDMI's classification. However, they are ideal for the purpose of evaluating implications of the plan to use a mixture of Type I and Type III wasterock from underground as 0.06%S would likely be a reasonable estimate of the bulk sulphur content for the underground waste material.

Scenario 2 is a worst-case geochemical scenario. It assumes a backfill leach quality estimated from the baseline long-term kinetic tests run on biotite schist with a sulphur content of 0.16%S. It is included to both illustrate a worst-case condition but also the relative insensitivity of the final water quality to the backfill leach quality. Table 5 lists the actual backfill leach water quality used to represent each of the backfill material types.

Table 6 shows the predicted mine water quality for each of the backfill options modeled. Despite differences in backfill leach water quality, the final mine water quality is unchanged because the final chemistry is dominated by the groundwater reporting to the drainage galleries.

Conclusion

There are environmental benefits to including Type III wasterock from underground to prepare backfill material for underground. This includes both the reduction in potential for poor quality surface runoff from surface exposure of Type III rock and elimination of short-term energy required to warm rock for use in underground. No impact on operational mine water quality has been predicted.

Please let me know if you require any further information.

Regards,

Gord Macdonald

Attachments:

Table 1 – Description of Backfill Scenarios Modeled
Table 2 – Flow rates assumed for open-pits, ramps, vents and drainage drifts.
Table 3C – Groundwater quality assumed for groundwater inflows.
Table 3D – Lake water quality assumed for lake water inflows.
Table 4 – Pit sump water quality assumed for open-pit sump inputs
Table 5 – Backfill leach water quality assumed for modeling.
Table 6 – Modeling results for various backfill materials.

TABLE 1
SCENARIOS MODELED: BACKFILL TYPES AND PERCENTAGE OF BACKFILL SEEPAGE
DIAVIK DIAMOND MINE

Backfill Type	Percentage of Water from Backfill [1]	Scenario Number
Acid Generating (AG) Rock - Sulphide-rich Biotite Schist	0.1%	Scenario 1
	10%	Scenario 2
Type I Stockpile - Coarse Rock	0.1%	Scenario 3
	10%	Scenario 4
Type I Stockpile - Paste Fill w/ 5% Cement	0.1%	Scenario 5
	10%	Scenario 6
Type I Stockpile - Paste Fill w/ 5% Intercem	0.1%	Scenario 7
	10%	Scenario 8
Type I Stockpile - Rock Fill	0.1%	Scenario 9
	10%	Scenario 10
Type III Stockpile - Coarse Rock	0.1%	Scenario 11
	10%	Scenario 12
Type III Stockpile - Paste Fill w/ 5% Cement	0.1%	Scenario 13
	10%	Scenario 14
Type III Stockpile - Paste Fill w/ 5% Intercem	0.1%	Scenario 15
	10%	Scenario 16
Type III Stockpile - Rock Fill	0.1%	Scenario 17
	10%	Scenario 18 [2]

Notes:

(1) Percentage of water from backfill:

(i) 0.1% Low flow − assumes that consolidation of backfill seepage will result in release of 0.1% of the total flow reporting to the drainage galleries.

(ii) 10% High flow − assumes that consolidation of backfill seepage will result in release of 10% of the total flow reporting to the drainage galleries.

(2) Scenario 18 was also simulated with the effect of upwelling of saline groundwater to the drainage galleries.

TABLE 2
FLOW RATE SCHEDULE FOR OPEN PITS, RAMPS, VENTS AND DRAINAGE DRIFTS
DIAVIK DIAMOND MINE

Flow Source	Annual Average Flow Rates (m^3/d)														
	2008	**2009**	**2010**	**2011**	**2012**	**2013**	**2014**	**2015**	**2016**	**2017**	**2018**	**2019**	**2020**	**2021**	**2022**
A154 Pit	16000	1600	1200	1100	1100	1100	1000	1000	1000	1000	900	900	1000	900	900
A418 Pit	1000	1000	1000	1000	1000	1000	1000	1000	1000	1000	1000	1000	1000	1000	1000
Ramps	1500	1600	1500	1400	1400	1800	2300	2200	2600	2500	2400	2400	2400	2500	2500
Vents	1800	1700	1300	1200	1100	1000	900	700	600	500	500	500	600	500	500
A154N Drifts															
9225 m	500	1700	1000	800	700	700	700	700	700	600	600	600	700	700	700
9150 m	900	15900	15200	11600	11500	11500	11400	11300	11300	11200	11200	11200	11300	11300	11300
9075 m	300	400	1000	8900	9000	9000	8900	8900	8800	8800	8800	8800	8900	8900	8900
9000 m	0	900	1000	700	700	700	700	600	600	600	600	600	600	600	600
8925 m	0	0	0	5900	5400	5100	3900	1700	1600	1400	1300	1400	2400	2900	2800
8850 m	0	0	0	0	0	0	1200	1900	1800	800	1000	1100	1500	1600	1600
8775 m	0	0	0	0	0	0	0	500	600	900	900	1200	2100	2100	2200
8700 m	0	0	0	0	0	0	0	1300	1200	1300	1300	2700	1100	1200	1200
8685 m	0	0	0	0	0	0	0	0	0	4300	4000	0	0	0	0
A154S Drifts															
9075 m	100	600	400	400	400	300	300	200	200	200	200	200	0	0	0
9000 m	100	9000	7800	700	600	600	400	300	200	300	300	300	0	0	0
8925 m	0	0	0	300	500	500	400	400	300	300	600	900	0	0	0
8850 m	0	0	0	0	0	100	900	1100	1000	1300	300	300	0	0	0
8835 m	0	0	0	0	0	0	0	2000	1800	0	0	0	0	0	0
A418 Drifts															
9165 m	1200	1200	800	700	700	700	600	600	600	500	500	500	500	500	500
9105 m	1800	1800	1500	1500	1500	1500	1300	1200	1200	1200	1200	1200	1200	1200	1200
9045 m	2700	2700	2300	2200	2200	2000	700	700	700	700	700	600	600	600	600
8980 m	0	0	0	0	0	0	1700	1200	500	500	500	500	500	500	500
8915 m	0	0	0	0	0	0	300	300	1000	900	900	900	900	900	900
8850 m	0	0	0	0	0	0	0	600	700	400	400	400	400	300	300
8785 m	0	0	0	0	0	0	0	0	700	700	700	600	300	300	300
8760 m	0	0	0	0	0	0	0	0	100	100	100	0	900	800	800
Underground Sources															
Total Flow	10900	37500	33800	36300	35700	35500	36600	38400	38800	40000	39000	36900	36900	37400	37400
% Lake Water	73	75	86	88	90	91	90	86	88	84	89	92	93	93	94
All Sources															
Total Flow	**27900**	**40100**	**36000**	**38400**	**37800**	**37600**	**38600**	**40400**	**40800**	**42000**	**40900**	**38800**	**38900**	**39300**	**39300**
% Underground	**39**	**94**	**94**	**95**	**94**	**94**	**95**	**95**	**95**	**95**	**95**	**95**	**95**	**95**	**95**

Note:
− Flow rates are derived from the July 2007 hydrogeologic numerical model.

TABLE 3C
SUMMARY OF MODEL INPUT WATER QUALITY: GROUNDWATER
DIAVIK DIAMOND MINE

Parameter	Units	Groundwater Quality [1]
Total Dissolved Solids (TDS)[2]	**mg/L**	**500−2800**
Total Dissolved Solids (TDS)[3]	**mg/L**	**271−2313**
Aluminum (Al)	mg/L	0.03
Ammonia (NH_4+NH_3)	mg/L as N	0.06
Arsenic (As)	mg/L	0.005
Chromium (Cr)	mg/L	*0.005*
Cobalt (Co)	mg/L	*0.0002*
Copper (Cu)	mg/L	*0.0008*
Iron (Fe)	mg/L	0.2
Lead (Pb)	mg/L	*0.00008*
Manganese (Mn)	mg/L	0.09
Molybdenum (Mo)	mg/L	0.009
Nickel (Ni)	mg/L	0.002
Nitrate (NO_3)	mg/L as N	0.01
Nitrite (NO_2)	mg/L as N	*0.002*
Phosphorus (P)[4]	mg/L	0.00005−0.2
Sulphate (SO_4)	mg/L	5
Uranium (U)	mg/L	0.0002
Vanadium (V)	mg/L	0.0008
Zinc (Zn)	mg/L	0.007

Notes:

0.0025 − denotes a value that is one half of the detection limit. Concentrations below detection were input into the model as one half of the detection limit.

(1) Groundwater Quality− taken from monitoring data collected from a depth of about 150 mbsl during a pumping test in 2006.

(2) Total Dissolved Solids− determined from the numerical hydrogeological model and considers the effect of upwelling of saline groundwater (Table 3B).

(3) Total Dissolved Solids− determined from the relationship between TDS and depth at Diavik and Lupin Mine sites (Table 3A; Figure 1).

(4) Phosphorous − determined from the relationship between P and depth (Table 3A; Figure 2).

TABLE 3D
SUMMARY OF MODEL INPUT WATER QUALITY: LAKE WATER
DIAVIK DIAMOND MINE

Parameter	Units	Lake Water Quality [1]
Total Dissolved Solids (TDS)	**mg/L**	**30**
Aluminum (Al)	mg/L	0.02
Ammonia (NH_4+NH_3)	mg/L as N	0.05
Arsenic (As)	mg/L	0.0003
Chromium (Cr)	mg/L	0.0001
Cobalt (Co)	mg/L	0.0003
Copper (Cu)	mg/L	0.001
Iron (Fe)	mg/L	0.01
Lead (Pb)	mg/L	0.0004
Manganese (Mn)	mg/L	0.004
Molybdenum (Mo)	mg/L	0.001
Nickel (Ni)	mg/L	0.002
Nitrate (NO_3)	mg/L as N	0.03
Nitrite (NO_2)	mg/L as N	0.01
Phosphorus (P)	mg/L	0.6 [2]
Sulphate (SO_4)	mg/L	1
Uranium (U)	mg/L	0.0004
Vanadium (V)	mg/L	0.0004
Zinc (Zn)	mg/L	0.005

Notes:

(1) Lake Water Quality − taken from Table 6-16 in DDMI (1998).

(2) Concentration of phosphorous assumed to be 0.6 mg/L. This assumption is based on observations of concentrations of phosphorous from previous pumping test data.

DRAFT

TABLE 4
SUMMARY OF MODEL INPUT WATER QUALITY:
OPEN PIT SUMPS
DIAVIK DIAMOND MINE

Parameter	Units	Water Quality Monitoring Data						Average Open Pit Sump Water Quality [1]
		SUMP 1 2003	SUMP 1 2004	SUMP 1 2005	NEW SUMP 1 8/26/2006	NEW SUMP 2 8/28/2006	NEW SUMP 2B 8/28/2006	
Total Dissolved Solids (TDS)	**mg/L**	**360**	**360**	**270**	**–**	**–**	**–**	**330**
Aluminum (Al)	mg/L	7	7	0.3	0.6	1	1	3
Ammonia (NH_4+NH_3)	mg/L as N	–	–	3	5	9	9	7
Arsenic (As)	mg/L	0.003	0.003	0.003	0.003	0.004	0.004	0.003
Chromium (Cr)	mg/L	0.02	0.02	0.003	0.01	0.03	0.03	0.02
Cobalt (Co)	mg/L	0.005	0.005	0.001	0.003	0.007	0.007	0.005
Copper (Cu)	mg/L	0.04	0.04	0.003	0.007	0.009	0.009	0.02
Iron (Fe)	mg/L	7	7	0.5	1	3	3	4
Lead (Pb)	mg/L	0.003	0.003	0.0005	0.004	0.001	0.001	0.002
Manganese (Mn)	mg/L	0.4	0.4	0.1	0.04	0.1	0.1	0.2
Molybdenum (Mo)	mg/L	0.03	0.03	0.02	0.05	0.03	0.04	0.03
Nickel (Ni)	mg/L	0.03	0.03	0.02	0.06	0.1	0.1	0.07
Nitrate (NO_3)	mg/L as N	9	9	5	12	16	17	11
Nitrite (NO_2)	mg/L as N	0.2	0.2	0.1	0.8	1.0	0.9	0.5
Phosphorus (P)	mg/L	–	–	0.4	0.3	0.2	0.2	0.3
Sulphate (SO_4)	mg/L	8	8	6	22	19	19	14
Uranium (U)	mg/L	0.03	0.03	0.01	0.005	0.007	0.007	0.02
Vanadium (V)	mg/L	0.02	0.02	0.003	0.003	0.005	0.006	0.008
Zinc (Zn)	mg/L	0.02	0.02	0.02	0.02	0.006	0.008	0.02

Notes:

0.0025 – denotes a value that is one half of the detection limit. Concentrations below detection were input into the model as one half of the detection limit.

(1) Average Open Pit Sump Water Quality – calculated from monitoring data collected from the open pit sumps from 2003 to 2006. Assumed to represent the water quality of the mixed water from the sumps in A154 and A418 pits.

DRAFT

TABLE 5
SUMMARY OF MODEL INPUT WATER QUALITY:
BACKFILL LEACH
DIAVIK DIAMOND MINE

Parameter	Units	Acid Generating Rock	Type I Stockpile Samples				Type III Stockpile Samples			
		Sulphide-rich Biotite Schist (2)	Coarse Rock	Paste Fill 5% Cement	Paste Fill 5% Intercem	Rock Fill	Coarse Rock	Paste Fill 5% Cement	Paste Fill 5% Intercem	Rock Fill
Total Dissolved Solids (TDS)	**mg/L**	**536**	**96**	**473**	**230**	**1518**	**102**	**348**	**243**	**1665**
Aluminum (Al)	mg/L	19	1	2	0.7	0.6	1	2	1.0	0.4
Ammonia (NH_4+NH_3)	mg/L as N	0.005	–	–	–	–	–	–	–	–
Arsenic (As)	mg/L	*0.0001*	0.0008	0.0003	0.001	*0.00005*	0.0008	0.0004	0.001	*0.00005*
Chromium (Cr)	mg/L	0.007	0.004	0.05	0.01	0.07	0.003	0.01	0.003	0.04
Cobalt (Co)	mg/L	0.4	*0.00001*	0.0008	0.00002	0.001	*0.00001*	0.0002	*0.00001*	0.001
Copper (Cu)	mg/L	2	0.0006	0.005	0.001	0.007	0.0003	0.003	0.0004	0.007
Iron (Fe)	mg/L	*3*	0.006	0.01	*0.0025*	*0.0025*	*0.0025*	0.01	*0.0025*	*0.0025*
Lead (Pb)	mg/L	0.02	*0.00001*	0.0003	0.0002	0.0002	*0.00001*	0.002	*0.00001*	0.0003
Manganese (Mn)	mg/L	0.6	0.00008	0.00005	0.0002	0.00004	0.00003	0.0001	0.00003	0.00007
Molybdenum (Mo)	mg/L	0.010	0.001	0.007	0.006	0.009	0.01	0.02	0.02	0.02
Nickel (Ni)	mg/L	2	*0.00025*	0.004	0.0008	0.006	*0.00025*	0.003	*0.00025*	0.008
Nitrate (NO_3)	mg/L as N	0.005	–	–	–	–	–	–	–	–
Nitrite (NO_2)	mg/L as N	0.01	–	–	–	–	–	–	–	–
Phosphorus (P)	mg/L	*0.05*	*0.05*	*0.05*	*0.05*	*0.05*	*0.05*	*0.05*	*0.05*	*0.05*
Sulphate (SO_4)	mg/L	451	17	69	83	208	21	90	97	6
Uranium (U)	mg/L	*0.02*	0.0002	*0.000005*	*0.000005*	*0.000005*	0.00007	*0.000005*	*0.000005*	*0.000005*
Vanadium (V)	mg/L	0.003	0.009	0.003	0.004	0.001	0.009	0.01	0.007	0.0006
Zinc (Zn)	mg/L	2	*0.00025*	*0.00025*	*0.00025*	*0.00025*	*0.00025*	*0.00025*	*0.00025*	*0.00025*

Notes:

0.0025 − denotes a value that is one half of the detection limit. Concentrations below detection were input into the model as one half of the detection limit.

(1) Backfill Leachate Water Quality− SPLP leach testing results conducted on samples of Type I and Type III coarse rock, rock fill and paste fill. The leach testing results are described in detail in Golder (2007).

(2) Biotite Schist − represents the acid generating rock material with relatively high concentrations of metals. These concentrations are an average of the last five weeks of kinetic testing of sample VR17699A as reported in the geochemistry baseline study by Sala/Geochimica (1998).

DRAFT

TABLE 6
SIMULATION RESULTS:
AVERAGE CONCENTRATIONS OVER LOM
DIAVIK DIAMOND MINE

Parameter	Units	Simulated Concentrations for Mine Discharge Water (Underground Sump Water + Open Pit Sump Water)																		DDMI Water License Criteria [1]
		Simulation Scenarios																		
		Acid Generating Rock		Type I - Stockpile Samples								Type III - Stockpile Samples								
		Sulphide-rich Biotite Schist		Coarse Rock		Paste Fill w/ 5% Cement		Paste Fill w/ 5% Intercem		Rock Fill		Coarse Rock		Paste Fill w/ 5% Cement		Paste Fill w/ 5% Intercem		Rock Fill		
		0.1%	10%	0.1%	10%	0.1%	10%	0.1%	10%	0.1%	10%	0.1%	10%	0.1%	10%	0.1%	10%	0.1%	10%	
Total Dissolved Solids (TDS)	**mg/L**	**174**	**174**	**174**	**174**	**174**	**174**	**174**	**174**	**174**	**175**	**174**	**174**	**174**	**174**	**174**	**174**	**174**	**175**	**–**
Aluminum (Al)	mg/L	0.3	0.3	0.3	0.3	0.3	0.3	0.3	0.3	0.3	0.3	0.3	0.3	0.3	0.3	0.3	0.3	0.3	0.3	1.5
Ammonia (NH_4+NH_3)	mg/L	1.3	1.3	1.3	1.3	1.3	1.3	1.3	1.3	1.3	1.3	1.3	1.3	1.3	1.3	1.3	1.3	1.3	1.3	10
Arsenic (As)	mg/L	0.001	0.001	0.001	0.001	0.001	0.001	0.001	0.001	0.001	0.001	0.001	0.001	0.001	0.001	0.001	0.001	0.001	0.001	0.05
Chromium (Cr)	mg/L	0.002	0.002	0.002	0.002	0.002	0.002	0.002	0.002	0.002	0.002	0.002	0.002	0.002	0.002	0.002	0.002	0.002	0.002	0.02
Cobalt (Co)	mg/L	0.001	0.001	0.001	0.001	0.001	0.001	0.001	0.001	0.001	0.001	0.001	0.001	0.001	0.001	0.001	0.001	0.001	0.001	–
Copper (Cu)	mg/L	0.003	0.005	0.003	0.003	0.003	0.003	0.003	0.003	0.003	0.003	0.003	0.003	0.003	0.003	0.003	0.003	0.003	0.003	0.02
Iron (Fe)	mg/L	0.4	0.4	0.4	0.4	0.4	0.4	0.4	0.4	0.4	0.4	0.4	0.4	0.4	0.4	0.4	0.4	0.4	0.4	–
Lead (Pb)	mg/L	0.0005	0.0005	0.0005	0.0005	0.0005	0.0005	0.0005	0.0005	0.0005	0.0005	0.0005	0.0005	0.0005	0.0005	0.0005	0.0005	0.0005	0.0005	0.01
Manganese (Mn)	mg/L	0.03	0.03	0.03	0.03	0.03	0.03	0.03	0.03	0.03	0.03	0.03	0.03	0.03	0.03	0.03	0.03	0.03	0.03	–
Molybdenum (Mo)	mg/L	0.004	0.004	0.004	0.004	0.004	0.004	0.004	0.004	0.004	0.004	0.004	0.004	0.004	0.004	0.004	0.004	0.004	0.004	–
Nickel (Ni)	mg/L	0.008	0.009	0.008	0.008	0.008	0.008	0.008	0.008	0.008	0.008	0.008	0.008	0.008	0.008	0.008	0.008	0.008	0.008	0.05
Nitrate (NO_3)	mg/L	1.6	1.6	1.6	1.6	1.6	1.6	1.6	1.6	1.6	1.6	1.6	1.6	1.6	1.6	1.6	1.6	1.6	1.6	–
Nitrite (NO_2)	mg/L	0.05	0.05	0.05	0.05	0.05	0.05	0.05	0.05	0.05	0.05	0.05	0.05	0.05	0.05	0.05	0.05	0.05	0.05	1
Phosphorous (P)	mg/L	0.52	0.52	0.52	0.52	0.52	0.52	0.52	0.52	0.52	0.52	0.52	0.52	0.52	0.52	0.52	0.52	0.52	0.52	– [2]
Sulphate (SO_4)	mg/L	3	3	3	3	3	3	3	3	3	3	3	3	3	3	3	3	3	3	–
Uranium (U)	mg/L	0.002	0.002	0.002	0.002	0.002	0.002	0.002	0.002	0.002	0.002	0.002	0.002	0.002	0.002	0.002	0.002	0.002	0.002	–
Vanadium (V)	mg/L	0.001	0.001	0.001	0.001	0.001	0.001	0.001	0.001	0.001	0.001	0.001	0.001	0.001	0.001	0.001	0.001	0.001	0.001	–
Zinc (Zn)	mg/L	0.006	0.009	0.006	0.006	0.006	0.006	0.006	0.006	0.006	0.006	0.006	0.006	0.006	0.006	0.006	0.006	0.006	0.006	0.01

Notes:

− All 18 scenarios are presented, including 9 different backfill types that were modeled using two backfill flow rates (0.1% and 10% of the total flow reporting to the drainage galleries).

(1) DDMI Water License Criteria are compliance limits outlined in the site water license N7L2-1645.

(2) Water license criteria for total phosphorous is defined as a load, not a concentration, at 1000 kg/year.